LAWRENCE
LIVERMORE
NATIONAL
LABORATORY

LLNL-TR-404620

Hydrologic Resources Management Program and Underground Test Area Project FY 2006 Progress Report

H. W. Culham, G. F. Eaton, V. Genetti, Q. Hu, A. B. Kersting, R. E. Lindvall, J. E. Moran, G. A. Blasiyh Nuno, B. A. Powell, T. P. Rose, M. J. Singleton, R. W. Williams, M. Zavarin, P. Zhao

June 12, 2008

Disclaimer

This work performed under the auspices of the U.S. Department of Energy by Lawrence Livermore National Laboratory under Contract DE-AC52-07NA27344.

LLNL-TR-404620

Hydrologic Resources Management Program and Underground Test Area Project FY 2006 Progress Report

EDITORS

Mavrik Zavarin
Annie B. Kersting
Rachel E. Lindvall
Timothy P. Rose

AUTHORS

H. W. Culham
Gail F. Eaton
Victoria Genetti
Qinhong (Max) Hu
Annie B. Kersting
Rachel E. Lindvall
Jean E. Moran
Guillermo A. Blasiyh Nuño
Brian A. Powell
Timothy P. Rose
Michael J. Singleton
Ross W. Williams
Mavrik Zavarin
Pihong Zhao

April 2008

Table of Contents

List of Figures

List of Tables

INTRODUCTION

Hydrologic Resources Management Program and Underground Test Area Project FY 2006 Progress Report

T.P. Rose[1], A.B. Kersting[2], and M. Zavarin[1]

[1]Chemical Sciences Division, Chemistry, Materials, Earth and Life Sciences
[2]Glenn T. Seaborg Institute, Chemistry, Materials, Earth and Life Sciences
Lawrence Livermore National Laboratory

This report describes FY 2006 technical studies conducted by the Chemical Biology and Nuclear Science Division (CBND) at Lawrence Livermore National Laboratory (LLNL) in support of the Hydrologic Resources Management Program (HRMP) and the Underground Test Area Project (UGTA). These programs are administered by the U.S. Department of Energy, National Nuclear Security Administration, Nevada Site Office (NNSA/NSO) through the Defense Programs and Environmental Restoration Divisions, respectively. HRMP-sponsored work is directed toward the responsible management of the natural resources at the Nevada Test Site (NTS), enabling its continued use as a staging area for strategic operations in support of national security. UGTA-funded work emphasizes the development of an integrated set of groundwater flow and contaminant transport models to predict the extent of radionuclide migration from underground nuclear testing areas at the NTS.

The report is organized on a topical basis and contains four chapters that highlight technical work products produced by CBND. However, it is important to recognize that most of this work involves collaborative partnerships with the other HRMP and UGTA contract organizations. These groups include the Energy and Environment Directorate at LLNL (LLNL-E&E), Los Alamos National Laboratory (LANL), the Desert Research Institute (DRI), the U.S. Geological Survey (USGS), Stoller-Navarro Joint Venture (SNJV), and National Security Technologies (NSTec).

Chapter 1 is a summary of FY 2006 sampling efforts at near-field "hot" wells at the NTS, and presents new chemical and isotopic data for groundwater samples from four near-field wells. These include PM-2 and U-20n PS#1DDh (CHESHIRE), UE-7ns (BOURBON), and U-19v PS#1ds (ALMENDRO).

Chapter 2 is a summary of the results of chemical and isotopic measurements of groundwater samples from three UGTA environmental monitoring wells. These wells are: ER-12-4 and U12S located in Area 12 on Rainier Mesa and USGS HGH#2 WW2 located in Yucca Flat. In addition, three springs were sampled White Rock Spring and Captain Jack Spring in Area 12 on Rainier Mesa and Topopah Spring in Area 29.

Chapter 3 is a compilation of existing noble gas data that has been reviewed and edited to remove inconsistancies in presentation of total vs. single isotope noble gas values reported in the previous HRMP and UGTA progress reports.

Chapter 4 is a summary of the results of batch sorption and desorption experiments performed to determine the distribution coefficients (K_d) of Pu(IV), Np(V), U(VI), Cs and Sr to zeolitized tuff (tuff confining unit, TCU) and carbonate (lower carbonate aquifer, LCA) rocks in synthetic NTS groundwater

Chapter 5 is a summary of the results of a series of flow-cell experiments performed to examine Np(V) and Pu(V) sorption to and desorption from goethite. Np and Pu desorption occur at a faster rate and to a greater extent than previously reported. In addition, oxidation changes occurred with the Pu whereby the surface-sorbed Pu(IV) was reoxidized to aqueous Pu(V) during desorption.

CHAPTER 1

FY 2006 Chemical and Isotopic Hot Well Groundwater Data

G.F. Eaton, V.Genetti, Q. (Max) Hu, R.E. Lindvall, J.E. Moran, T.P. Rose, R.W. Williams, M. Zavarin, and P. Zhao

Chemical Sciences Division
Lawrence Livermore National Laboratory

1.1 Introduction

This chapter summarizes the results of chemical and isotopic analyses of groundwater samples collected from near-field "hot" wells at the NTS during FY 2006. This work is the latest contribution to a long-standing effort aimed at understanding radionuclide transport processes at the NTS. These data are required in the development and verification of contaminant transport models for the Underground Test Area (UGTA) project. Collaborating agencies in the hot well sampling effort include Los Alamos National Laboratory (LANL), the U.S. Geological Survey (USGS), the Desert Research Institute (DRI), National Security Technologies (NSTec), and Stoller-Navarro Joint Venture (SNJV).

Groundwater samples were collected from four NTS near-field wells during FY 2006. These include PM-2 located approximately 270 meters northwest of the SCHOONER test, U-20n PS1ddh completed in the cavity of CHESHIRE, UE-7ns (located 137 m southeast of BOURBON), and U-19v PS#1ds (ALMENDRO). **Figure 1.1** shows the locations of these wells at the NTS. Laboratory analytical protocols are fully described in the LLNL Standard Operating Procedures written in support of the UGTA Project (LLNL, 2004). **Tables 1.1** through **1.7** contain the analytical results for the FY 2006 samples together with comparative data for samples collected over the past several years. Significant features of the FY 2006 data are highlighted in the sections that follow.

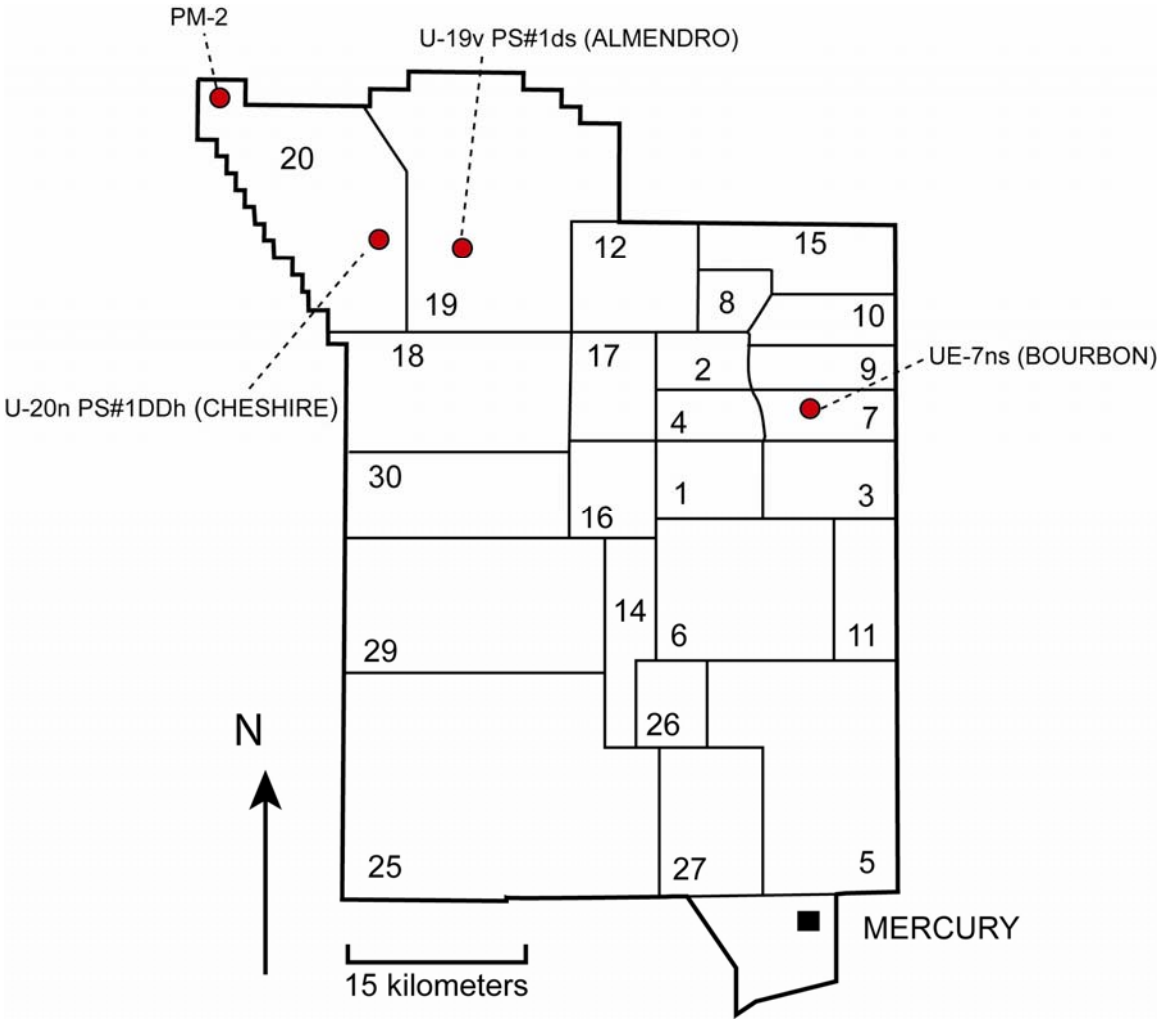

Figure 1.1 Map of the NTS showing Hotwell sampling locations for FY2006.

1.2 PM-2

PM-2 is located at the extreme northwest corner of area 20 of the Nevada Test Site (NTS). It was constructed between May 20 and October 13, 1964. The nearest underground nuclear test is the SCHOONER test (12/8/1968, U-20u, 30 kt, 108.2 meter depth) (DOE, 2000) detonated approximately 270 meters southeast of PM-2 (Russell and Locke, 1997). Construction details and sample locations for well PM-2 are shown in **Figure 1.2**. The PM-2 borehole was last sampled for radiochemical characterization in May 1994, and has not been a part of the regular hot well sampling program. SCHOONER was part of the Plowshare program designed to test the effects of cratering. This detonation resulted in debris and ejecta temporarily burying PM-2. Schooner was detonated at burial depth of 111m, well above the regional water table. Radionuclides detected in the deep groundwater (305-915 m-bgs) at PM-2 implies either significant vertical transport of contaminants through the thick unsaturated zone on Pahute Mesa, or dragged-down surface contamination. Our present interest in PM-2 is related to the extremely wet 2004-05 winter season, which should have produced a major pulse of groundwater recharge on Pahute Mesa. Under these circumstances, we expect to observe (1) an increase in PM-2 water

levels relative to previous measurements, and (2) a correlated increase in radionuclide concentrations.

The water table depth at PM-2 was measured at 262 m-bgs, not corrected for hole deviations. This water level is in good agreement with water levels measured in the 1990's. Interestingly, it does not appear that there was an increase in water levels as a result of increased recharge (as observed in 1993).

Groundwater characterization samples were collected from well PM-2 on October 26, 2005 using evacuated steel pressure tubes, lowered into the hole with the USGS wire-line bailer. A total of four samples were collected at four depth intervals. The first sample was collected near the water table (264 m-bgs). Subsequent samples were taken at successively deeper intervals (300, 600, and 800 m-bgs). For the 800 m-bgs sample, the pressure tube sampling valve was difficult to close. The valve successfully closed only when sampler was raised to 400 m-bgs. Thus, this sample represents a mixture of groundwater from 400 to 800 m-bgs.

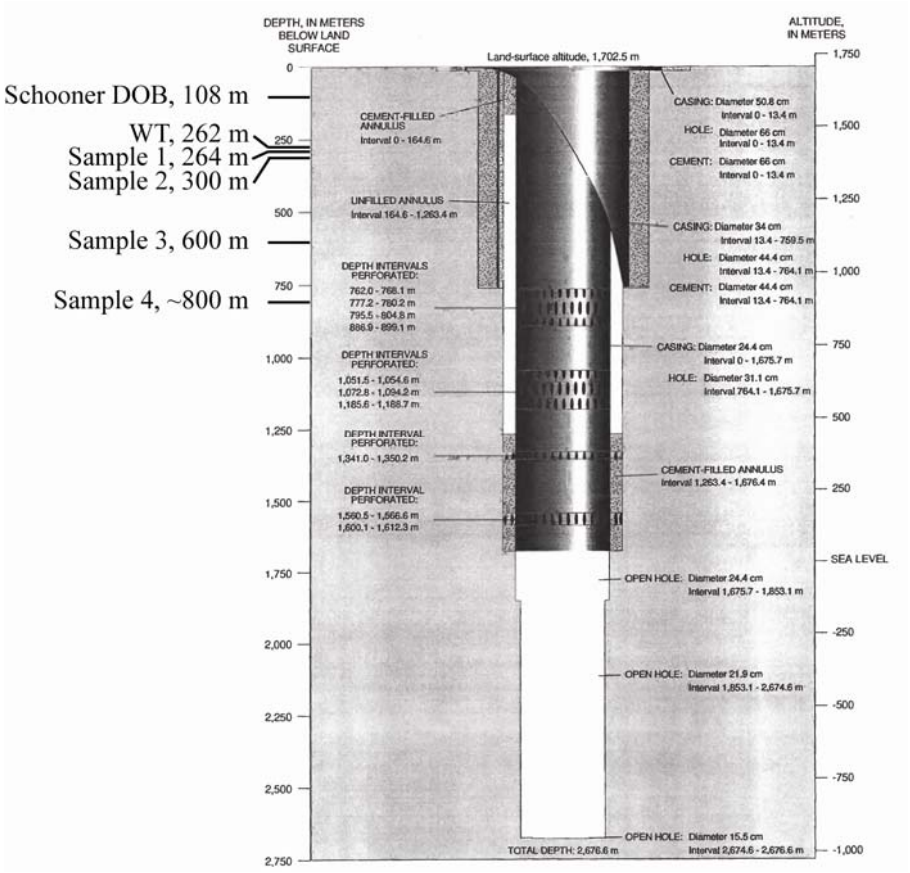

Figure 1.2 Construction details of PM-2 and sampling locations. Diagram from Russell and Locke, 1993).

The composition of PM-2 groundwater varies dramatically with depth (**Table 1.2**). For the two shallow groundwater samples, the water is a low ionic strength Na-HCO_3 type groundwater that is low in Cl^- and SO_4^{2-}. In the deeper intervals, the Na concentration increases to over 1000

mg/L; the DIC increases to over 2000 mg/L. The Ca, Mg, and SO_4^{2-} concentrations decrease with depth and the SO_4 concentrations are anomalously low at the deepest interval. These trends are generally consistent with sampling and analysis that occurred in 1994. It should also be noted that the sample collected at the deepest interval was dark brown in color, suggestive of high organic material content. In fact, a number of organic compounds were identified in the deeper samples in 1994. Furthermore, the low SO_4^{2-} and the high TIC is suggestive of microbial decomposition of organic matter and resulting reducing conditions.

PM-2 has $\delta^{18}O$ and δD values that decrease with depth. The $\delta^{18}O$ decreases from -11.1 to -13.6 while the δD decreases from -80 to -105. Based on these values, the upper interval samples appear to be dominated by recent recharge. Importantly, we cannot say whether this water reached the water table by migration through fractured rock or by preferential flow in/near the wellbore. In the lowest sampling interval, the $\delta^{18}O$ and δD values as well as the Cl^- concentration are approaching the composition of regional groundwater observed in nearby wells (PM-3, ER-EC-1).

The tritium activity at PM-2 increases with depth. This was observed in tritium sampling in 1993-1994 as well. However, in 1993-1994, ^3H activity at 300 meters was 300 to 1000 Bq/L. When decay corrected to 1993, activity in 2005 samples is much higher (~4000 Bq/L). In the deeper intervals, the ^3H concentration has not changed significantly since the 1993-1994 sampling events. The depth-dependence of tritium concentrations suggests that tritium enters the PM-2 wellbore through the uppermost perforated intervals at 800 m-bgs.

Total inorganic carbon (TIC) in PM-2 increases dramatically with depth. Much of this TIC may be related to decomposition of anthropogenic organic materials identified at the bottom of PM-2. It is not expected to be representative of formation water. The ^{14}C value in sample 3 (600 m-bgs) of 1.4×10^2 pmc corresponds to a dissolved ^{14}C activity of 0.91 pCi/L. It is anthropogenic in origin and is likely to have originated from the SCHOONER test. The $\delta^{13}C$ value in the 300 m-bgs samples is -12.2 ‰ and consistent with a significant component of local recharge. The $\delta^{13}C$ value increases dramatically with depth. The high $\delta^{13}C$ in the deepest interval is consistent with microbial decomposition of organic matter.

Chlorine-36 is a long-lived neutron activation product ($t_{1/2} = 3 \times 10^5$ years) that is produced during nuclear detonations, and is highly mobile as the soluble chloride anion. PM-2 groundwater has $^{36}Cl/Cl$ ratios that decrease slightly with depth and are one to two orders of magnitude above the modern atmospheric ratio for southern Nevada ($\sim 5 \times 10^{-13}$, Fabryka-Martin et al., 1993). In terms of pCi/L, the ^{36}Cl concentration changes very little with depth. The ^{36}Cl activity in PM-2 groundwater is ~0.015 pCi/L. Interestingly, these values are one to two orders of magnitude higher than those measured in 1993 (5×10^{-4} to 4×10^{-3} pCi/L).

The fission products ^{99}Tc and ^{129}I were measured in PM-2 groundwater by ICP-MS and AMS, respectively. Technetium and iodine are both highly mobile as soluble anions under oxidizing conditions. Under reducing conditions, they may be effectively sequestered. The measured ^{99}Tc

activity was $<7.6 \times 10^{-2}$ pCi/L at 600 m-bgs. The ^{129}I activity was 9.74×10^{-4} and 6.46×10^{-4} pCi/L at 300 m-bgs and 600 m-bgs, respectively.

PM-2 groundwater from sample 3 (600 m-bgs) has a $^{87}Sr/^{86}Sr$ ratio of 0.70759, a $\delta^{87}Sr$ value of -2.27 ‰, and a Sr concentration of 4360 µg/L. The Sr concentration in this sample is extremely high. The origin for this high Sr is unclear. The concentration of dissolved uranium (0.2 µg/L) is quite low. However, the $^{235}U/^{238}U$ ratio indicates that the uranium is natural in origin. The $^{234}U/^{238}U$ activity ratio (2.43) reveals little or no enrichment in dissolved ^{234}U. The low U concentrations and low $^{234}U/^{238}U$ activity ratio may reflect a significant component of local recharge.

Plutonium was positively detected in only the deepest groundwater sample ($^{239,240}Pu$ 0.006 pCi/L). A positive value may have been measured in the 600 m-bgs sample but potential sample contamination during sample preparation could not be ruled out. The Pu activity reported in Russell and Locke (1997) was 0.04 and 0.1 pCi/L at 823 and 915 m-bgs, respectively. The activity in 2005 samples is significantly lower. However, it still suggests that Pu contamination from SCHOONER may have reached the deeper intervals of PM-2. The form of the Pu (colloidal or otherwise) could not be determined due to the very low activity and small sample volumes collected.

1.3 U-20n PS1-DDh (CHESHIRE)

The CHESHIRE test was detonated in the U-20n emplacement hole on 14 February 1976 at a depth of 3,829 ft (1,167 m) beneath the surface of Pahute Mesa and produced a yield in the range of 200-500 kt (DOE, 2000). A post-shot hole was drilled soon after the test, and later was converted to a monitoring well (U-20n PS1-DDh) for radionuclide migration investigations. The well has been modified several times over during its history, but has afforded periodic access to the CHESHIRE cavity and/or chimney region for groundwater sampling since September 1976 (Sawyer et al., 1999). A diagram of the emplacement hole and postshot hole is shown in **Figure 1.3**. The cumulative data set that was gathered for the CHESHIRE site provides valuable insight into how the hydrologic source term (HST) evolves over time, and was recently used in the calibration of an HST model for the CHESHIRE test (Pawloski et al., 2001).

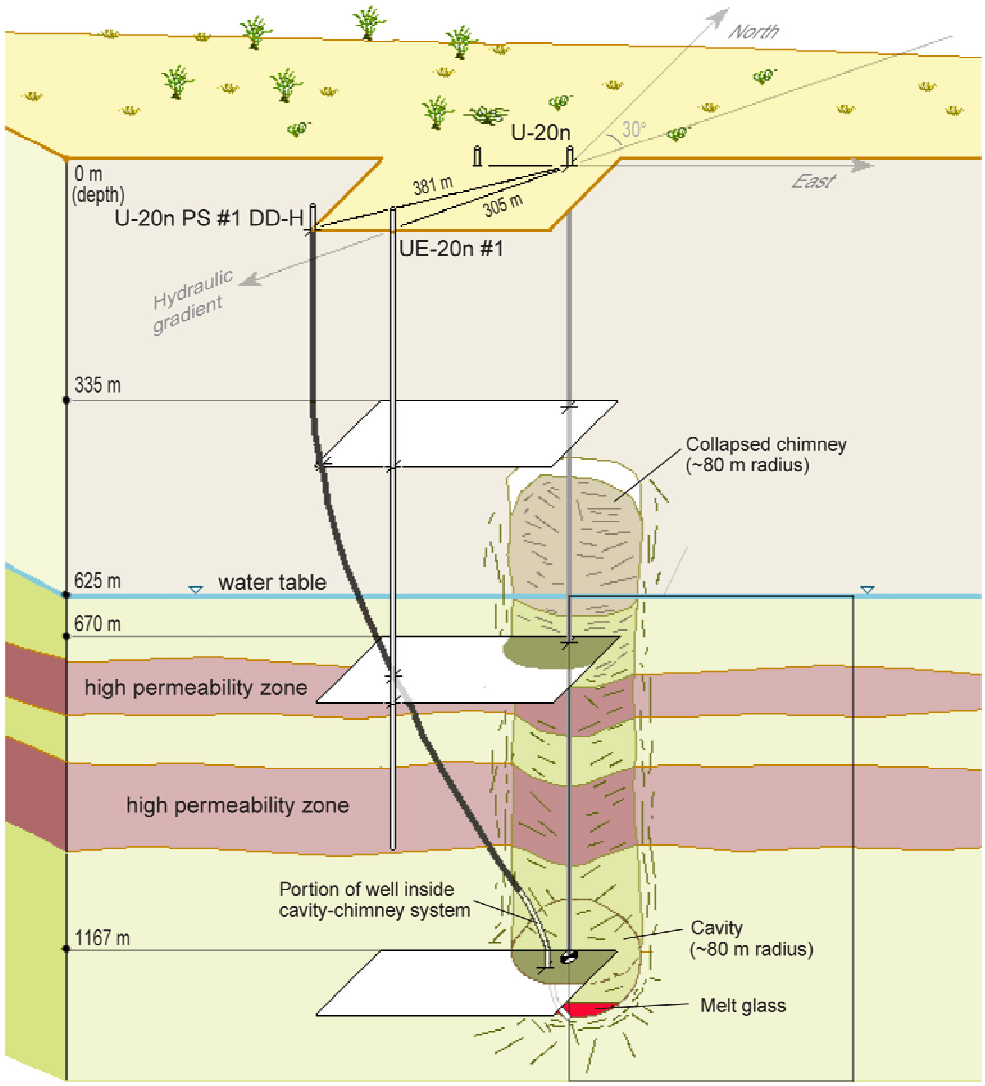

Figure 1.3 Schematic of the near-field CHESHIRE test (Pawloski et al. 2001). The unclassified cavity radius estimate (~80 meters) was based on the maximum announced yield (200-500 kt, DOE, 2000) and the cavity radius equation $Rc = 70.2 \times 500^{1/3}/(2.11 \times 1167)^{1/4}$ defined in Pawloski (1999).

Groundwater characterization samples were collected from U-20n PS1-DDh on 15 November 2005. The samples were pumped from the depth interval 1,250–1,253 m (4,100–4,110 ft) below the surface, within the CHESHIRE test cavity. Prior to the 2005 sampling event, the well was sampled on 9 July 2003, and 12 October 1999 from the same depth interval, allowing a direct comparison of the 1999, 2003 and 2005 data sets. Further discussion of the 1999 and 2003 data is found in Rose et al. (2002) and Rose et al. (2004) respectively.

Comparison of water quality parameters and major dissolved constituents for the 1999, 2003 and 2005 Cheshire samples shows little change in the water chemistry with time. The water has a

dilute sodium bicarbonate composition that is typical of the volcanic aquifers in the eastern part of Pahute Mesa (east of the Purse Fault). The stable isotope (δD and $\delta^{18}O$) composition of the water reveals it is linked to the regional flow system beneath Pahute Mesa, with probable source area(s) located to the north of the NTS (e.g. Rose and Davisson, 2003).

The tritium activity in the July 2005 CHESHIRE sample was 3.3×10^7 pCi/L (corrected to the sampling date). In comparison, the 2003 sample had an activity of 4.4×10^7 pCi/L and the 1999 sample 5.1×10^7 pCi/L at the time of sampling. When these data are decay corrected to time zero, the 1999 (1.9×10^8 pCi/L), 2003 (1.8×10^8 pCi/L) and 2005 (1.8×10^8 pCi/L) results suggest little or no change in tritium over the past 6 years.

The ^{14}C value of dissolved inorganic carbon (DIC) in CHESHIRE groundwater is 1.58×10^5 percent modern carbon (pmc). This is similar to the values measured in 1999 (1.54×10^5 pmc), and 2003 (1.69×10^5 pmc); these are some of the highest ^{14}C values measured for any test at the NTS despite the relatively low DIC concentration in the water. The $^{36}Cl/Cl$ ratio measured in 2005 (1.20×10^{-9}) is four orders of magnitude above the modern atmospheric ratio for southern Nevada ($\sim 5 \times 10^{-13}$, Fabryka-Martin et al., 1993), is slightly less than the ratio measured in 2003 (2.22×10^{-9}), and very similar to the 1999 value (1.15×10^{-9}). There does not appear to be a consistent increase or decrease in ^{36}Cl over the past 6 years. The dissolved $^{129}I/^{127}I$ ratio is 1.13×10^{-4} and falls between that measured in 1999 (4.91×10^{-5}) and 2003 (2.74×10^{-4}). In terms of ^{129}I activity, differences between the last 3 sampling events are also small. Interestingly, the ^{99}Tc activity appears to be decreasing with time. The ^{99}Tc activity was 22.3 pCi/L in 1999, 12.3 pCi/L in 2003, and 0.93 pCi/L in 2005. This trend is particularly unusual given the stable concentration of most other measured geochemical parameters over this sampling time. Continued monitoring of ^{99}Tc at CHESHIRE should reveal whether this trend will continue into the future.

In 2005, the CHESHIRE groundwater had an $^{87}Sr/^{86}Sr$ ratio (0.71102) that reflects equilibration of the water with the volcanic host rock, and the measured $^{235}U/^{238}U$ ratio (0.00728) consistent with the natural isotopic abundance of uranium. Enrichment in the $^{234}U/^{238}U$-activity ratio (3.29) reflects the preferential leaching of ^{234}U from uranium-bearing minerals in the host rock following α-decay of ^{238}U. Sr and U isotopes ratios are, essentially, unchanged since 1999. However, the measured U concentration dropped to 0.36 μg/L.

Plutonium was present at detectable levels in the 2005 CHESHIRE samples. Unfiltered groundwater had a total plutonium concentration of 6.0 pg/L and a $^{239}Pu + ^{240}Pu$ activity of 0.46 pCi/L. This result compares well with earlier Pu measurements and suggests little or no change in the CHESHIRE cavity/chimney Pu concentrations. The 2003 CHESHIRE sample had a slightly lower plutonium concentration (4.1 pg/L) and $^{239}Pu + ^{240}Pu$ activity (0.31 pCi/L); the 1999 CHESHIRE sample had a slightly higher Pu concentration (7.0 pg/L) and $^{239}Pu + ^{240}Pu$ activity (0.51 pCi/L). Filtration experiments performed on the 2003 samples showed that >90% of the plutonium is associated with mineral colloids in the water. Small differences in the Pu activity may be due to the different colloids concentrations in the samples.

Overall, it appears that the groundwater chemistry, stable isotope composition, and radionuclide concentrations in the CHESHIRE cavity/chimney have not changed in the past 6 years. An exception is the steady decrease in ^{99}Tc concentrations; future sampling will reveal whether this trend continues. Based on the last 3 sampling events, there is no indication of rapid radionuclide migration away from the CHESHIRE cavity since 1999. (note: RN detected in satellite well indicates migration)

1.4 UE-7ns (BOURBON)

UE-7ns was completed in 1976 to a depth of 672 m and is located in Area 7 approximately 137 m southeast of the BOURBON test. The BOURBON test was detonated in emplacement hole U-7n on 20 January 1967 with a yield of 20 – 200 kt (DOE, 2000). Both the working point of the BOURBON test (559.7 m-bgs) and UE-7ns satellite well were completed in the Paleozoic carbonate rock of the Lower Carbonate Aquifer (LCA). The rock at the BOURBON working point is a silty limestone and located very close to the tuff-paleozoic carbonate boundary. The tuff-paleozoic carbonate boundary at UE-7ns is at 503 m-bgs (Buddemeier & Isherwood, 1985). The working point of the BOURBON test is above the water table (600.9 m-bgs). However, it is expected that the bottom of the BOURBON cavity intersects the water table (**Figure 1.4**).

On December 13, 2005, groundwater characterization samples were collected from well UE-7ns using evacuated steel pressure tubes, lowered into the hole with a USGS wire-line bailer. All the samples were collected from the same depth (617 m-bgs). The water table depth at the time of sampling was 600.9 m-bgs; the water table depth has not changed since the well was last sampled in August of 2001 (~ 601 m-bgs).

The water from UE-7ns is a Na-K-HCO_3 groundwater with very low SO_4. It resembles water found in tuffaceous volcanic rocks beneath Yucca Flat, though the Cl is slightly elevated (SNJV, 2006). The water chemistry suggests some mixing of LCA groundwater with the overlying volcanic tuff aquifers. However, UE-7ns water has $\delta^{18}O$ and δD values that are depleted in heavy isotopes ($\delta^{18}O$ = -14.1 ‰; δD = -105 ‰) relative to local precipitation and other Yucca Flat wells. These depleted values are more indicative of an LCA source.

Water chemistry, $\delta^{18}O$, and δD data from 2001 and 2005 sampling events are nearly identical. However, the reported pH was significantly lower in 2005. Based on charge balance and calcite saturation calculations, this measured pH is lower than expected.

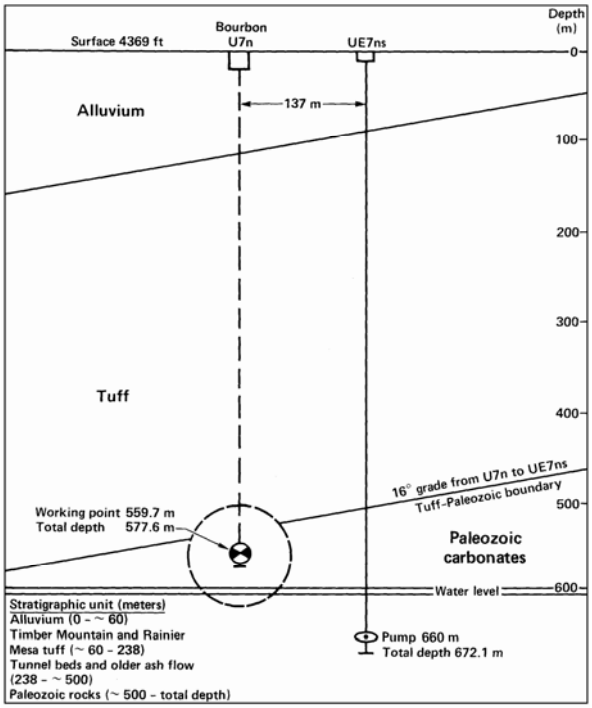

Figure 1.4 The BOURBON near-field (cavity radius not to scale). From Buddemeier and Isherwood (1985).

The tritium activity of the UE-7ns groundwater, measured at LLNL by the helium accumulation method, is 130 pCi/L. This value is two orders of magnitude lower than in 2001. This drop in activity was observed for several radionuclides, as described below.

Total inorganic carbon (TIC) in UE-7ns groundwater has a ^{14}C value of 55.0 pmc, a measured TIC concentration of 204 mg/L, and a dissolved ^{14}C activity of 0.14 pCi/L. The high ^{14}C activity relative to undisturbed LCA groundwater suggests that ^{14}C migrated from the BOURBON test. The measured ^{14}C in 2005 and 2001 is essentially the same. The $\delta^{13}C$ value was -5.3 ‰, 3.3 ‰ lighter than in 2001. However, the value is still consistent with the typical isotopically heavy $\delta^{13}C$ values found in LCA groundwater.

Chlorine-36 is a long-lived neutron activation product ($t_{1/2} = 3 \times 10^5$ years) that is produced during nuclear detonations, and is highly mobile as the soluble chloride anion. UE-7ns groundwater has a $^{36}Cl/Cl$ ratio of 2.95×10^{-13} that is similar to the modern atmospheric ratio for southern Nevada ($\sim 5 \times 10^{-13}$, Fabryka-Martin et al., 1993). The total ^{36}Cl activity in the UE-7ns groundwater is 2.43×10^{-4} pCi/L, about 1 order of magnitude lower than in 2001 (1.4×10^{-3} pCi/L), and consistent with the observed decrease in tritium activity.

The fission products ^{99}Tc and ^{129}I were measured in UE-7ns groundwater by ICP-MS and AMS, respectively. Technetium and iodine are both highly mobile as soluble anions under oxidizing conditions. For comparative purposes, the ^{99}Tc and ^{129}I concentrations in archival samples collected in 2001 were also analyzed. The measured ^{99}Tc activity was <0.043 pCi/L in the 2005

sample and <1 pCi/L in the 2001 sample. The ^{129}I activity was 4.1×10^{-5} pCi/L in the 2005 sample and 6.1×10^{-4} pCi/L in the 2001 sample. The significant drop in ^{129}I activity in 2005 is consistent with ^{36}Cl and tritium measurements.

UE-7ns groundwater has an $^{87}Sr/^{86}Sr$ ratio of 0.71263, and a $\delta^{87}Sr$ value of 4.84 ‰. This ratio is intermediate between the high ratios observed in many LCA groundwater samples and the lower values observed in volcanic aquifers. The Sr concentration in UE-7ns is also suggestive of mixing between LCA and overlying volcanic aquifer waters. The concentration of dissolved uranium (0.06 μg/L) is quite low but consistent with the 2001 measurement. The $^{235}U/^{238}U$ ratio indicates that the uranium is natural in origin. The $^{234}U/^{238}U$ activity ratio (2.77) reveals only a modest enrichment in dissolved ^{234}U due to preferential leaching of this isotope from the aquifer matrix following α-decay of ^{238}U. The $^{234}U/^{238}U$ activity ratio is low when compared to other carbonate aquifer measurements in Yucca Flat and suggests possible mixing with non-LCA waters (SNJV, 2006).

Plutonium was not detected in the groundwater from UE-7ns ($^{239,240}Pu$ <0.04 pCi/L). Plutonium was measured on a bulk sample which includes both the colloidal and aqueous fractions of the groundwater.

Because well UE-7ns was not purged prior to sampling, it is possible that the drop in tritium, 36Cl, and 129I activity is a sampling artifact. To explore the potential migration of these tracers away from UE-7ns in detail, pump installation and well purging is recommended**.**

1.5 U-19v PS#1ds (ALMENDRO)

U-19v PS#1ds is the post-shot re-entry hole for the ALMENDRO underground test, which was conducted on June 6, 1973 at a vertical depth of 3,487 ft (1,063 m) beneath the surface of Pahute Mesa and had a yield in the range of 200-1000 kt (DOE, 2000). The post-shot hole was later developed for use as a near-field monitoring well. Groundwater characterization samples were first collected at this site in 1993 at a vertical depth of 3091 feet (942 m); additional samples were collected in 1996, 1998, 1999, 2000, 2001, and 2003 at vertical depths of 3089 ft (942 m), 3350 ft (1021 m), 2999 ft (914 m), 3089 ft (942 m), 3089 ft (942 m) and 3089 ft (942 m) respectively. Sampling was conducted using a wireline bailer due to the narrow diameter of the borehole and the anomalously high water temperature in the cavity region. A borehole temperature log run in 1996 recorded a maximum value of 157°C at 1,073 m vertical depth. The persistence of elevated temperatures more than 20 years after the test was detonated suggests the ALMENDRO cavity may be effectively isolated from the surrounding groundwater.

Groundwater samples were collected at U-19v PS#1ds on 18 April 2006 using the USGS wireline bailer. The water level was tagged at a vertical depth of 2192 ft (668 m) and sampling occurred at a vertical depth of 3,089 ft (941.5 m).

The chemical characteristics of U-19v PS#1ds groundwater have not changed appreciably during the past several sampling events (see Rose et al., 2003). The water contains Na^+ and HCO_3^- as the major dissolved ions, with relatively high Cl^- (75.7 mg/L) and low SO_4^{2-} (4.3 mg/L)

concentrations. ALMENDRO cavity water also shows strong enrichments in As (228 μg/L) and Mo (1.238 mg/L) compared to environmental samples. U-19v PS#1ds groundwater shows a strong ^{18}O-enrichment relative to other Pahute Mesa regional groundwaters, but lacks a correlated enrichment in deuterium. This is interpreted to reflect oxygen isotope exchange between the water and rock at elevated temperatures, a process that is known to occur in natural geothermal systems (Craig, 1963). Interestingly, it may be possible to take advantage of this isotopic shift to deduce glass dissolution rates in the Almendro cavity. However, this would require understanding ^{18}O enrichment rates as a function of temperature and glass alteration.

Total inorganic carbon (TIC) in U-19v PS#1ds groundwater exhibits an unusually high $\delta^{13}C$ value (+35.9‰ in 2006). The observed ^{13}C-enrichment is consistent with methanogenic reduction of CO_2, which is associated with a large carbon isotope fractionation between CH_4 and CO_2. These data, together with the $\delta^{18}O$ and temperature data for ALMENDRO provide a strong indication that the Almendro cavity is undergoing only limited mass exchange with the surrounding environment. The total organic carbon (TOC) $\delta^{13}C$ value is similar to other wells at the NTS. The isotopic composition of TOC is not being controlled by the same processes as the inorganic carbon. The concentration, however, is high (20 mg/L as C) and may be a carbon source for microbial reactions.

The tritium activity in U-19v PS#1ds groundwater was 1.1×10^8 pCi/L at the time of sampling. The $^{36}Cl/Cl$ ratio in U-19v PS#1ds groundwater (1.88×10^{-9}) is nearly four orders of magnitude above the natural environmental level. $^{36}Cl/Cl$ ratios have remained fairly constant over time. The ALMENDRO samples consistently exhibit the highest $^{129}I/^{127}I$ ratios and highest ^{129}I activity of any near-field wells at the NTS although the low concentration of dissolved iodine and long half-life translates to a fairly low activity (2.58 pCi/L in 2006). The relatively high activity may, in part, result from reducing conditions at this site which promote reduction of slightly sorbing iodate (IO_3^-) to very weakly sorbing iodide (I^-).

The $^{87}Sr/^{86}Sr$ ratio in the ALMENDRO cavity fluid is similar to other volcanic aquifer groundwaters from Pahute Mesa (e.g. Thomas et al., 2002), and is inferred to reflect the equilibration of groundwater with strontium in the aquifer host rocks. The $^{235}U/^{238}U$ ratio (0.00722) indicates the dissolved uranium is natural in origin, and the low $^{234}U/^{238}U$-activity ratio (2.18) implies that ^{234}U and ^{238}U are close to secular equilibrium. The close-to-secular-equilibrium condition is consistent with bulk dissolution of the wall rock and/or melt glass (Paces et al., 2002), and is likely facilitated by the high temperature conditions within the cavity. The lack of measurable enrichment in ^{235}U in the water is probably due to the large amount of natural uranium in the rocks, which masks the small contribution of enriched ^{235}U from the test. The low U concentration overall (30 ppt) may be an indication of reducing conditions, consistent with stable isotope and other data.

ALMENDRO groundwater samples were also analyzed for ^{236}U (which originates *only* from the test). While ^{236}U was not detected in 2003 ($<1.1 \times 10^{-6}$ pCi/L), it was measured in the 2006 sample (3.4×10^{-6} pCi/L) and the 2001 (3.4×10^{-6} pCi/L) sample just above the detection limit. ^{236}U was also measured well above detection limits in the 2000 (1.4×10^{-5} pCi/L) sample. In

2006, a large 4 liter sample was used to reduce our Pu detection limit to 0.004 pCi/L ^{239,240}Pu. The detection limit in the 2003 sample (1 liter sample) was 0.02 pCi/L ^{239,240}Pu. The Pu activity was below detection in both samples. Pu was observed in ALMENDRO fluid samples collected in 1999 (9.5 pCi/L ^{239,240}Pu) and 2001 (0.18 pCi/L ^{239,240}Pu) (Rose et al., 2003). We do not presently have a good explanation for the variability in the Pu data. It is possible that the physiochemical conditions within the ALMENDRO cavity are evolving over time, which may influence (among other things) the redox state of the groundwater. High temperature mineral alteration in the cavity may also provide an overall sink for Pu over time.

1.6 References

Buddemeier, R.W. and Isherwood, D. (1985) Radionuclide Migration Project 1984 Progress Report. Lawrence Livermore National Laboratory, UCRL-53628, Livermore, CA, 71 p.

Craig, H. (1963) The isotopic geochemistry of water and carbon in geothermal areas. In: E. Tongiorgi, ed., *Nuclear Geology on Geothermal Areas*, Spoleto, 9-13 September 1963. Consiglio Nazionale delle Ricerche, Laboratorio di Geologia Nucleare, Pisa, p. 17-53.

Department of Energy (2000). United States Nuclear Tests, July 1945 through September 1992, DOE/NV-209 (Rev. 15).

Fabryka-Martin, J., Wightman, S.J., Murphy, W.J., Wickham, M.P., Caffee, M.W., Nimz, G.J., Southon, J.R., and Sharma, P. (1993) *Distribution of chlorine-36 in the unsaturated zone at Yucca Mt.: An indicator of fast transport paths*. FOCUS '93: Site Characterization and Model Validation, Las Vegas, NV, 26-29 Sept 1993.

LLNL (2004) Analytical Measurements: Standard Operating Procedures, Underground Test Area Project. Chemical Biology and Nuclear Science Division, Lawrence Livermore National Laboratory, 30 June 2004

Paces, J.B., Ludwig, K.R., Peterman, Z.E., and Neymark, L.A. (2002) ^{234}U/^{238}U evidence for local recharge and patterns of groundwater flow in the vicinity of Yucca Mountain, Nevada, USA. Applied Geochemistry, v. 17, p. 751-779

Pawloski, G. A. (1999) Development of Phenomenological Models of Underground Nuclear Tests on Pahute Mesa, Nevada Test Site—BENHAM and TYBO, UCRL-ID-136003, Lawrence Livermore National Laboratory, Livermore.

Pawloski, G.A., Tompson, A.F.B., and Carle, S.F., eds. (2001) Evaluation of the hydrologic source term from underground nuclear tests on Pahute Mesa at the Nevada Test Site: The CHESHIRE test. Lawrence Livermore National Laboratory Report UCRL-ID-147023, May 2001.

Rose, T.P., and Davisson, M.L. (2003) Isotopic and geochemical evidence for Holocene-age groundwater in regional flow systems of south-central Nevada. In: Enzel, Y., Wells., S.G., and Lancaster, N., eds., *Paleoenvironments and Paleohydrology of the Mojave and Southern Great Basin Deserts.* Geological Society of America Special Paper 368, p. 143-164.

Rose, T.P., Eaton, G.F., and Kersting, A.B., eds. (2003) Hydrologic Resources Management Program and Underground Test Area Project FY 2001-2002 Progress Report. Lawrence Livermore National Laboratory Report, UCRL-ID-154357, 135 p

Rose, T.P., Eaton, G.F., and Yamamoto, R.I., eds. (2002) Hydrologic Resources Management Program and Underground Test Area Project FY 2000 Progress Report. Lawrence Livermore National Laboratory Report, UCRL-ID-145167, June 2002, 141 p.

Rose, T.P., Eaton, G.F., and Yamamoto, R.I., eds. (2004) Hydrologic Resources Management Program and Underground Test Area Project FY 2003 Progress Report. Lawrence Livermore National Laboratory Report, UCRL-TR-206661, August 2004, 81 p.

Russell, G.M., and G.L. Locke 1997. Summary of Data Concerning Radiological Contamination at Well PM-2, Nevada Test Site, Nye County, Nevada, Open File Report 96-599, U.S. Geological Survey, Carson City, Nevada.

Sawyer, D.A., Thompson, J.L., and Smith, D.K. (1999) The CHESHIRE migration experiment: A summary report. Los Alamos National Laboratory Report LA-13555-MS, October 1999, 32 p.

SNJV (2006) Geochemical and Isotopic Evaluation of Groundwater Movement in Corrective Action Unit 97: Yucca Flat/Climax Mine, Nevada Test Site, Nevada, S-N/99205—070, Las Vegas, NV

Thomas, J.M., Benedict, F.C., Jr., Rose, T.P., Hershey, R.L., Paces, J.B., Peterman, Z.E., Farnham, I.M., Johannesson, K.H., Singh, A.K., Stetzenbach, K.J., Hudson, G.B., Kenneally, J.M., Eaton, G.F., and Smith, D.K. (2002) Geochemical and isotopic interpretations of groundwater flow in the Oasis Valley flow system, southern Nevada. Desert Research Institute Publication No. 45190, August 2002, 202 p.

Table 1.1 Hotwell Site Information.

Well name	Test Name	Test Date	Latitude	Longitude	Surface Elevation	Well Depth	Open Interval	Water Depth	Sample Method	Volume pumped	Sample Depth	Sample date
Units			*(d m s)*	*(d m s)*	*(ft)*	*(ft bgs)*	*(ft bgs)*	*(ft bgs)*		*(gal)*	*(ft bgs)*	
Hot Wells - Frenchman Flat												
UE5n	CAMBRIC	14-May-65	36 49 34	116 06 59	3112	1690	720-730	---	pump	---	---	12-Feb-04
UE5n	CAMBRIC	14-May-65	36 49 34	116 06 59	3112	1690	720-730	702	pump	---	702	19-Apr-01
UE5n	CAMBRIC	14-May-65	36 49 34	116 06 59	3112	1690	720-730	705	pump	---	730	9-Sep-99
RNM-1	CAMBRIC	14-May-65	36 49 28	115 58 01	3135	1302	919-927 and 938-947 (Zone 5), 984-995 (Zone 4)	789	pump	1.68E+04	---	3-Jun-04
RNM-1	CAMBRIC	14-May-65	36 49 28	115 58 01	3135	1302	919-927 and 938-947 (Zone 5), 984-995 (Zone 4)	789	pump	---	---	28-Jun-00
RNM-2S	CAMBRIC	14-May-65	36 49 21	115 58 01	3133	1120	1038-1119	725	pump	6.39E+07	---	10-Jul-03
RNM-2S	CAMBRIC	14-May-65	36 49 21	115 58 01	3133	1120	1038-1119	725	pump	1.00E+07	---	9-May-03
RNM-2S	CAMBRIC	14-May-65	36 49 21	115 58 01	3133	1120	1038-1119	725	pump	---	---	14-Jun-00
RNM-2S	CAMBRIC	14-May-65	36 49 21	115 58 01	3133	1120	1038-1119	725	pump	---	800	11-Oct-99
Hot Wells - Yucca Flat												
U4u PS2a	DALHART	13-Oct-88	37 05 13	116 02 51	4117	2280	1548-1644	1636	pump	7.06E+03	---	9-Oct-03
U4u PS2a	DALHART	13-Oct-88	37 05 13	116 02 51	4117	2280	1548-1644	1636	pump	---	1640	16-Aug-99
UE-7ns	BOURBON	20-Jan-67	37 05 56	116 00 09	4369	2205	1995-2199	1969	bailer	---	2025	13-Dec-05
UE-7ns	BOURBON	20-Jan-67	37 05 56	116 00 09	4369	2205	1995-2199	1969	bailer	---	2025	21-Aug-01
UE-2ce	NASH	19-Jan-67	37 08 31	116 08 07	4764	1650	1385-1624	1448	bailer	---	1580	12-Jul-05
UE-2ce	NASH	19-Jan-67	37 08 31	116 08 07	4764	1650	1385-1624	1470	bailer	---	1550	22-Aug-01
U-3cn PS#2	BILBY	13-Sep-63	37 03 38	116 01 19	3994	2603	1680-1729	1550	pump	1.51E+04	1652-1656	9-Dec-04
U-3cn PS#2	BILBY	13-Sep-63	37 03 38	116 01 19	3994	2603	1680-1729	1550	pump	---	1652-1656	18-Dec-01
Hot Wells - Pahute Mesa												
U20n PS1 DDh	CHESHIRE	14-Feb-76	37 14 25	116 25 24	6468	4253	4100-4110	---	pump	2.30E+04		15-Nov-05
U20n PS1 DDh	CHESHIRE	14-Feb-76	37 14 25	116 25 24	6468	4253	4100-4110	2051	pump	---	4100	9-Jul-03
U20n PS1 DDh	CHESHIRE	14-Feb-76	37 14 25	116 25 24	6468	4253	4100-4110	2051	pump	---	4100	12-Oct-99
U19ad PS1A	CHANCELLOR	1-Sep-83	37 16 13	116 21 17	6656	2609*	2407-2579*	2240*	pump	2.04E+05	2370*	27-Sep-04
U19q PS1d	CAMEMBERT	26-Jun-75	37 16 49	116 21 54	6740	4991*	3665-3678*	2185*	pump	---	3000*	16-Jul-03
U19q PS1d	CAMEMBERT	26-Jun-75	37 16 49	116 21 54	6740	4991*	3665-3678*	2185*	pump	1.47E+04	3000*	21-Oct-98
U19v PS1ds	ALMENDRO	6-Jun-73	37 14 53	116 20 57	6842	3837*	4,100-4,110	2342*	bailer	---	3300	18-Apr-06
U19v PS1ds	ALMENDRO	6-Jun-73	37 14 53	116 20 57	6842	3837*	---	---	bailer	---	3300	23-Jul-03
U19v PS1ds	ALMENDRO	6-Jun-73	37 14 53	116 20 57	6842	3837*	---	2187*	bailer	---	3300	31-May-01
U19v PS1ds	ALMENDRO	6-Jun-73	37 14 53	116 20 57	6842	3837*	---	2170*	bailer	---	3300	26-Sep-00
U19v PS1ds	ALMENDRO	6-Jun-73	37 14 53	116 20 57	6842	3837*	---	2170*	bailer	---	3204	18-Aug-99
ER-20-5 #1	TYBO/BENHAM†	14-May-75	31 13 12	116 28 38	6242	2823	2301-2573	2055	pump	---	2300-2572	30-Nov-04
ER-20-5 #1	TYBO/BENHAM†	14-May-75	31 13 12	116 28 38	6242	2823	2301-2573	2055	pump	---	2300-2572	9-Jul-98
ER-20-5 #3	TYBO/BENHAM†	14-May-75	37 13 11	116 28 38	6242	4294	3430-3882	2060	pump	---	3383-3405	29-Nov-04
ER-20-5 #3	TYBO/BENHAM†	14-May-75	37 13 11	116 28 38	6242	4294	3430-3882	2060	pump	---	3383-3405	15-Nov-01
ER-20-5 #3	TYBO/BENHAM†	14-May-75	37 13 11	116 28 38	6242	4294	3430-3882	2060	pump	---	3383-3405	30-Apr-98
PM-2	SCHOONER	8-Dec-68	37 34 50	116 56 81	5586	8781	2507-8781	861	bailer	---	865	26-Oct-05
PM-2	SCHOONER	8-Dec-68	37 34 50	116 56 81	5586	8781	2507-8781	861	bailer	---	985	26-Oct-05
PM-2	SCHOONER	8-Dec-68	37 34 50	116 56 81	5586	8781	2507-8781	861	bailer	---	1970	26-Oct-05
PM-2	SCHOONER	8-Dec-68	37 34 50	116 56 81	5586	8781	2507-8781	861	bailer	---	2625-1300	26-Oct-05

*reported values are measured depths along a slanted borehole. Approximate slant angles: RNM-1(21˚); U19ad PS1A (22˚); U19v PS1ds (20.6˚); U19q PS1d (unknown)

† Both the TYBO and BENHAM tests are listed since the ER-20-5 well cluster was drilled in the near-field (~300 m from the surface ground zero) environment of the TYBO test. Test date is reflective of the TYBO test.

Table 1.2 Field parameter and anion data.

Well name	Test	Sample date	pH	T	Cond.	F	Cl	Br	NO_2	NO_3	SO_4	Na	K	Ca	Mg	Li
Units		*date*		*(°C)*	*(µS/cm)*	*(mg/L)*	*(mg/L)*	*(mg/L)*	*(mg/L)*	*(mg/L)*	*(mg/L)*	*(mg/L)*	*(mg/L)*	*(mg/L)*	*(mg/L)*	*(mg/L)*
Hot Wells - Frenchman Flat																
UE5n	CAMBRIC	12-Feb-04	8.2*	---	452*	0.7	11.7	0.1	---	6.0	31.9	86.7	7.7	8.3	2.2	<0.01
UE5n	CAMBRIC	19-Apr-01	8.7	23.0	408	0.7	12.9	<0.1	---	6.7	32.0	76.0	8.0	8.6	2.0	0.02
UE5n	CAMBRIC	9-Sep-99	8.4	26.5	453	0.8	12.0	<0.03	---	8.1	31.8	86.0	8.0	7.5	2.0	<0.05
RNM-1	CAMBRIC	3-Jun-04	7.8*	---	432*	0.4	9.7	0.1	---	13.4	34.7	45.5	7.5	26.8	10.4	0.03
RNM-1	CAMBRIC	28-Jun-00	8.0	26.0	416	0.3	12.3	0.2	---	16.2	36.5	44.0	8.0	26.0	9.4	0.03
RNM-2S	CAMBRIC	10-Jul-03	8.0	24.4	418	0.5	13.5	0.6	---	12.6	38.0	56.7	7.8	15.1	5.7	0.02
RNM-2S	CAMBRIC	9-May-03	8.2	24.0	450	0.5	13.6	0.6	---	12.5	38.0	57.2	7.9	16.3	5.9	0.02
RNM-2S	CAMBRIC	14-Jun-00	7.8*	---	429*	0.4	14.8	0.2	---	14.3	36.8	62.0	9.7	18.0	5.2	0.02
RNM-2S	CAMBRIC	11-Oct-99	8.2	24.6	440	0.6	13.7	<0.03	---	13.9	37.0	63.0	9.2	17.0	5.6	<0.05
Hot Wells - Yucca Flat																
U4u PS2a	DALHART	9-Oct-03	6.7	---	385	1.6	5.1	<0.03	---	2.5	12.3	87.0	22.1	12.7	1.2	0.02
U4u PS2a	DALHART	16-Aug-99	8.2*	---	352*	0.7	5.8	<0.03	---	18.5	12.0	72.0	14.0	13.1	2.7	0.14
UE-7ns	BOURBON	13-Dec-05	6.5	---	380	1.2	26.9	<0.01	---	0.2	1.4	50.6§	4.4§	18.8§	3.2§	0.05§
UE-7ns	BOURBON	21-Aug-01	8.0*	---	375*	0.8	22.9	<0.1	---	<0.09	1.6	67.4	4.9	20.9	3.6	0.06
UE-2ce	NASH	12-Jul-05	7.3	---	466	1.1	14.2	<0.02	---	1.6	16.6	38.1	17.6	46.0	24.9	0.08
UE-2ce	NASH	22-Aug-01	7.9*	---	435*	0.3	15.5	<0.1	---	<0.09	11.1	45.6	21.8	49.1	25.4	0.10
U-3cn PS#2	BILBY	9-Dec-04	8.1*	---	528	1.38	17.3	1.0	---	7.2	19.2	89.4	15.3	11.9	3.3	0.02
U-3cn PS#2	BILBY	18-Dec-01	8.1*	---	490*	0.8	8.6	0.6	---	5.8	20.3	98.4	18.3	14.4	3.3	0.05
Hot Wells - Pahute Mesa																
U20n PS1 DDh	CHESHIRE	15-Nov-05	8.3	27.6	340	4.4	12.0	<0.01	---	1.4	33.2	62.4	1.7	2.0	0.1	0.06
U20n PS1 DDh	CHESHIRE	9-Jul-03	8.5	38.4	330	3.6	10.9	0.6	---	1.9	27.9	60.7	1.9	3.8	0.1	0.06
U20n PS1 DDh	CHESHIRE	12-Oct-99	8.2	38.2	324	3.6	11.1	<0.03	---	2.3	28.2	65.0	2.2	4.7	0.1	<0.05
U19ad PS1A	CHANCELLOR	27-Sep-04	9.4	47.0	941	36.0	43.5	<0.02	---	3.0	106.4	156.2	6.6	0.8	0.0	0.73
U19q PS1d	CAMEMBERT	16-Jul-03	---	---	---	15.5	7.2	<0.03	---	0.5	20.8	199.0	9.0	5.0	0.2	0.49
U19q PS1d	CAMEMBERT	21-Oct-98	7.2	33.0	959	31.5	10.4	<0.1	---	<0.07	29.7	342.0	10.3	3.2	0.0	1.06
U19v PS1ds	ALMENDRO	18-Apr-06	9.8	26.7	797	9.6	75.7	<0.2	<0.2	<0.2	4.3	151§	13§	0.25§	0.04§	---
U19v PS1ds	ALMENDRO	23-Jul-03	9.3	35.7	517	8.9	53.2	0.1	---	0.7	0.8	140.0	8.8	1.0	0.1	0.17
U19v PS1ds	ALMENDRO	31-May-01	---	---	---	9.7	66.5	<0.1	---	<0.09	2.5	173.0	14.0	1.5	0.2	0.28
U19v PS1ds	ALMENDRO	26-Sep-00	9.3*	---	742*	9.5	48.2	<0.1	---	<0.09	3.8	131.0	11.6	0.7	0.1	0.24
U19v PS1ds	ALMENDRO	18-Aug-99	8.2*	---	728*	9.9	40.5	<0.03	---	<0.02	3.9	162.0	9.8	0.9	0.2	0.42
ER-20-5 #1	TYBO/BENHAM†	30-Nov-04	8.1*	---	545*	10.8	24.7	0.1	---	1.8	43.2	117.5	4.6	6.2	0.1	<0.01
ER-20-5 #1	TYBO/BENHAM†	9-Jul-98	8.1	32.3	510	9.6	24.5	<0.04	---	1.4	40.4	106.0	5.7	7.2	0.4	0.09
ER-20-5 #3	TYBO/BENHAM†	29-Nov-04	8.2*	---	376*	4.1	17.4	0.1	---	1.7	35.3	80.4	3.5	3.5	<0.04	<0.01
ER-20-5 #3	TYBO/BENHAM†	15-Nov-01	8.0*	---	345*	3.6	18.9	0.8	---	2.6	35.3	87.1	3.3	4.4	0.1	0.07
ER-20-5 #3	TYBO/BENHAM†	30-Apr-98	8.2	35.3	335	3.2	17.3	<0.02	---	1.2	33.3	68.0	2.1	1.8	0.1	0.07
PM-2, 865	SCHOONER	26-Oct-05	---	---	---	0.88	10.5	<0.01	---	0.62	1.85	120	4.3	1.9	0.46	0.03
PM-2, 985	SCHOONER	26-Oct-05	---	---	---	1.02	10.6	<0.01	---	0.15	1.65	124	4.6	1.3	0.39	0.03
PM-2, 1970, main	SCHOONER	26-Oct-05	7.9	---	813	2.14	19.7	<0.01	---	0.25	0.35	264	4.8	0.6	0.20	0.05
PM-2, 2625-1300	SCHOONER	26-Oct-05	---	---	---	<0.03	69.9	0.35	---	0.43	0.37	1080	9.8	0.3	0.15	0.15

* pH and conductivity values marked with an asterisk are laboratory measurements

† Both the TYBO and BENHAM tests are listed since the ER-20-5 well cluster was drilled in the near-field (~300 m from the surface ground zero) environment of the TYBO test.

§ Analyses performed by ICPMS

Table 1.3 Cations and metals data.

Well name	Test	Sample date	Al	Si	Fe	Be	B	Ti	Mn	As	Se	Sr	Mo	Sb	I	Ba	Pb	U	Pu, total
Unit			*(mg/L)*	*(mg/L)*	*(mg/L)*	*(mg/L)*	*(mg/L)*	*(mg/L)*	*(mg/L)*	*(mg/L)*	*(mg/L)*	*(mg/L)*	*(mg/L)*	*(mg/L)*	*(mg/L)*	*(mg/L)*	*(mg/L)*	*(mg/L)*	*(pg/L)*
Hot Wells - Frenchman Flat																			
UE5n	CAMBRIC	12-Feb-04	0.0207	41.3	1.08	0.3	---	2.8	44	11.9	1.5	28	6.1	0.39	19.0	4.7	2.8	4.45	<0.2
UE5n	CAMBRIC	19-Apr-01	<0.05	27.4	<0.04	---	---	---	<6	22	---	22	4	---	20.3	21	---	0.41	---
UE5n	CAMBRIC	9-Sep-99	<0.02	---	0.06	---	0.3	---	10	9	<2	50	5	---	30.0	<5	0.37	4.00	---
RNM-1	CAMBRIC	3-Jun-04	0.005367	50.5	0.003	0.1	---	2.2	9.9	9.7	1.6	166	4.4	0.18	16.2	19.3	3.4	3.84	0.17
RNM-1	CAMBRIC	28-Jun-00	0.4	20	0.18	0.1	---	4.2	<6	9.8	1.5	300	5.1	0.15	17.9	18.5	0.01	3.97	---
RNM-2S	CAMBRIC	10-Jul-03	<0.05	37.2	<0.04	---	0.9	---	<6	<20	<24	102	<3	---	12.2	6	<14	4.91	<0.2
RNM-2S	CAMBRIC	9-May-03	<0.05	35.5	<0.04	---	1.0	---	<6	27	<24	101	<3	---	12.1	5	<14	4.93	<0.2
RNM-2S	CAMBRIC	14-Jun-00	0.4	35	0.18	0.0	---	3.6	<6	10.5	1.6	140	4.4	0.14	12.0	17.3	<0.01	5.00	---
RNM-2S	CAMBRIC	11-Oct-99	<0.02	32	0.01	---	0.2	---	<2	5	<2	110	3	---	11.0	<5	0.24	4.00	---
Hot Wells - Yucca Flat																			
U4u PS2a	DALHART	9-Oct-03	10.7	61.6	1.99	0.6	---	112	125	13.9	0.9	25	5.1	0.54	7.1	27.3	17.6	7.43	5.0
U4u PS2a	DALHART	16-Aug-99	12.0	37	1.30	---	0.1	---	90	4	<1	30	<1	---	3.1	30	8.6	4.20	8.7
UE-7ns	BOURBON	13-Dec-05	0.0053	5.9	2	<0.006	0.2	<2.9	45.2	5.6	< 0.27	103	19.2	< 0.3	44.6	59.8	22.25	0.06	<0.15
UE-7ns	BOURBON	21-Aug-01	<0.05	10.0	0.21	---	---	---	55	21	<24	70	26	---	19.2	77	<14	0.04	<0.6
UE-2ce	NASH	12-Jul-05	0.0	13	12	<0.33	0.2	< 5.1	199.6	5.5	< 0.6	194	8.9	1.09	4.0	22.5	551	2.00	<1
UE-2ce	NASH	22-Aug-01	<0.05	22.2	0.11	---	---	---	66	<20	<24	160	17	---	7.4	47	<14	0.39	<0.6
U-3cn PS#2	BILBY	9-Dec-04	1.23	46.9	4.23	0.1	---	12.0	173	5.6	1.5	21	7.2	0.88	9.5	18.7	104	10.31	---
U-3cn PS#2	BILBY	18-Dec-01	0.3	28.7	0.30	---	---	---	78	<20	<24	24	3.5	---	9.1	4	<14	10.67	<0.6
Hot Wells - Pahute Mesa																			
U20n PS1 DDh	CHESHIRE	15-Nov-05	0.6	11.3	4.53	< 0.45	0.1	< 5.7	187	7.9	< 0.9	10	11.8	0.54	4.2	16.5	2.86	0.36	6.0
U20n PS1 DDh	CHESHIRE	9-Jul-03	0.7	30.9	0.81	---	1.0	---	170	<20	<24	12	9.1	---	2.0	3	<14	2.07	4.1
U20n PS1 DDh	CHESHIRE	12-Oct-99	0.1	24	1.4	---	0.1	---	110	3	<2	10	10	---	13.0	<5	0.67	2.30	7.0
U19ad PS1A	CHANCELLOR	27-Sep-04	9.69	115.3	2.02	1.9	---	170	357	232	2.4	17	1024	30.6	19.4	72.9	21.8	2.60	369.9
U19q PS1d	CAMEMBERT	16-Jul-03	50	20.2	11.53	1.5	---	153	586	14.6	0.3	7.9	40.7	0.89	4.0	9.7	16.4	2.61	<0.2
U19q PS1d	CAMEMBERT	21-Oct-98	70	32	5.77	---	0.9	---	530	4	<3	<0.01	40	---	10.0	<10	0.60	<0.5	---
U19v PS1ds	ALMENDRO	18-Apr-06	0.112	---	2.202	< 0.18	---	---	33.4	228.2	< 0.27	75.3	1298	49	20.3	50.5	11	0.03	<0.06
U19v PS1ds	ALMENDRO	23-Jul-03	0.04	22.8	10.6	0.1		3.3	160	341	0.08	18	2059	250	10.1	60	82	0.11	<0.2
U19v PS1ds	ALMENDRO	31-May-01	0.3	2.0	3.7	---	---	---	330	140	<24	44	1200	---	13.7	60	250	0.03	2.1
U19v PS1ds	ALMENDRO	26-Sep-00	0.3	6.6	0.19	---	---	---	---	50	<24	---	1100	---	11.4	20	22	0.02	---
U19v PS1ds	ALMENDRO	18-Aug-99	0.5	11	12.0	---	1.5	---	250	1716	8	40	1226	---	7.4	70	63	<0.5	58.2
ER-20-5 #1	TYBO/BENHAM†	30-Nov-04	6.53	67.9	0.40	2.3	---	28.3	22	10.3	0.9	21	40.2	1.30	5.4	13.3	9.1	14.09	6.4
ER-20-5 #1	TYBO/BENHAM†	9-Jul-98	5.76	48.4	1.32	---	0.3	---	50	3.1	<3	20	0.03	---	7.0	<10	2.9	15.00	---
ER-20-5 #3	TYBO/BENHAM†	29-Nov-04	8.53	54.6	2.24	4.6	---	95.5	129	14.4	0.9	30	10.4	0.46	4.7	28.8	18.2	5.64	0.6
ER-20-5 #3	TYBO/BENHAM†	15-Nov-01	3.60	29	1.9	---	---	---	75	23	<24	31	5.8	---	5.8	17	<14	12.80	<0.6
ER-20-5 #3	TYBO/BENHAM†	30-Apr-98	1.03	24	0.46	---	0.1	---	20	4.8	<3	7	<0.01	---	8.0	<10	0.9	2.70	---
PM-2, 865	SCHOONER	26-Oct-05	---	---	---	---	---	---	---	---	---	---	---	---	---	---	---	---	---
PM-2, 985	SCHOONER	26-Oct-05	---	---	---	---	---	---	---	---	---	---	---	---	4.65	---	---	---	<0.06
PM-2, 1970, main	SCHOONER	26-Oct-05	0.03	3	1.03	<0.54	0.2	14.3	26.2	4.8	< 0.9	4360	55.8	0.34	8.39	573	60.7	0.24	0.2*
PM-2, 2625-1300	SCHOONER	26-Oct-05	---	---	---	---	---	---	---	---	---	---	---	---	---	---	---	---	0.1

† Both the TYBO and BENHAM tests are listed since the ER-20-5 well cluster was drilled in the near-field (~300 m from the surface ground zero) environment of the TYBO test.
* Pu value is probably the result of contamination.

Table 1.4 Trace metal data.

Well name	Test	Sample date	V	Cr	Co	Ni	Cu	Zn	Br	Rb	Nb	Tc	Ru	Ag	Cd	Sn	Cs	Eu	W	Hg	Tl
Unit			*(mg/L)*	*(mg/L)*	*(mg/L)*	*(mg/L)*	*(mg/L)*	*(mg/L)*	*(mg/L)*	*(mg/L)*	*(mg/L)*	*(ng/L)*	*(mg/L)*	*(mg/L)*	*(mg/L)*	*(mg/L)*	*(mg/L)*	*(mg/L)*	*(mg/L)*	*(mg/L)*	*(mg/L)*
Hot Wells - Frenchman Flat																					
UE5n	CAMBRIC	12-Feb-04	15.5	1.29	0.17	0.65	BD*	37.0	129	8.4	0.22	3.3E-04	0.078	0.73	0.09	0.83	0.09	0.05	1.7	42.7	0.25
UE5n	CAMBRIC	19-Apr-01	---	---	---	---	---	---	---	---	---	---	---	---	---	---	---	---	---	---	---
UE5n	CAMBRIC	9-Sep-99	---	---	---	---	---	---	---	---	---	1.3E-04	---	---	---	---	---	---	---	---	---
RNM-1	CAMBRIC	3-Jun-04	12.6	1.89	0.08	3.24	BD*	21.5	119	8.1	0.08	< 2E-04	0.019	0.19	0.04	1.05	0.05	0.02	1.1	25.7	0.15
RNM-1	CAMBRIC	28-Jun-00	12.8	2.15	0.05	1.95	BD*	BD*	123	8.3	0.15	---	0.007	0.06	0.01	0.06	0.02	BD	0.86	12.3	0.06
RNM-2S	CAMBRIC	10-Jul-03	---	---	---	---	---	---	---	---	---	8.9E-05	---	---	---	---	---	---	---	---	---
RNM-2S	CAMBRIC	9-May-03	---	---	---	---	---	---	---	---	---	---	---	---	---	---	---	---	---	---	---
RNM-2S	CAMBRIC	14-Jun-00	15.8	3.58	0.08	0.75	BD*	BD*	139	10	0.10	---	0.003	0.02	0.01	0.02	0.03	BD*	0.83	8.4	0.04
RNM-2S	CAMBRIC	11-Oct-99	---	---	---	---	---	---	---	---	---	7.6E-05	---	---	---	---	---	---	---	---	---
Hot Wells - Yucca Flat																					
U4u PS2a	DALHART	9-Oct-03	7.0	3.02	0.18	0.99	BD*	38.8	50	46	4.25	2.1	0.004	0.08	0.07	0.20	1.47	0.05	0.64	6.5	0.25
U4u PS2a	DALHART	16-Aug-99	---	---	---	---	---	---	---	---	---	7.7E-01	---	---	---	---	---	---	---	---	---
UE-7ns	BOURBON	13-Dec-05	<0.9	< 0.51	< 0.12	< 1.2	< 1.2	219	---	6	< 0.18	---	< 0.39	< 0.33	< 0.42	---	< 0.99	< 0.018	0.1	---	< 0.012
UE-7ns	BOURBON	21-Aug-01	---	---	---	---	---	---	---	---	---	---	---	---	---	---	---	---	---	---	---
UE-2ce	NASH	12-Jul-05	< 0.9	3.4	1.43	9	38.8	488	---	39.7	< 0.09	---	< 0.42	< 0.21	< 0.6	---	< 0.6	< 0.012	< 0.036	---	< 0.035
UE-2ce	NASH	22-Aug-01	---	---	---	---	---	---	---	---	---	---	---	---	---	---	---	---	---	---	---
U-3cn PS#2	BILBY	9-Dec-04	5.8	1.55	0.43	11.6	BD*	126	68	51	0.15	3.7	BD*	0.09	0.92	0.06	0.40	BD*	0.90	4.7	0.05
U-3cn PS#2	BILBY	18-Dec-01	---	---	---	---	---	---	---	---	---	4.8	---	---	---	---	---	---	---	---	---
Hot Wells - Pahute Mesa																					
U20n PS1 DDh	CHESHIRE	15-Nov-05	1.6	<0.48	<0.2	4.7	4.9	286	---	8	< 0.12	5.4E-02	< 0.45	< 0.33	< 0.54	---	1.17	< 0.006	4.2	---	< 0.012
U20n PS1 DDh	CHESHIRE	9-Jul-03	---	---	---	---	---	---	---	---	---	7.2E-01	---	---	---	---	---	---	---	---	---
U20n PS1 DDh	CHESHIRE	12-Oct-99	---	---	---	---	---	---	---	---	---	1.3	---	---	---	---	---	---	---	---	---
U19ad PS1A	CHANCELLOR	27-Sep-04	101	0.44	0.19	1.42	BD*	42.3	158	80	9.10	2.7	0.003	0.20	0.58	0.69	11.7	0.44	334	6.1	0.26
U19q PS1d	CAMEMBERT	16-Jul-03	1.5	3.86	0.66	50.1	BD*	336	56	57	3.95	---	0.002	0.15	0.12	1.61	3.69	0.01	7.0	3.3	0.13
U19q PS1d	CAMEMBERT	21-Oct-98	---	---	---	---	---	---	---	---	---	4.9E-03	---	---	---	---	---	---	---	---	---
U19v PS1ds	ALMENDRO	18-Apr-06	0.87	1.93	0.94	< 1.8	5.1	304	---	39.3	< 0.036	5.8E-03	< 0.36	< 0.12	1.4	< 0.18	2.51	< 0.018	94.3	---	0.03
U19v PS1ds	ALMENDRO	23-Jul-03	1.4	0.09	0.37	1.63	BD*	65.6	127	66	0.25	---	0.005	6.47	0.78	0.02	1.24	BD	177	4.7	0.004
U19v PS1ds	ALMENDRO	31-May-01	---	---	---	---	---	---	---	---	---	---	---	---	---	---	---	---	---	---	---
U19v PS1ds	ALMENDRO	26-Sep-00	---	---	---	---	---	---	---	---	---	---	---	---	---	---	---	---	---	---	---
U19v PS1ds	ALMENDRO	18-Aug-99	---	---	---	---	---	---	---	---	---	---	---	---	---	---	---	---	---	---	---
ER-20-5 #1	TYBO/BENHAM†	30-Nov-04	3.2	0.98	0.11	61.5	BD*	42.0	134	27	1.24	2.0E-02	0.002	0.09	0.05	0.16	2.86	0.004	2.0	2.0	0.03
ER-20-5 #1	TYBO/BENHAM†	9-Jul-98	---	---	---	<0.01	---	---	---	---	---	1.6E-02	---	---	---	---	---	---	---	---	---
ER-20-5 #3	TYBO/BENHAM†	29-Nov-04	6.1	1.94	0.38	68.9	BD*	54.4	102	38	4.89	9.9E-04	0.001	0.12	0.20	0.56	2.74	0.03	13.1	2.2	0.19
ER-20-5 #3	TYBO/BENHAM†	15-Nov-01	---	---	---		---	---	---	---	---	---	---	---	---	---	---	---	---	---	---
ER-20-5 #3	TYBO/BENHAM†	30-Apr-98	---	---	---	<0.01	---	---	---	---	---		---	---	---	---	---	---	---	---	---
PM-2, 865	SCHNOONER	26-Oct-05	---	---	---	---	---	---	---	---	---	---	---	---	---	---	---	---	---	---	---
PM-2, 985	SCHNOONER	26-Oct-05	---	---	---	---	---	---	---	---	---	---	---	---	---	---	---	---	---	---	---
PM-2, 1970, main	SCHNOONER	26-Oct-05	3.7	3.3	< 0.12	< 3.6	6	322	---	15.1	< 0.12	---	< 0.6	< 0.18	< 0.51	---	5.5	< 0.044	57.5	---	< 0.024
PM-2, 2625-1300	SCHNOONER	26-Oct-05	---	---	---	---	---	---	---	---	---	---	---	---	---	---	---	---	---	---	---

† Both the Tybo and Benham tests are listed since the ER-20-5 well cluster was drilled in the near-field (~300 m from the surface ground zero) environment of the Tybo test.
* BD is below detection limit.

Table 1.5 Stable Isotope data.

Well name	Test	Sample date	dD_{SMOW}	$d^{18}O_{SMOW}$	TIC	TOC	$d^{13}C_{PDB}$ TIC	$d^{13}C_{PDB}$ TOC	^3He	^4He	R/R_a	Ne total	Ar total	Xe total	$^{87}Sr/^{86}Sr$	$d^{87}Sr$
			‰	‰	ppm C	ppm C	‰	‰	atoms/g	atoms/g	$^3He/^4He$ sample/air	atoms/g	atoms/g	atoms/g	ratio	‰
Hot Wells - Frenchman Flat																
UE5n	CAMBRIC	12-Feb-04	-105	-13.5	35	---	-8.0	---	---	---	---	---	---	---	0.70871	-0.69
UE5n	CAMBRIC	19-Apr-01	-105	-13.4	32	---	-6.7	---	2.70E+09	2.34E+12	8.36E+02	5.15E+12	8.33E+15	2.78E+11	0.71039	1.68
UE5n	CAMBRIC	9-Sep-99	-106	-13.4	36	---	-8.3	---	1.95E+09	3.16E+12	4.48E+02	8.01E+12	1.04E+16	2.90E+11	---	---
RNM-1	CAMBRIC	3-Jun-04	-104	-12.8	33	---	-8.5	---	---	---	---	---	---	---	0.70772	-2.09
RNM-1	CAMBRIC	28-Jun-00	-104	-12.7	---	---	---	---	1.43E+09	2.05E+12	5.05E+02	4.58E+12	7.66E+15	---	---	---
RNM-2S	CAMBRIC	10-Jul-03	-105	-13.1	33	---	-9.5	---	4.29E+10	1.94E+13	1.60E+03	7.17E+13	---	8.85E+11	0.71049	1.82
RNM-2S	CAMBRIC	9-May-03	-105	-13.1	30	---	-8.2	---	2.53E+10	2.77E+12	6.62E+03	3.34E+12	---	3.29E+11	0.71051	1.85
RNM-2S	CAMBRIC	14-Jun-00	-105	-13.0	26	---	-5.3	---	2.50E+10	6.43E+12	2.84E+03	6.08E+12	9.15E+15	---	---	---
RNM-2S	CAMBRIC	11-Oct-99	-104	-12.9	33	---	-9.3	---	2.35E+10	6.40E+12	2.65E+03	4.81E+12	8.08E+15	---	---	---
Hot Wells - Yucca Flat																
U4u PS2a	DALHART	9-Oct-03	-104.5	-13.5	34	---	-9.4	---	5.56E+11	5.57E+12	7.23E+04	1.33E+13	---	2.63E+11	0.71275	5.01
U4u PS2a	DALHART	16-Aug-99	-100	-12.8	31	---	-8.7	---	---	---	---	---	---	---	---	---
UE-7ns	BOURBON	13-Dec-05	-105	-14.1	40	---	-5.3	---	---	---	---	---	---	---	0.71263	4.84
UE-7ns	BOURBON	21-Aug-01	-106	-14.0	33	---	-2.0	---	1.93E+10	2.45E+12	5.71E+03	7.21E+12	9.34E+15	2.68E+11	---	---
UE-2ce	NASH	12-Jul-05	-98	-12.6	66	---	-6.6	---	---	---	---	---	---	---	0.71137	3.06
UE-2ce	NASH	22-Aug-01	-100	-12.9	61	---	-5.3	---	4.78E+09	2.36E+12	1.47E+03	7.89E+12	9.35E+15	2.66E+11	---	---
U-3cn PS#2	BILBY	9-Dec-04	-110	-13.9	53	---	-7.0	---	---	---	---	---	---	---	0.70984	0.9
U-3cn PS#2	BILBY	18-Dec-01	-108	-13.9	56	---	-3.8	---	5.98E+11	3.59E+12	1.21E+05	8.19E+12	9.34E+15	2.44E+11	0.70974	0.76
Hot Wells - Pahute Mesa																
U20n PS1 DDh	CHESHIRE	15-Nov-05	-114	-14.9	18	---	-6.4	---	---	---	---	---	---	---	0.71102	2.57
U20n PS1 DDh	CHESHIRE	9-Jul-03	-114	-15.0	18	---	-4.0	---	2.12E+12	1.02E+13	1.51E+05	5.63E+12	---	3.02E+11	0.71088	2.37
U20n PS1 DDh	CHESHIRE	12-Oct-99	-113	-15.0	21	---	-6.0	---	2.01E+12	1.01E+13	1.44E+05	6.30E+12	6.48E+15	---	0.71078	2.23
U19ad PS1a	CHANCELLOR	27-Sep-04	-112	-14.7	22	---	-8.6	---	---	---	---	---	---	---	0.71049	1.82
U19q PS1d	CAMEMBERT	16-Jul-03	-114	-15.0	98	---	+0.5	---	---	---	---	---	---	---	0.71190	3.81
U19q PS1d	CAMEMBERT	21-Oct-98	-113	-14.6	200	---	+1.5	---	2.02E+12	1.85E+14	7.90E+03	8.54E+12	---	---	0.71260	4.79
U19v PS1ds	ALMENDRO	18-Apr-06	-113	-13.7	41	20.0	+35.9	-24.5	---	---	---	---	---	---	0.70790	-1.83
U19v PS1ds	ALMENDRO	23-Jul-03	-112	-13.4	41	---	+35.4	---	7.64E+10	9.52E+11	5.82E+04	5.74E+12	---	4.12E+11	0.71113	2.72
U19v PS1ds	ALMENDRO	31-May-01	-112	-13.3	49	---	+30.1	---	3.75E+11	1.50E+12	1.81E+05	4.89E+12	1.45E+16	9.41E+11	---	---
U19v PS1ds	ALMENDRO	26-Sep-00	-111	-13.4	52	---	+30.2	---	---	---	---	---	---		---	---
U19v PS1ds	ALMENDRO	18-Aug-99	-111	-13.4	24	---	+45.0	---	---	---	---	---	---		---	---
ER-20-5 #1	TYBO/BENHAM†	30-Nov-04	-115	-14.9	38	---	-4.7	---	---	---	---	---	---	---	0.71047	7.79
ER-20-5 #1	TYBO/BENHAM†	9-Jul-98			36	---	-2.48	---	4.15E+12	2.64E+13	1.14E+05		---	---	---	2.59
ER-20-5 #3	TYBO/BENHAM†	29-Nov-04	-114	-15.1	27	---	-9.3	---	---	---	---	---	---	---	0.70841	-1.11
ER-20-5 #3	TYBO/BENHAM†	15-Nov-01	-114	-15.0	22	---	-4.0	---	8.09E+09	7.48E+12	7.84E+02	8.28E+12	---	2.76E+11	0.70864	-0.79
ER-20-5 #3	TYBO/BENHAM†	30-Apr-98	---	---	21	---	-5.6	---	1.21E+10	1.21E+13	7.23E+02	1.18E+13	---	---	---	-0.73
PM-2, 865	SCHOONER	26-Oct-05	-80	-11.1	---	---	---	---	---	---	---	---	---	---	---	---
PM-2, 985	SCHOONER	26-Oct-05	-80	-11.1	58	---	-12.2	---	---	---	---	---	---	---	---	---
PM-2, 1970, main	SCHOONER	26-Oct-05	-83	-11.4	105	---	-6.3	---	---	---	---	---	---	---	0.70759	-2.27
PM-2, 2625-1300	SCHOONER	26-Oct-05	-105	-13.6	441	---	-1.6	---	---	---	---	---	---	---	---	---

† Both the Tybo and Benham tests are listed since the ER-20-5 well cluster was drilled in the near-field (~300 m from the surface ground zero) environment of the Tybo test.

Table 1.6 Radiochemical data.

Well name	Test	Sample date	^{3}H	^{3}H	^{14}C	^{14}C	$^{36}Cl/Cl$	^{36}Cl	^{85}Kr	^{99}Tc	$^{129}I/^{127}I$	^{129}I
Unit		date	(pCi/L)	(pCi/L)	(pmc)	(pCi/L)	ratio	(pCi/L)	(pCi/L)	(pCi/L)	ratio	(pCi/L)
Half-life (a)		collected	12.32	12.32	5730	5730		3.01E+05	10.73	2.13E+05		1.57E+07
Ref. date		in field	collect.	time zero	collect.	collect.		collect.	collect.	collect.		collect.
Hot Wells - Frenchman Flat												
UE5n	CAMBRIC	12-Feb-04	1.5E+05	1.3E+06	1.66E+01	3.55E-02	6.49E-10	2.51E-01	---	5.6E-03	5.02E-07	1.70E-03
UE5n	CAMBRIC	19-Apr-01	1.4E+05	1.1E+06	2.84E+01	5.53E-02	5.38E-10	2.29E-01	---	---	---	---
UE5n	CAMBRIC	9-Sep-99	1.3E+05	8.9E+05	1.88E+01	4.14E-02	6.01E-10	2.38E-01	<40	2.3E-03	3.51E-09	---
RNM-1	CAMBRIC	3-Jun-04	3.4E+02	3.1E+03	1.22E+03	2.44E+00	1.38E-12	4.42E-04	---	<0.0034	2.06E-07	5.96E-04
RNM-1	CAMBRIC	28-Jun-00	2.8E+04	2.1E+05	---	---	1.06E-12	4.30E-04	---	---	---	---
RNM-2S	CAMBRIC	10-Jul-03	1.3E+05	1.1E+06	3.64E+02	7.35E-01	2.30E-10	1.03E-01	---	1.5E-03	6.16E-07	1.35E-03
RNM-2S	CAMBRIC	9-May-03	1.5E+05	1.3E+06	3.87E+02	7.07E-01	2.55E-10	1.15E-01	---	---	4.82E-07	9.07E-04
RNM-2S	CAMBRIC	14-Jun-00	1.9E+05	1.4E+06	---	---	1.62E-10	7.92E-02	---	---	---	---
RNM-2S	CAMBRIC	11-Oct-99	2.3E+05	1.6E+06	4.13E+02	8.34E-01	1.64E-10	7.40E-02	<40	1.3E-03	2.12E-07	4.18E-04
Hot Wells - Yucca Flat												
U4u PS2a	DALHART	9-Oct-03	2.7E+07	6.2E+07	1.56E+05	3.26E+02	1.74E-07	2.93E+01	---	3.51E+01	1.04E-04	1.32E-01
U4u PS2a	DALHART	16-Aug-99	1.6E+07	3.1E+07	1.19E+05	2.29E+02	4.45E-08	8.52E+00	---	1.31E+01	5.32E-05	2.85E-02
UE-7ns	BOURBON	13-Dec-05	1.3E+02	1.15E+03	5.50E+01	1.35E-01	2.95E-13	2.43E-04	---	<0.043	5.08E-09	4.10E-05
UE-7ns	BOURBON	21-Aug-01	4.6E+03	3.2E+04	6.97E+01	1.39E-01	1.85E-12	1.40E-03	---	---	1.75E-07	6.05E-04
UE-2ce	NASH	12-Jul-05	9.3E+04	8.3E+05	2.01E+02	8.15E-01	9.54E-10	4.47E-01	---	<2.4e-3	5.02E-06	0.024
UE-2ce	NASH	22-Aug-01	1.4E+05	9.9E+05	2.17E+02	8.01E-01	1.62E-09	8.27E-01	---	---	2.40E-05	0.032
U-3cn PS#2	BILBY	9-Dec-04	7.9E+06	8.0E+07	1.15E+05	3.72E+02	4.46E-08	2.55E+01	---	6.26E+01	1.48E-04	2.52E-01
U-3cn PS#2	BILBY	18-Dec-01	9.9E+06	8.6E+07	8.78E+04	3.03E+02	1.52E-07	4.32E+01	---	8.26E+01	7.38E-04	1.58E-01
Hot Wells - Pahute Mesa												
U20n PS1 DDh	CHESHIRE	15-Nov-05	3.3E+07	1.8E+08	1.58E+05	1.78E+02	1.20E-09	4.75E-01	---	9.25E-01	1.13E-04	1.43E-01
U20n PS1 DDh	CHESHIRE	9-Jul-03	4.4E+07	2.1E+08	1.69E+05	1.83E+02	2.22E-09	7.99E-01	---	1.23E+01	2.74E-04	1.47E-01
U20n PS1 DDh	CHESHIRE	12-Oct-99	5.1E+07	190000000	1.54E+05	2.00E+02	1.15E-09	4.20E-01	2.77E+04	2.23E+01	4.91E-05	1.14E-01
U19ad PS1A	CHANCELLOR	27-Sep-04	2.2E+07	5.3E+07	3.06E+05	4.04E+02	6.39E-09	9.18E+00	---	4.60E+01	5.59E-04	1.94E+00
U19q PS1d	CAMEMBERT	16-Jul-03	1.1E+07	5.4E+07	4.92E+04	2.93E+02	7.73E-11	1.84E-02	---	---	2.85E-06	1.98E-03
U19q PS1d	CAMEMBERT	21-Oct-98	2.1E+07	7.8E+07	1.07E+05	1.31E+03	5.28E-11	1.81E-02	1.10E+05	8.4E-02	2.27E-06	4.07E-03
U19v PS1ds	ALMENDRO	18-Apr-06	1.1E+08	6.8E+08	N/A*	N/A*	1.88E-09	4.68E+00	---	1.00E-01	7.08E-04	2.58E+00
U19v PS1ds	ALMENDRO	23-Jul-03	1.4E+08	7.7E+08	2.99E+04	7.44E+01	3.20E-09	5.62E+00	---	---	1.89E-03	2.54E+00
U19v PS1ds	ALMENDRO	31-May-01	1.8E+08	9.0E+08	3.11E+04	9.33E+01	1.63E-09	3.58E+00	---	---	1.54E-03	2.33E+00
U19v PS1ds	ALMENDRO	26-Sep-00	1.5E+08	710000000	3.19E+04	1.01E+02	2.30E-09	3.66E+00	---	---	2.09E-03	2.76E+00
U19v PS1ds	ALMENDRO	18-Aug-99	1.6E+08	680000000	2.47E+04	3.56E+01	1.60E-09	2.14E+00	---	---	7.81E-03	1.39E+00
ER-20-5 #1	TYBO/BENHAM†	30-Nov-04	3.8E+07	2.0E+08	9.63E+04	2.24E+02	4.39E-09	3.57E+00	---	3.5E-01	1.99E-04	1.92E-01
ER-20-5 #1	TYBO/BENHAM†	9-Jul-98	6.2E+07	2.3E+08	8.17E+04	1.79E+02	4.11E-09	3.32E+00	502.00	2.7E-01	2.14E-04	2.68E-01
ER-20-5 #3	TYBO/BENHAM†	29-Nov-04	1.1E+05	6.0E+05	1.68E+03	2.73E+00	2.27E-11	1.31E-02	---	1.7E-02	1.66E-06	1.40E-03
ER-20-5 #3	TYBO/BENHAM†	15-Nov-01	1.4E+05	6.3E+05	1.57E+03	2.08E+00	3.49E-11	2.18E-02	---	---	1.34E-05	1.20E-03
ER-20-5 #3	TYBO/BENHAM†	30-Apr-98	1.6E+05	5.7E+05	1.35E+03	1.73E+00	1.93E-11	1.10E-02	<15	---	---	---
PM-2, 865	SCHOONER	26-Oct-05	4.9E+04	3.9E+05	---	---	3.82E-11	1.32E-02	---	---		
PM-2, 985	SCHOONER	26-Oct-05	4.8E+04	3.8E+05	---	---	3.64E-11	1.27E-02	---	---	1.17E-06	9.74E-04
PM-2, 1970, main	SCHOONER	26-Oct-05	7.7E+04	6.1E+05	1.42E+02	9.11E-01	2.10E-11	1.37E-02	---	<0.076	4.30E-07	6.46E-04
PM-2, 2625-1300	SCHOONER	26-Oct-05	2.6E+05	2.0E+06	---	---	7.19E-12	1.66E-02	---	---		

N/A* Data will be provided in the FY07 HRMP report when analyses are complete.

† Both the Tybo and Benham tests are listed since the ER-20-5 well cluster was drilled in the near-field (~300 m from the surface ground zero) environment of the Tybo test.

Table 1.7 Radiochemical data continued.

Well name	Test	Sample date	$^{234}U/^{238}U$	$^{234}U/^{238}U$ activity ratio	$^{234}U/^{235}U$	$^{236}U/^{235}U$	$^{235}U/^{238}U$	^{234}U	^{235}U	^{236}U	^{238}U	Pu, total
Unit *Half-life (a)* *Ref. date*		*date collected in field*	*ratio*	*ratio*	*ratio*	*ratio*	*ratio*	*(pCi/L)* *2.46E+05* *collect.*	*(pCi/L)* *7.04E+08* *collect.*	*(pCi/L)* *2.34E+07* *collect.*	*(pCi/L)* *4.47E+09* *collect.*	*(pCi/L)* *total* *collect.*
Hot Wells - Frenchman Flat												
UE5n	CAMBRIC	12-Feb-04	8.95E+03	2.03	1.54E-02	---	7.25E-03	3.07E+00	6.92E-02	---	1.49E+00	<0.02
UE5n	CAMBRIC	19-Apr-01	1.13E-04	2.06	1.56E-02	< 2.1E-05	7.25E-03	2.90E-01	6.00E-03	---	1.40E-01	---
UE5n	CAMBRIC	9-Sep-99	---	---	---	---	---	---	---	---	---	---
RNM-1	CAMBRIC	3-Jun-04	1.34E-04	2.44	1.85E-02	< 2.1E-05	7.25E-03	3.18E+00	5.97E-02	< 3.8E-05	1.28E+00	<0.02
RNM-1	CAMBRIC	28-Jun-00	1.36E-04	2.48	1.87E-02	9.6E-04	7.29E-03	3.33E+00	6.00E-02	1.79E-03	1.33E+00	---
RNM-2S	CAMBRIC	10-Jul-03	1.23E-04	2.25	1.70E-02	< 2.1E-05	7.26E-03	3.72E+00	7.60E-02	< 4.82E-05	1.64E+00	<0.02
RNM-2S	CAMBRIC	9-May-03	1.23E-04	2.25	1.70E-02	< 2.1E-05	7.26E-03	3.75E+00	7.70E-02	< 4.85E-05	1.65E+00	<0.02
RNM-2S	CAMBRIC	14-Jun-00	1.23E-04	2.24	1.69E-02	---	7.29E-03	3.77E+00	8.00E-02	---	1.66E+00	---
RNM-2S	CAMBRIC	11-Oct-99	---	---	---	---	---	---	---	---	---	---
Hot Wells - Yucca Flat												
U4u PS2a	DALHART	9-Oct-03	2.02E-04	3.69	2.78E-02	2.10E-05	7.26E-03	9.25E+00	1.16E-01	---	2.48E+00	0.32
U4u PS2a	DALHART	16-Aug-99	---	---	---	---	---	---	---	---	---	1.2
UE-7ns	BOURBON	13-Dec-05	1.52E-04	2.77	2.10E-02	< 5E-06	7.25E-03	5.80E-02	1.00E-03	---	2.10E-02	<0.04
UE-7ns	BOURBON	21-Aug-01	1.69E-04	3.08	2.31E-02	< 2.1E-05	7.30E-03	4.60E-02	7.00E-04	---	1.50E-02	<0.04
UE-2ce	NASH	12-Jul-05	1.94E-04	3.53	2.67E-02	---	7.25E-03	2.39E+00	3.10E-02	---	6.69E-01	<0.07
UE-2ce	NASH	22-Aug-01	2.05E-04	3.74	2.82E-02	< 2.1E-05	7.26E-03	5.00E-01	6.00E-03	---	1.30E-01	<0.04
U-3cn PS#2	BILBY	9-Dec-04	1.54E-04	2.80	2.12E-02	2.80E-05	7.25E-03	9.77E+00	1.60E-01	---	3.44E+00	<0.01
U-3cn PS#2	BILBY	18-Dec-01	1.60E-04	2.92	2.21E-02	< 2.1E-05	7.25E-03	1.05E+01	1.66E-01	---	3.56E+00	<0.04
Hot Wells - Pahute Mesa												
U20n PS1 DDh	CHESHIRE	15-Nov-05	1.80E-04	3.29	2.48E-02	1.40E-03	7.28E-03	3.95E-01	6.00E-03	---	1.19E-01	0.46
U20n PS1 DDh	CHESHIRE	9-Jul-03	1.93E-04	3.53	2.66E-02	---	7.26E-03	2.46E+00	3.20E-02	8.70E-04	6.91E-01	0.31
U20n PS1 DDh	CHESHIRE	12-Oct-99	1.89E-04	3.44	2.63E-02	---	7.17E-03	3.00E+00	4.00E-02	---	8.60E-01	0.51
U19ad PS1A	CHANCELLOR	27-Sep-04	8.90E-05	1.62	1.18E-02	4.37E-03	7.56E-03	1.43E+00	4.21E-02	5.50E-03	8.68E-01	26.8
U19q PS1d	CAMEMBERT	16-Jul-03	1.05E-04	1.92	1.45E-02	< 2.1E-05	7.25E-03	1.69E+00	4.10E-02	---	8.72E-01	<0.02
U19q PS1d	CAMEMBERT	21-Oct-98	1.65E-04	3.02	2.25E-02	---	7.35E-03	<0.509	<0.008	---	<0.167	0.019
U19v PS1ds	ALMENDRO	18-Apr-06	1.20E-04	2.18	1.66E-02	2.38E-04	7.22E-03	2.24E-02	4.71E-04	3.37E-06	1.02E-02	<0.004
U19v PS1ds	ALMENDRO	23-Jul-03	6.96E-05	1.27	9.59E-03	< 2.1E-05	7.25E-03	4.80E-02	2.00E-03	< 1.1E-06	3.80E-02	<0.02
U19v PS1ds	ALMENDRO	31-May-01	1.77E-04	3.24	2.44E-02	2.40E-04	7.25E-03	3.40E-02	5.00E-04	3.40E-06	1.00E-02	0.18
U19v PS1ds	ALMENDRO	26-Sep-00	1.72E-04	3.15	2.38E-02	1.55E-03	7.23E-03	1.70E-02	3.00E-04	1.40E-05	5.00E-03	<0.041
U19v PS1ds	ALMENDRO	18-Aug-99	---	---	---		---	---	---	---	---	9.45
ER-20-5 #1	TYBO/BENHAM†	30-Nov-04	1.59E-04	2.90	2.20E-02	5.30E-05	7.25E-03	1.38E+01	2.19E-01	---	4.71E+00	0.42
ER-20-5 #1	TYBO/BENHAM†	9-Jul-98	1.65E-04	3.01	2.27E-01	---	7.27E-03	1.52E+01	2.34E-01	---	5.01E+00	0.59
ER-20-5 #3	TYBO/BENHAM†	29-Nov-04	1.39E-04	2.53	1.92E-02	1.70E-05	7.25E-03	4.83E+00	8.77E-02	---	1.88E+00	<0.04
ER-20-5 #3	TYBO/BENHAM†	15-Nov-01	6.35E-05	1.16	8.76E-03	1.56E-05	7.25E-03	5.01E+00	2.00E-01	---	4.27E+00	<0.04
ER-20-5 #3	TYBO/BENHAM†	30-Apr-98	1.58E-04	2.89	2.18E-02	---	7.27E-03	2.64E+00	4.20E-02	---	9.02E-01	---
PM-2, 865	SCHNOONER	26-Oct-05	---	---	---	---	---	---	---	---	---	---
PM-2, 985	SCHNOONER	26-Oct-05	---	---	---	---	---	---	---	---	---	<0.004
PM-2, 1970, main	SCHNOONER	26-Oct-05	1.34E-04	2.43	1.84E-02	< 5E-06	7.25E-03	1.95E-01	4.00E-03	---	7.90E-02	---
PM-2, 2625-1300	SCHNOONER	26-Oct-05	---	---	---	---	---	---	---	---	---	0.006

N/A* Data will be provided in the FY07 HRMP report when analyses are complete.

† Both the Tybo and Benham tests are listed since the ER-20-5 well cluster was drilled in the near-field (~300 m from the surface ground zero) environment of the Tybo test.

CHAPTER 2

FY 2006 Chemical and Isotopic Environmental Well Groundwater Data

H. W. Culham, G.F. Eaton, V.Genetti, Q. (Max) Hu, R.E. Lindvall, J.E. Moran, T.P. Rose, R.W. Williams, M. Zavarin, and P. Zhao

Chemical Sciences Division, Chemistry Materials Earth and Life Sciences Directorate
Lawrence Livermore National Laboratory

2.1 Introduction

This chapter summarizes the results of chemical and isotopic analyses of groundwater samples collected from the UGTA project environmental monitoring wells during FY 2006. Geochemical data gathered through this effort provide an independent means of evaluating groundwater flow model predictions for the NTS. The sampling program is a coordinated effort between the various UGTA contractors including Lawrence Livermore National Laboratory (LLNL), Los Alamos National Laboratory (LANL), the Desert Research Institute (DRI), the U.S. Geological Survey (USGS), Stoller-Navarro Joint Venture (SNJV), and National Security Technologies (NSTec). During FY 2006, groundwater characterization samples were collected from three environmental wells ER-12-4 and U-12s on Rainier Mesa and USGS HTH #2 (aka Water Well 2 (WW-2)) in Yucca Flat Area 2. Samples were also collected from three springs, White Rock Spring and Captain Jack Spring on Rainier Mesa and Topopah Spring in Area 29. The locations of all sampling events are found in **Figure 2.1**. The analytical results from these sampling events are compiled in **Tables 2.1-2.7**. Laboratory analytical protocols are fully described in the LLNL Standard Operating Procedures written in support of the UGTA Project (LLNL, 2004).

Groundwater characterization samples were collected from ER-12-4 on April 25, 2006. Samples from U-12s and WW-2 were collected on 22 August 2006 and 7 September 2006. Samples from White Rock Spring, Captain Jack Spring and Topopah Spring were collected on September 26, 27 and 28, 2006 respectively.

Significant features of the ER-12-4 data are highlighted in the following section. The remaining wells and springs were collected in part for the Rainier Mesa / Shoshone Mountain Geochemical Evaluation. Data interpretation for these samples will be presented in the Rainier Mesa / Shoshone Mountain Geochemical Evaluation Report.

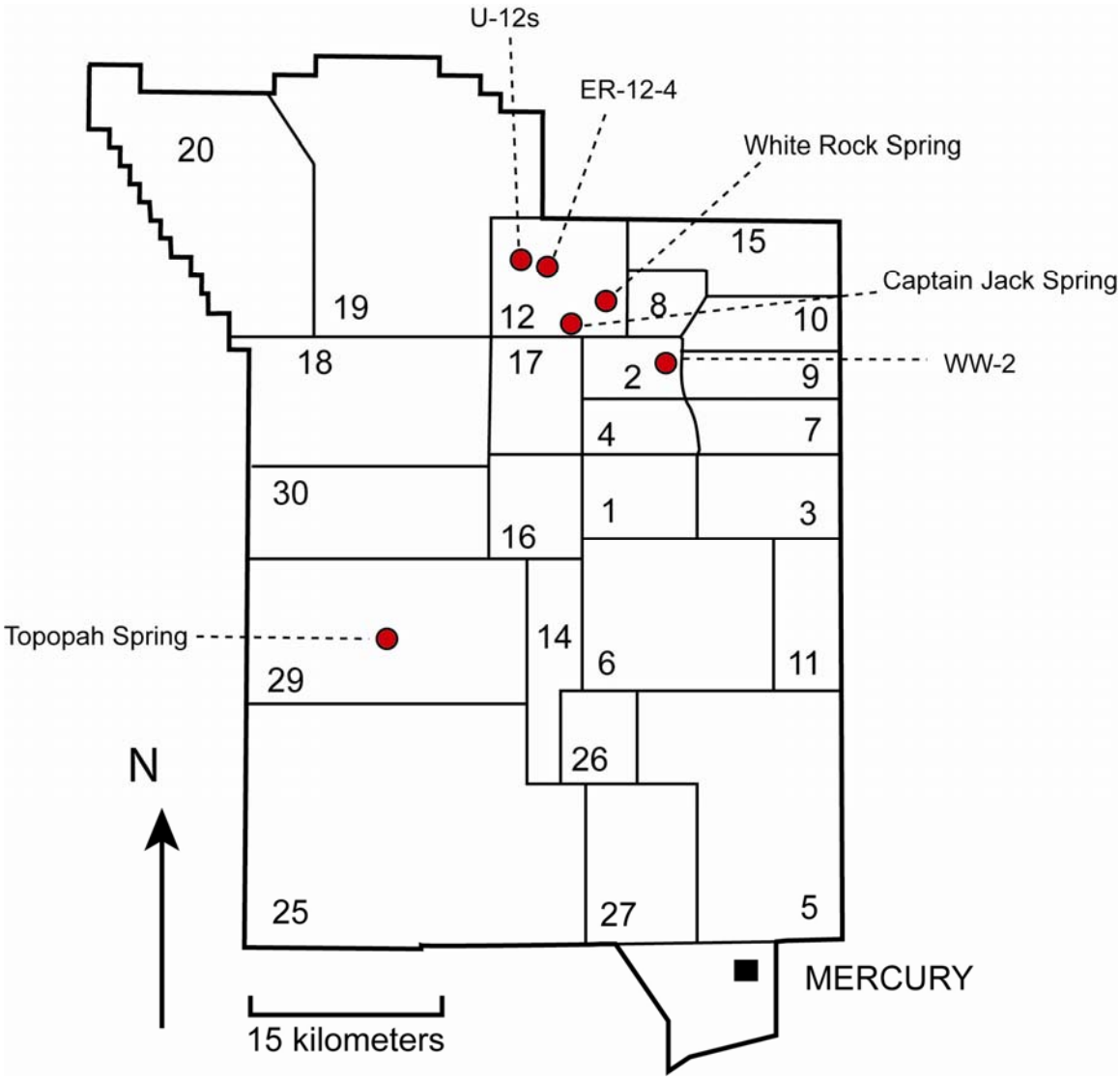

Figure 2.1 Map of the NTS showing environmental well sampling locations for FY2006.

2.2 ER-12-4

Well ER-12-4 was constructed in Area 12 on Rainier Mesa and drilled into the carbonate aquifer with the objective of acquiring data on the radiological and hydrogeologic environment beneath Rainier Mesa. Well completion, development, lithology and hydraulic testing data are summarized in a preliminary report by Stoller-Navarro Joint Venture (SNJV, 2005). ER-12-4 was completed to a total depth of 1,132 m-bgs on June 1, 2005 with 7 intervals of slotted casing, each about 43 ft in length. The top of the uppermost interval 948 m-bgs and the bottom of the lowermost interval is 1,118 m-bgs. Saturated rocks consist of some Paleozoic dolomite but primarily Paleozoic limestone with little apparent porosity but populated with numerous hairline fractures mostly cemented by later stage calcite deposits (SNJV, 2005). Interestingly, significant water production was only observed in the limestone. Also, production rates were significantly lower than those observed in ER-12-3. The original pump installed in ER-12-4 had a capacity of 10 to 30 gallons per minutes, which proved to be unsustainable. Between April 17 and 27, 2006,

a low-volume submersible pump was installed and used to collect samples described in this well report (SNJV, 2006).

Groundwater characterization samples were collected from well ER-12-4 on April 25, 2006. At the time of sampling, the depth to water was measured at 707 m-bgs, the pump rate was 4.5 gpm, and the cumulative purge volume was ~2.3×10^4 gallons of water. Previous well completion activities conducted in 2005 had purged ~4.9×10^4 gallons of water.

Well ER-12-4 produces a dilute mixed type Ca-Mg-Na-HCO_3 groundwater with a low conductivity value (211 µS/cm) and a pH of 7.8. The stable isotope composition of the water is -100 ‰ for δD and -13.9 ‰ for $\delta^{18}O$. The stable isotope composition is not unlike that of other northern Yucca Flat wells completed in the carbonate aquifer. However, the major element composition suggests that a fraction of the water may be derived from perched volcanic aquifers.

The tritium activity of groundwater from well ER-12-4 was determined by the helium accumulation method (Surano et al., 1992). The tritium activity is <1 pCi/L. The higher tritium value observed in 2005 (89.7 pCi/L) was likely an artifact of drilling and insufficient well purging. The new sample indicates no significant transport of tritium from the overlying perched groundwater to the regional aquifer.

Dissolved inorganic carbon (DIC) in ER-12-4 groundwater has a $\delta^{13}C$-DIC value of -6.7 ‰ and a $\delta^{13}C$-DOC value of -25.6 ‰. The relatively heavy $\delta^{13}C$-DIC is indicative of groundwater interaction with LCA rock. The dissolved inorganic carbon (DIC) was 14.1 mg/L as C, and the dissolved organic carbon (DOC) was 1.0 mg/L as C. It should be noted that the DIC is unusually low for LCA waters. However, it is consistent with the previous measurement in 2005. ^{14}C analysis has not been completed but will be submitted as an addendum at a later date.

The ^4He value is quite low (1.6×10^{12} atoms/g). ^4He is not appreciably enriched relative to the equilibrium atmospheric helium solubility for this location. It suggests that the noble gas data are not representative of ambient waters in ER-12-4. A similar result was reported for the sample collected in 2005. It does not appear that the additional purging improved the noble gas results. The low groundwater production from this well makes collection of an undisturbed noble gas sample difficult.

ER-12-4 groundwater has a chloride concentration of 9.0 mg/L and a $^{36}Cl/Cl$ ratio (5.7×10^{-13}) that is in the normal range for the modern atmospheric ratio for southern Nevada (~5×10^{-13}, Fabryka-Martin et al., 1993). It is significantly higher than most LCA $^{36}Cl/Cl$ ratios and may, again, be an indication of mixing with overlying perched volcanic aquifer waters.

The groundwater from ER-12-4 has a $^{87}Sr/^{86}Sr$ ratio of 0.71087 and a $\delta^{87}Sr$ value of +2.35 ‰. The relatively low Sr concentration (53.2 µg/L) and isotope ratios are also suggestive of significant mixing with overlying perched volcanic aquifers. The concentration of dissolved uranium (0.37 µg/L) is on the lower end of the normal range of values for groundwater from the

NTS, and the $^{235}U/^{238}U$ ratio shows the uranium is natural in origin. The $^{234}U/^{238}U$-activity ratio is 2.08.

2.3 References

Fabryka-Martin, J., Wightman, S.J., Murphy, W.J., Wickham, M.P., Caffee, M.W., Nimz, G.J., Southon, J.R., and Sharma, P. (1993) Distribution of chlorine-36 in the unsaturated zone at Yucca Mt.: An indicator of fast transport paths. FOCUS '93: Site Characterization and Model Validation, Las Vegas, NV, 26-29 Sept 1993.

LLNL (2004) Analytical Measurements: Standard Operating Procedures, Underground Test Area Project. Chemical Biology and Nuclear Science Division, Lawrence Livermore National Laboratory, 30 June 2004.

SNJV (2005) Rainier Mesa ER-12-4 Well Data Report, Preliminary, Rev. 0., Stoller-Navarro Joint Venture, Las Vegas, NV, September 2005, 116 p.

SNJV (2006) Rainier Mesa ER-12-4 Sampling Report, Preliminary, Stoller-Navarro Joint Venture, Las Vegas, NV, 11p.

Surano, K.A., Hudson, G.B., Failor, R.A., Sims, J.M., Holland, R.C., MacLean, S.C., and Garrison, J.C. (1992) Helium-3 mass spectrometry for low-level tritium analysis of environmental samples. Jour. Radioanal. Nuclear Chem. Articles, v. 161, p. 443-453.

Table 2.1 Environmental Well Site Information.

Well name	Test Name	Test Date	Latitude	Longitude	Surface Elevation	Well Depth	Open Interval	Water Depth	Sample Method	Volume pumped	Sample Depth	Sample date
Units			*(d m s)*	*(d m s)*	*(ft)*	*(ft bgs)*	*(ft bgs)*	*(ft bgs)*		*(gal)*	*(ft bgs)*	
Clean Wells - Frenchman Flat												
Water Well 5a	---	---	36 46 35	115 57 29	3092	910	642-877	695	pump	---	---	14-Aug-00
Water Well 5c	---	---	36 47 08	115 57 44	3081	1200	887-1187	689	pump	---	---	7-Aug-00
Water Well 5b	---	---	36 48 05	115 58 08	3093	900	700-900	683	pump	---	---	7-Aug-00
ER-5-4	---	---	36 49 28	115 57 48	3127	3732	1770-2113; 3136-3350	726	pump	3.74E+06	---	5-Jul-01
ER-5-4 #2	---	---	36 49 27	115 57 48	3127	7000	6486-6658	697	pump	4.00E+06	---	21-Nov-02
UE-5c WW	---	---	36 50 11	115 58 47	3216	2682	1100-2682	806	pump	---	---	8-Aug-00
UE-5 PW-3	---	---	36 52 01	115 58 16	3297	955	891-955	891	pump	---	---	9-Aug-00
ER-5-3	---	---	36 52 23	115 56 17	3334	2606	1480-1737; 2420-2549	927	pump	3.16E+06	---	28-Mar-01
ER-5-3 #2	---	---	36 52 23	115 56 18	3334	5683	4674-4868	952	pump	3.46E+06	---	17-May-01
Water Well 4a	---	---	36 54 12	116 01 39	3604	1517	944-1502	835	pump	---	---	8-Aug-00
Clean Wells - Yucca Flat												
ER-2-1	---	---	37 07 31	116 03 42	4222	2600	1642-2076	1723.0	pump	2.15E+04	---	3-Sep-03
ER-6-1 #2	---	---	36 59 01	115 59 35	3934	3200	1775-3200	1545	pump	3.80E+06	---	16-Jan-03
ER-6-2	---	---	36 57 40	116 04 34	4231	3408	1746-3430	1789	pump	3.37E+06	---	4-Aug-04
ER-7-1	---	---	37 04 24	115 59 43	4247	2500	2182-2479	1854.0	pump	3.54E+07	---	17-Jul-03
WW2 (USGS HTH #2)	---	---	37 09 58	116 05 15	4470	3422	2700 – 2950; 3166 - 3414	2052	pump	2.80E+04	2443	7-Sep-06
Clean Wells - Rainier Mesa												
ER-12-1	---	---	37 11 06	116 11 03	5817	3434	1641-1846	1538	pump	1.95E+04	---	8-Dec-04
ER-12-2	---	---	37 10 19	116 07 21	4705	6883	2958-6883	191	pump	3.52E+05	---	01-Apr-03
ER-12-3	---	---	37 11 42	116 12 51	7385	4850	3591-3805; 4919-4834	3100	pump	6.22E+02	---	6-Jul-05
ER-12-4	---	---	37 13 11	116 10 59	6883	3715	3111-3669	2321	pump	2.30E+04	---	25-Apr-06
ER-12-4	---	---	37 13 11	116 10 59	6883	3715	3111-3669	2600	pump	4.93E+04	2916	16-Aug-05
U12S	---	---	37 13 42	116 12 57	6794	1467	12-1480	908	pump	5.58E+04	1248	22-Aug-06
Springs - Rainier Mesa												
White Rock Springs	---	---	37 12 05	116 07 54	5025	---	---	---	grab	---	---	26-Sep-06
Captain Jack Springs	---	---	37 10 06	116 10 07	5765	---	---	---	grab	---	---	27-Sep-06
Springs												
Topopah Springs	---	---	36 56 17	116 16 15	5700	---	---	---	grab	---	---	28-Sep-06
Clean Wells - Pahute Mesa-Oasis Valley												
ER-EC-1	---	---	37 12 23	116 31 44	6026	5000	2298-2821; 3348-3760; 4449-4750	1859	pump	2.02E+05	---	3-Jun-03
ER-EC-1	---	---	37 12 23	116 31 44	6026	5000	2298-2821; 3348-3760; 4449-4750	1859	pump	---	---	1-Feb-00
ER-EC-2A	---	---	37 08 52	116 34 05	4904	4974	1707-2179; 3077-3549; 4487-4916	748	pump	2.66E+04	---	8-Jul-03
ER-EC-2A	---	---	37 08 52	116 34 05	4904	4974	1707-2179; 3077-3549; 4487-4916	748	pump	---	---	27-Jul-00
ER-EC-4	---	---	37 09 39	116 37 52	4760	3487	989-1224; 1910-2253; 3103-3404	749	pump	1.23E+05	---	24-Jun-03
ER-EC-4	---	---	37 09 39	116 37 52	4760	3487	989-1224; 1910-2253; 3103-3404	749	pump	---	---	17-Aug-00
ER-EC-5	---	---	37 05 05	116 33 49	5077	2500	1197-1399; 1892-2094; 2246-2417	1017	pump	2.21E+05	---	15-Jul-03
ER-EC-5	---	---	37 05 05	116 33 49	5077	2500	1197-1399; 1892-2094; 2246-2417	1017	pump	---	---	25-May-00
ER-EC-6	---	---	37 11 26	116 29 48	5605	5000	1628-1871; 2195-2507; 3438-3811; 4421-4904	1426	pump	2.15E+05	---	10-Jun-03
ER-EC-6	---	---	37 11 26	116 29 48	5605	5000	1628-1871; 2195-2507; 3438-3811; 4421-4904	1426	pump	---	---	10-Feb-00
ER-EC-7	---	---	36 59 10	116 28 41	4800	1386	920-979; 1215-1304	719	pump	2.90E+05	---	21-Jul-03
ER-EC-7	---	---	36 59 10	116 28 41	4800	1386	920-979; 1215-1304	719	pump	---	---	5-Jun-00
ER-EC-8	---	---	37 06 17	116 37 53	4245	2000	683-984; 1447-1507; 1677-1908	323	pump	2.34E+05	---	1-Jul-03
ER-EC-8	---	---	37 06 17	116 37 53	4245	2000	683-984; 1447-1507; 1677-1908	323	pump	---	---	12-Jul-00
ER-18-2	---	---	37 06 21	116 22 22	5436	2500	1930-1960; 2000-2030; 2071-2101	1213	pump	9.76E+04	---	17-Jun-03
ER-18-2	---	---	37 06 21	116 22 22	5436	2500	1930-1960; 2000-2030; 2071-2101	1213	pump	---	---	21-Mar-00

Table 2.2 Environmental well field parameter and anion data.

Well name	Test	Sample date	pH	T	Cond.	F	Cl	Br	NO_2	NO_3	SO_4	Na	K	Ca	Mg	Li
Units		*date*		*(°C)*	*(mS/cm)*	*(mg/L)*	*(mg/L)*	*(mg/L)*	*(mg/L)*	*(mg/L)*	*(mg/L)*	*(mg/L)*	*(mg/L)*	*(mg/L)*	*(mg/L)*	*(mg/L)*
Clean Wells - Frenchman Flat																
Water Well 5a	---	14-Aug-00	8.9	22.3	600	1.1	11.1	<0.2	---	3.7	28.5	147.0	5.5	1.7	0.8	---
Water Well 5c	---	7-Aug-00	8.7	28.2	601	1.0	11.3	<0.2	---	7.4	29.3	149.0	7.0	1.9	0.7	---
Water Well 5b	---	7-Aug-00	8.5	24.6	512	0.7	23.4	<0.2	---	12.8	55.0	101.0	12.6	7.3	2.5	---
ER-5-4	---	5-Jul-01	8.7	30.2	885	6.2	26.8	<0.3	---	4.0	120.0	124.0	7.1	2.2	0.2	---
ER-5-4 #2	---	21-Nov-02	8.7	38.1	1249	63.9	51.7	<0.5	---	<0.1	119.4	334.0	4.3	0.7	0.3	0.07
UE-5c WW	---	8-Aug-00	8.5	25.8	463	1.8	12.8	<0.2	---	7.5	43.7	100.0	6.7	6.9	1.8	---
UE-5 PW-3	---	9-Aug-00	8.3	21.5	371	0.9	9.4	<0.2	---	14.6	31.8	61.8	5.0	16.4	6.7	---
ER-5-3	---	28-Mar-01	8.3	30.0	445	2.5	15.5	<0.1	---	7.0	40.0	78.9	4.0	14.3	3.9	---
ER-5-3 #2	---	17-May-01	6.7	33.8	1158	1.3	38.0	<0.1	---	<0.09	64.0	145.0	15.8	86.1	32.6	---
Water Well 4a	---	8-Aug-00	7.9	26.5	409	1.2	13.2	<0.2	---	17.4	39.8	57.3	6.2	23.1	8.3	---
Clean Wells - Yucca Flat																
ER-2-1	---	3-Sep-03	9.3	21.3	368	1.8	4.4	<0.03	---	2.4	15.9	73.0	3.8	3.1	0.3	0.02
ER-6-1 #2	---	16-Jan-03	7.6	39.9	408	0.8	10.0	0.8	---	1.1	34.0	47.1	6.3	33.6	14.0	0.06
ER-6-2	---	4-Aug-04	7.5	34.9	617	1.4	23.9	0.1	---	1.4	52.4	72.1	10.2	67.4	22.3	0.18
ER-7-1	---	17-Jul-03	7.6	49.4	488	0.8	9.5	0.1	---	0.1	34.4	41.6	5.6	27.1	13.3	0.04
WW2 (USGS HTH #2)	---	7-Sep-06	7.62‡	31.86‡	339‡	<0.1	7.2	<0.4	<0.4	3.7	21.3	25.2§	5.5§	27.2§	12.8§	---
Clean Wells - Rainier Mesa																
ER-12-1	---	8-Dec-04	7.5	25.0	984	0.3	17.7	0.4	---	0.1	355.4	38.3	3.0	88.4	58.8	0.26
ER-12-2	---	1-Apr-03	8.1	35.2	528	2.2	7.0	0.7	---	<0.2	27.4	117.2	2.1	6.5	2.1	0.19
ER-12-3	---	6-Jul-05	8.2	30.6	306	1.5	5.7	<0.02	---	0.8	24.6	30.7	2.2	13.8	7.9	<0.03
ER-12-4	---	25-Apr-06	7.8	26.0	211	0.82	9.01	<0.2	<0.2	3.09	12.6	28.9§	4.2§	9.3§	3.8§	---
ER-12-4	---	16-Aug-05	8.8	23.9	196	0.3	9.1	<0.02	---	8.5	11.4	28.3	3.1	8.4	3.5	<0.005
U12S	---	22-Aug-06	9.6‡	22.34‡	208‡	<0.1	9.25	<0.2	8.33	2.92	11.7	25.2§	4.5§	16.5§	0.86§	---
Springs - Rainier Mesa																
White Rock Springs	---	26-Sep-06	7.06‡	15.67‡	283‡	<0.1	15.1	<0.4	<0.4	7.16	37.3	48.9§	6.3§	6.9§	0.5§	---
Captain Jack Springs	---	27-Sep-06	7.03‡	16.59‡	179‡	<0.1	4.3	<0.4	<0.4	<0.4	6.19	37.2§	2.2§	2.4§	0.3§	---
Springs																
Topopah Springs	---	28-Sep-06	5.41‡	25.14‡	103‡	<0.1	2.2	<0.4	<0.4	<0.4	3.24	15.3§	6.6§	7.2§	1.9§	---
Clean Wells - Pahute Mesa-Oasis Valley																
ER-EC-1	---	3-Jun-03	8.1	34.8	782	2.3	97.0	1.4	---	2.1	119.0	143.7	4.9	18.7	0.4	0.11
ER-EC-1	---	1-Feb-00	7.9	37.0	818	2.4	97.0	1.1	---	2.5	145.0	154.0	6.0	19.0	0.4	0.15
ER-EC-2A	---	8-Jul-03	8.1	35.2	616	3.9	55.5	1.1	---	1.9	84.5	127.8	2.2	8.7	0.2	0.15
ER-EC-2A	---	27-Jul-00	7.8	40.4	706	5.9	63.0	0.6	---	1.2	99.0	123.0	2.5	13.1	2.5	0.14
ER-EC-4	---	24-Jun-03	7.8	35.9	750	3.0	80.6	1.2	---	2.4	109.0	118.7	8.1	26.1	5.0	0.09
ER-EC-4	---	17-Aug-00	7.9	38.5	793	3.6	95.7	1.3	---	3.2	130.0	116.0	8.7	25.9	3.8	0.09
ER-EC-5	---	15-Jul-03	7.9	29.7	412	4.3	15.9	0.7	---	1.7	36.3	70.8	1.1	19.8	0.8	0.09
ER-EC-5	---	25-May-00	7.9	29.9	424	4.6	16.1	n.d.	---	1.2	35.0	75.0	1.8	21.0	0.6	0.01
ER-EC-6	---	10-Jun-03	8.1	33.9	516	2.7	51.7	0.9	---	2.0	75.4	119.6	1.8	4.6	0.2	0.10
ER-EC-6	---	10-Feb-00	8.1	37.9	613	3.1	44.0	0.8	---	2.0	56.0	128.0	2.0	4.0	0.0	0.15
ER-EC-7	---	21-Jul-03	8.0	27.3	263	1.2	3.8	<0.03	---	5.6	13.6	28.0	2.0	20.2	2.2	0.02
ER-EC-7	---	5-Jun-00	7.9	30.0	315	1.3	5.2	n.d.	---	5.8	15.0	35.0	2.8	22.0	2.0	0.04
ER-EC-8	---	1-Jul-03	8.1	36.7	642	5.2	47.3	1.0	---	1.4	76.1	120.4	4.9	10.1	0.3	0.15
ER-EC-8	---	12-Jul-00	8.0	38.2	647	5.5	57.6	0.4	---	1.3	94.0	120.0	5.6	11.0	0.5	0.15
ER-18-2	---	17-Jun-03	7.9	43.0	1277	12.5	12.3	<0.2	---	<0.2	52.9	344.0	2.1	5.9	0.5	0.22
ER-18-2	---	21-Mar-00	7.6	55.2	1439	12.6	13.3	n.d.	---	<1.0	53.0	365.0	1.8	6.1	0.2	0.28

‡ Values provided by Stoller Navarro Joint Venture
§ Analyses performed by ICPMS

Table 2.3 Environmental well cations and metals data.

Well name	Test	Sample date	Al	Si	Fe	Be	B	Ti	Mn	As	Se	Sr	Mo	Sb	I	Ba	Pb	U
Unit			*(mg/L)*	*(mg/L)*	*(mg/L)*	*(mg/L)*	*(mg/L)*	*(mg/L)*	*(mg/L)*	*(mg/L)*	*(mg/L)*	*(mg/L)*	*(mg/L)*	*(mg/L)*	*(mg/L)*	*(mg/L)*	*(mg/L)*	*(mg/L)*
Clean Wells - Frenchman Flat																		
Water Well 5a	---	14-Aug-00	<0.05	18.8	<0.04	---	---	---	<6	37	<24	<13	8.3	---	---	1	<14	---
Water Well 5c	---	7-Aug-00	<0.05	25	<0.04	---	---	---	<6	32	<24	<13	7.3	---	---	1	<14	---
Water Well 5b	---	7-Aug-00	<0.05	26.3	<0.04	---	---	---	<6	<20	<24	<13	3.2	---	---	2	<14	---
ER-5-4	---	5-Jul-01	0.2	24.5	0	---	---	---	<6	47	<24	35	63	---	---	8	21	1.60
ER-5-4 #2	---	21-Nov-02	1.9	34.7	1	---	---	---	98	<20	<24	3.3	82	---	---	8	<14	36.40
UE-5c WW	---	8-Aug-00	0.6	33.3	0	---	---	---	<6	<20	<24	33	11	---	---	89	<14	---
UE-5 PW-3	---	9-Aug-00	<0.05	27.6	<0.04	---	---	---	<6	<20	<24	120	3.8	---	---	13	<14	---
ER-5-3	---	28-Mar-01	---	---	---	---	---	---	<6	30	<24	64	6.9	---	---	3	<14	0.97
ER-5-3 #2	---	17-May-01	---	---	---	---	---	---	92	35	<24	1018	4.3	---	---	230	<14	0.50
Water Well 4a	---	8-Aug-00	<0.05	28.0	<0.04	---	---	---	<6	<20	<24	130	5.8	---	---	3	<14	---
Clean Wells - Yucca Flat																		
ER-2-1	---	3-Sep-03	0.1	55.8	2.20	---	---	---	110	<20	40	6.7	<3	---	5.3	9	<14	3.40
ER-6-1 #2	---	16-Jan-03	<0.05	16.4	<0.04	---	0.1	---	7	<20	<24	208	<3	---	---	160	<14	3.21
ER-6-2	---	4-Aug-04	0.01021	40.1	0.03	0.1	---	2.3	38.3	38	0.905	231	5.4	3.15	---	154	0.35	2.17
ER-7-1	---	17-Jul-03	<0.05	18.3	<0.04	---	---	---	<6	<20	<24	156	10	---	8.1	230	<14	1.42
WW2 (USGS HTH #2)	---	7-Sep-06	< 0.0009	---	0.573	< 0.054	0.128	---	98	1.787	1.09	84.7	2.32	0.16	---	31.6	0.071	1.034
Clean Wells - Rainier Mesa																		
ER-12-1	---	8-Dec-04	0.000317	29.34	4.99	0.1	---	3.7	141	106	0.457	210	10.6	0.48	---	35	BD	1.63
ER-12-2	---	1-Apr-03	<0.05	6.9	0.26	---	0.5	---	22	<20	<24	317	4.7	---	---	210	<14	0.02
ER-12-3	---	6-Jul-05	0.003	6.8	0.3	<0.3	0.1	< 9	26.6	7.5	< 1.5	102	5.9	0.36	3.6	24.88	0.3	1.83
ER-12-4	---	25-Apr-06	0.0438	---	0.2258	< 0.042	---	---	20.2	3	1	53.2	1.06	< 0.18	9.1	23	0.94	0.37
ER-12-4	---	16-Aug-05	0.02	3.53	1.0	<0.12	0.04	< 9	45.3	< 4.2	< 1.5	63	2	< 0.3	---	12.6	0.24	0.30
U12S	---	22-Aug-06	0.038	---	0.195	< 0.15	0.069	---	16.6	1.47	0.28	1200	1.33	0.064	12.4	142	1.26	0.922
Springs - Rainier Mesa																		
White Rock Springs	---	26-Sep-06	0.938	---	0.587	< 0.18	0.13	---	5.89	3.77	1.5	3.06	1.24	0.079	---	1.78	0.998	1.565
Captain Jack Springs	---	27-Sep-06	0.691	---	0.194	< 0.27	0.06	---	6.78	1.504	0.135	2.69	0.24	< 0.033	---	5.01	0.421	0.672
Springs																		
Topopah Springs	---	28-Sep-06	0.503	---	0.264	< 0.36	0.082	---	1.95	1.99	0.178	20.5	0.4	0.071	---	2.63	0.555	0.302
Clean Wells - Pahute Mesa-Oasis Valley																		
ER-EC-1	---	3-Jun-03	0.2	28.7	<0.04	---	1.2	---	<6	<20	<24	16	<3	---	---	1	<14	9.51
ER-EC-1	---	1-Feb-00	<0.4	23	0.64	---	0.3	---	---	---	---	27	---	---	---	---	---	8.12
ER-EC-2A	---	8-Jul-03	0.1	26.5	<0.04	---	1.1	---	<6	<20	<24	28	6.8	---	---	15	<14	7.05
ER-EC-2A	---	27-Jul-00	<0.11	15	0.25	---	---	---	---	---	---	74	---	---	---	---	---	9.20
ER-EC-4	---	24-Jun-03	0.2	40.3	0.05	---	1.2	---	<6	<20	<24	136	4.7	---	---	2	<14	4.08
ER-EC-4	---	17-Aug-00	<0.11	21	0.18	---	---	---	---	---	---	160	---	---	---	---	---	4.10
ER-EC-5	---	15-Jul-03	<0.05	24.5	<0.04	---	1.1	---	<6	<20	<24	128	6.2	---	---	3	<14	3.34
ER-EC-5	---	25-May-00	0.2	15	0.13	---	---	---	---	---	---	170	---	---	---	---	---	3.30
ER-EC-6	---	10-Jun-03	0.2	27.4	<0.04	---	1.1	---	<6	<20	<24	4.1	<3	---	---	2	<14	5.43
ER-EC-6	---	10-Feb-00	<0.4	22	0.42	---	0.2	---	---	---	---	14	---	---	---	---	---	4.72
ER-EC-7	---	21-Jul-03	<0.05	20.7	<0.04	---	---	---	<6	<20	<24	81	2.4	---	---	4	<14	1.86
ER-EC-7	---	5-Jun-00	0.4	13	0.23	---	---	---	---	---	---	160	---	---	---	---	---	2.10
ER-EC-8	---	1-Jul-03	<0.05	28.4	<0.04	---	0.6	---	<6	<20	<24	2.2	10	---	---	2	<14	4.81
ER-EC-8	---	12-Jul-00	0.2	22	0.11	---	---	---	---	---	---	41	---	---	---	---	---	4.80
ER-18-2	---	17-Jun-03	0.3	26.1	<0.04	---	1.4	---	25	42	27	212	7.8	---	---	15	<14	8.53
ER-18-2	---	21-Mar-00	<0.4	22	0.06	---	0.4	---	---	---	---	230	---	---	---	---	---	7.26

Table 2.4 Environmental well trace metal data.

Well name	Test	Sample date	V	Cr	Co	Ni	Cu	Zn	Br	Rb	Nb	Tc	Ru	Ag	Cd	Sn	Cs	Eu	W	Hg	Tl
Unit			*(mg/L)*	*(mg/L)*	*(mg/L)*	*(mg/L)*	*(mg/L)*	*(mg/L)*	*(mg/L)*	*(mg/L)*	*(mg/L)*	*(ng/L)*	*(mg/L)*	*(mg/L)*	*(mg/L)*	*(mg/L)*	*(mg/L)*	*(mg/L)*	*(mg/L)*	*(mg/L)*	*(mg/L)*
Clean Wells - Frenchman Flat																					
Water Well 5a	---	14-Aug-00	---	---	---	---	---	---	---	---	---	---	---	---	---	---	---	---	---	---	---
Water Well 5c	---	7-Aug-00	---	---	---	---	---	---	---	---	---	---	---	---	---	---	---	---	---	---	---
Water Well 5b	---	7-Aug-00	---	---	---	---	---	---	---	---	---	---	---	---	---	---	---	---	---	---	---
ER-5-4	---	5-Jul-01	---	---	---	---	---	---	---	---	---	---	---	---	---	---	---	---	---	---	---
ER-5-4 #2	---	21-Nov-02	---	---	---	---	---	---	---	---	---	---	---	---	---	---	---	---	---	---	---
UE-5c WW	---	8-Aug-00	---	---	---	---	---	---	---	---	---	---	---	---	---	---	---	---	---	---	---
UE-5 PW-3	---	9-Aug-00	---	---	---	---	---	---	---	---	---	---	---	---	---	---	---	---	---	---	---
ER-5-3	---	28-Mar-01	---	---	---	---	---	---	---	---	---	---	---	---	---	---	---	---	---	---	---
ER-5-3 #2	---	17-May-01	---	---	---	---	---	---	---	---	---	---	---	---	---	---	---	---	---	---	---
Water Well 4a	---	8-Aug-00	---	---	---	---	---	---	---	---	---	---	---	---	---	---	---	---	---	---	---
Clean Wells - Yucca Flat																					
ER-2-1	---	3-Sep-03	---	---	---	---	---	---	---	---	---	---	---	---	---	---	---	---	---	---	---
ER-6-1 #2	---	16-Jan-03	---	---	---	---	---	---	---	---	---	---	---	---	---	---	---	---	---	---	---
ER-6-2	---	4-Aug-04	4.1	0.08	10.8	21.7	BD	32.3	230	41	0.04	---	0.001	0.11	0.01	0.01	7.75	0.01	5.1	17.1	0.78
ER-7-1	---	17-Jul-03	---	---	---	---	---	---	---	---	---	---	---	---	---	---	---	---	---	---	---
WW2 (USGS HTH #2)	---	7-Sep-06	2.01	1.09	< 0.057	6.39	1.26	11.6	---	10.9	< 0.003	---	< 0.009	< 0.5	< 0.03	< 0.034	0.158	< 0.011	0.4	---	< 0.0333
Clean Wells - Rainier Mesa																					
ER-12-1	---	8-Dec-04	0.6	0.10	0.41	15.2	BD	6.5	702	7.7	0.01	---	0.002	0.004	0.01	0.03	0.17	BD	1.6	1.4	0.004
ER-12-2	---	1-Apr-03	---	---	---	---	---	---	---	---	---	---	---	---	---	---	---	---	---	---	---
ER-12-3	---	6-Jul-05	2.2	< 0.24	< 0.27	<2.9	< 0.9	259	---	7.3	< 0.042	---	< 0.3	< 0.24	< 0.6	---	< 0.99	< 0.012	2.51	---	0.17
ER-12-4	---	25-Apr-06	2.78	0.52	< 0.21	48.6	1.8	320	---	10.12	< 0.054	---	< 0.42	< 0.12	< 0.39	< 0.09	0.44	< 0.006	1.25	---	0.037
ER-12-4	---	16-Aug-05	1.2	1.6	< 0.36	14.1	5.8	538	---	10.3	< 0.24	---	< 0.27	< 0.18	< 0.33	---	< 0.9	< 0.006	1.37	---	< 0.04
U12S	---	22-Aug-06	3.7	0.73	< 0.09	2.88	1.88	13.4	---	4.31	< 0.0054	---	< 0.018	< 0.5	< 0.039	< 0.05	< 0.07	< 0.024	0.9	---	< 0.03
Springs - Rainier Mesa																					
White Rock Springs	---	26-Sep-06	4.29	0.65	< 0.042	< 0.21	0.79	30.3	---	17.4	0.046	---	< 0.009	< 0.5	< 0.033	< 0.052	0.324	< 0.039	< 0.148	---	< 0.068
Captain Jack Springs	---	27-Sep-06	1.4	0.58	< 0.036	< 0.12	< 0.25	1.5	---	6.7	< 0.0036	---	< 0.012	< 0.5	< 0.039	< 0.042	0.197	< 0.0123	< 0.124	---	< 0.046
Springs																					
Topopah Springs	---	28-Sep-06	1.9	1.14	< 0.054	< 0.3	< 0.42	1.29	---	13.6	0.084	---	< 0.006	< 0.5	< 0.057	< 0.063	1.44	< 0.019	< 0.17	---	< 0.05
Clean Wells - Pahute Mesa-Oasis Valley																					
ER-EC-1	---	3-Jun-03	---	---	---	---	---	---	---	---	---	---	---	---	---	---	---	---	---	---	---
ER-EC-1	---	1-Feb-00	---	---	---	---	---	---	---	---	---	---	---	---	---	---	---	---	---	---	---
ER-EC-2A	---	8-Jul-03	---	---	---	---	---	---	---	---	---	---	---	---	---	---	---	---	---	---	---
ER-EC-2A	---	27-Jul-00	---	---	---	---	---	---	---	---	---	---	---	---	---	---	---	---	---	---	---
ER-EC-4	---	24-Jun-03	---	---	---	---	---	---	---	---	---	---	---	---	---	---	---	---	---	---	---
ER-EC-4	---	17-Aug-00	---	---	---	---	---	---	---	---	---	---	---	---	---	---	---	---	---	---	---
ER-EC-5	---	15-Jul-03	---	---	---	---	---	---	---	---	---	---	---	---	---	---	---	---	---	---	---
ER-EC-5	---	25-May-00	---	---	---	---	---	---	---	---	---	---	---	---	---	---	---	---	---	---	---
ER-EC-6	---	10-Jun-03	---	---	---	---	---	---	---	---	---	---	---	---	---	---	---	---	---	---	---
ER-EC-6	---	10-Feb-00	---	---	---	---	---	---	---	---	---	---	---	---	---	---	---	---	---	---	---
ER-EC-7	---	21-Jul-03	---	---	---	---	---	---	---	---	---	---	---	---	---	---	---	---	---	---	---
ER-EC-7	---	5-Jun-00	---	---	---	---	---	---	---	---	---	---	---	---	---	---	---	---	---	---	---
ER-EC-8	---	1-Jul-03	---	---	---	---	---	---	---	---	---	---	---	---	---	---	---	---	---	---	---
ER-EC-8	---	12-Jul-00	---	---	---	---	---	---	---	---	---	---	---	---	---	---	---	---	---	---	---
ER-18-2	---	17-Jun-03	---	---	---	---	---	---	---	---	---	---	---	---	---	---	---	---	---	---	---
ER-18-2	---	21-Mar-00	---	---	---	---	---	---	---	---	---	---	---	---	---	---	---	---	---	---	---

Table 2.5 Stable Isotope Data

Well name	Test	Sample date	δD_{SMOW}	$\delta^{18}O_{SMOW}$	TIC	TOC	$\delta^{13}C_{PDB}$ TIC	$\delta^{13}C_{PDB}$ TOC	^{3}He	^{4}He	R/R_a	Ne total	Ar total	Kr total	Xe total	$^{87}Sr/^{86}Sr$	$\delta^{87}Sr$
		fixed	*‰*	*‰*	*ppm C*	*ppm C*	*‰*	*‰*	*atoms/g*	*atoms/g*	*$^{3}He/^{4}He$ sample/air*	*atoms/g*	*atoms/g*	*atoms/g*	*atoms/g*	*ratio*	*‰*
Clean Wells - Frenchman Flat																	
Water Well 5a	---	14-Aug-00	-110	-13.8	62	---	-4.8	---	4.62E+06	3.16E+12	1.06	1.04E+13	1.59E+16	---	---	---	---
Water Well 5c	---	7-Aug-00	-110.5	-14.0	60	---	-6.0	---	3.41E+06	8.67E+12	0.28	6.23E+12	9.90E+15	---	---	---	---
Water Well 5b	---	7-Aug-00	-108	-13.1	34	---	-9.5	---	3.85E+06	3.90E+12	0.71	6.10E+12	9.04E+15	---	---	---	---
ER-5-4	---	5-Jul-01	-109	-13.6	62	---	-4.6	---	4.10E+06	5.45E+13	0.054	1.00E+13	1.09E+16	2.10E+12	2.90E+11	0.71056	1.92
ER-5-4 #2	---	21-Nov-02	-101	-13.3	78	---	+0.2	---	1.65E+06	1.35E+12	0.89	4.97E+12	8.25E+15	1.81E+12	2.43E+11	0.70902	-0.25
UE-5c WW	---	8-Aug-00	-106.5	-13.7	35	---	-7.2	---	5.18E+06	1.89E+13	0.20	5.42E+12	8.85E+15	---	---	---	---
UE-5 PW-3	---	9-Aug-00	-105.5	-13.5	30	---	-7.5	---	4.34E+06	2.15E+12	1.46	7.77E+12	1.15E+16	---	---	---	---
ER-5-3	---	28-Mar-01	-108.5	-14.1	33	---	-8.0	---	3.09E+06	5.20E+12	0.43	9.33E+12	9.87E+15	---	---	0.71017	1.37
ER-5-3 #2	---	17-May-01	-110	-14.1	157	---	-4.3	---	2.42E+07	1.28E+13	1.37	5.00E+12	4.75E+15	1.02E+12	1.34E+11	0.71538	8.71
Water Well 4a	---	8-Aug-00	-101	-12.8	31	---	-8.4	---	2.42E+06	3.16E+12	0.55	5.14E+12	8.02E+15	---	---	---	---
Clean Wells - Yucca Flat																	
ER-2-1	---	3-Sep-03	-109.5	-14.2	37	---	-12.1	---	7.36E+07	3.76E+12	14.2	7.65E+12	9.66E+15	2.02E+12	2.62E+11	0.71210	4.09
ER-6-1 #2	---	16-Jan-03	-105	-14.1	50	---	-5.9	---	---	---	---	---	---	---	---	0.71295	5.29
ER-6-2	---	4-Aug-04	-105	-14.1	85	---	-4.0	---	6.67E+06	7.05E+12	0.68	4.06E+12	5.15E+15	1.19E+12	1.70E+11	0.71281	5.09
ER-7-1	---	17-Jul-03	-106	-14.1	48	---	-5.8	---	3.28E+07	4.07E+13	0.58	4.79E+12	7.43E+15	1.81E+12	2.66E+11	0.71306	5.44
WW2 (USGS HTH #2)	---	7-Sep-06	-104	-14.1	33.5	0.7	-8.8	-23.5	4.74E+06	1.50E+13	0.23	4.55E+12	6.85E+15	1.53E+12	2.12E+11	0.71311	5.51
Clean Wells - Rainier Mesa																	
ER-12-1	---	8-Dec-04	-94.5	-12.6	51	---	-10.7	---	4.24E+06	6.84E+12	0.45	1.12E+13	1.28E+16	2.67E+12	3.65E+11	0.71230	4.37
ER-12-2	---	1-Apr-03	-101	-13.5	60	---	-4.9	---	3.51E+06	9.24E+13	0.03	8.08E+12	1.03E+16	1.91E+12	1.16E+11	0.71662	10.46
ER-12-3	---	6-Jul-05	-106	-14.5	25	---	-5.4	---	3.24E+06	1.79E+13	0.13	8.07E+12	9.73E+15	2.14E+12	2.83E+11	0.71055	1.90
ER-12-4	---	25-Apr-06	-100	-13.9	14.1	1.0	-6.7	-25.6	1.41E+06	1.62E+12	0.63	4.31E+12	6.46E+15	1.53E+12	2.39E+11	0.71087	2.35
ER-12-4	---	16-Aug-05	-103	-13.7	17	---	-7.6	---	7.81E+05	1.08E+12	0.52	4.95E+12	7.66E+15	1.82E+12	2.89E+11	0.71065	2.04
U12S	---	22-Aug-06	-97	-13.1	8.5	1.8	-15.2	-25.8	5.74E+07	5.43E+13	0.77	2.22E+14	3.73E+16	1.29E+13	1.39E+12	0.70544	-5.30
Springs - Rainier Mesa																	
White Rock Springs	---	26-Sep-06	-96	-12.9	15.5	1.3	-10.2	-22.1	---	---	---	---	---	---	---	0.70975	0.78
Captain Jack Springs	---	27-Sep-06	-103	-13.9	16.7	3.2	-10.7	-24.0	---	---	---	---	---	---	---	0.70988	0.96
Springs																	
Topopah Springs	---	28-Sep-06	-91	-12.6	15.4	2.5	-13.9	-24.1	---	---	---	---	---	---	---	0.71175	3.60
Clean Wells - Pahute Mesa-Oasis Valley																	
ER-EC-1	---	3-Jun-03	-116	-14.9	29	---	-3.1	---	9.44E+06	1.13E+13	0.60	7.21E+12	7.68E+15	1.58E+12	2.29E+11	0.71056	1.92
ER-EC-1	---	1-Feb-00	-116	-14.8	29	---	-4.0	---	9.03E+06	9.24E+12	0.71	9.93E+12	9.11E+15	---	2.34E+11	0.71023	1.45
ER-EC-1	---	1-Feb-00							9.03E+06	9.24E+12	0.71	8.05E+12	---	---	---		
ER-EC-2A	---	8-Jul-03	-116.5	-14.9	32	---	-2.0	---	8.36E+06	6.97E+12	0.87	4.28E+12	5.68E+15	1.21E+12	1.93E+11	0.70912	-0.11
ER-EC-2A	---	27-Jul-00	-116	-14.9	34	---	-1.5	---	1.03E+07	7.92E+12	0.94	1.07E+13	1.02E+16	---	---	0.70939	0.26
ER-EC-4	---	24-Jun-03	-114	-14.6	30	---	-1.1	---	2.00E+07	1.41E+13	1.02	6.78E+12	7.15E+15	1.42E+12	1.97E+11	0.71010	1.27
ER-EC-4	---	17-Aug-00	-115	-14.6	31	---	-1.5	---	1.83E+07	1.30E+13	1.01	7.66E+12	8.55E+15	---	---	0.70998	1.11
ER-EC-5	---	15-Jul-03	-113	-14.9	35	---	-2.8	---	9.77E+06	6.07E+12	1.16	5.23E+12	6.53E+15	1.34E+12	1.96E+11	0.70916	-0.06
ER-EC-5	---	25-May-00	-113	-14.9	35	---	-2.5	---	1.06E+07	7.09E+12	1.08	8.88E+12	9.51E+15	---	1.84E+11	0.70912	-0.11
ER-EC-6	---	10-Jul-03	-117	-15.0	29	---	-2.7	---	1.72E+07	1.79E+13	0.69	4.76E+12	6.63E+15	1.49E+12	2.26E+11	0.71038	1.66
ER-EC-6	---	10-Feb-00	-116	-15.0	30	---	-3.4	---	1.76E+07	1.75E+13	0.73	6.90E+12	8.78E+15	---	2.29E+11	0.70982	0.88
ER-EC-7	---	21-Jul-03	-98	-13.2	17	---	-5.5	---	6.81E+06	5.87E+12	0.84	5.38E+12	7.41E+15	1.59E+12	2.22E+11	0.70948	0.39
ER-EC-7	---	5-Jun-00	-98	-13.2	23	---	-6.3	---	8.81E+06	7.46E+12	0.86	7.44E+12	8.23E+15	---	2.35E+11	0.70932	0.17
ER-EC-8	---	1-Jul-03	-115	-14.9	34	---	-0.9	---	5.18E+06	3.81E+12	0.98	4.68E+12	5.63E+15	1.13E+12	1.64E+11	0.70922	0.03
ER-EC-8	---	12-Jul-00	-116	-14.8	34	---	-1.0	---	6.43E+06	3.69E+12	1.26	5.16E+12	6.46E+15	---	---	0.70882	-0.54
ER-18-2	---	17-Jun-03	-111	-14.7	173	---	-0.5	---	5.11E+08	1.83E+14	2.01	2.94E+12	3.51E+15	6.94E+11	1.08E+11	0.70877	-0.61
ER-18-2	---	21-Mar-00	-112	-14.7	171	---	-0.7	---	6.81E+08	1.70E+14	2.89	3.83E+12	4.22E+15	---	---	0.70861	-0.84

Table 2.6 Environmental well radiochemical data.

Well name	Test	Sample date	^{3}H	^{14}C	^{14}C	$^{36}Cl/Cl$	^{36}Cl
Unit		*date*	*(pCi/L)*	*(pmc)*	*(pCi/L)*	*ratio*	*(pCi/L)*
Half-life (a)		*collected*	*12.32*	*5730*	*5730*		*3.01E+05*
Ref. date		*in field*	*collect.*	*collect.*	*collect.*		*collect.*
Clean Wells - Frenchman Flat							
Water Well 5a	---	14-Aug-00	1.5	2.60E+00	9.64E-03	8.43E-13	3.1E-04
Water Well 5c	---	7-Aug-00	< 1.5	3.40E+00	1.24E-02	---	---
Water Well 5b	---	7-Aug-00	< 1.5	1.31E+01	2.68E-02	7.83E-13	6.0E-04
ER-5-4	---	5-Jul-01	2.5	1.50E+00	5.72E-03	3.94E-13	3.5E-04
ER-5-4 #2	---	21-Nov-02	156.8	1.00E+00	4.69E-03	1.76E-13	3.0E-04
UE-5c WW	---	8-Aug-00	< 1.5	6.50E+00	1.39E-02	---	---
UE-5 PW-3	---	9-Aug-00	< 1.5	1.60E+01	2.94E-02	---	---
ER-5-3	---	28-Mar-01	<1.5	8.50E+00	1.73E-02	8.42E-13	4.3E-04
ER-5-3 #2	---	17-May-01	<1.5	1.60E+00	1.55E-02	2.29E-13	2.9E-04
Water Well 4a	---	8-Aug-00	< 1.5	1.83E+01	3.45E-02	6.47E-13	4.4E-04
Clean Wells - Yucca Flat							
ER-2-1	---	3-Sep-03	227.7	1.82E+01	4.14E-02	7.19E-13	1.04E-04
ER-6-1 #2	---	16-Jan-03	≤ 30.8	2.40E+00	7.39E-03	4.33E-13	1.4E-04
ER-6-2	---	4-Aug-04	92.2	1.56E+00	8.12E-03	2.00E-13	1.6E-04
ER-7-1	---	17-Jul-03	117.2	5.30E+00	1.56E-02	3.77E-13	1.18E-04
WW2 (USGS HTH #2)	---	7-Sep-06	< 1	N/A*	N/A*	6.4E-13	1.5E-04
Clean Wells - Rainier Mesa							
ER-12-1	---	8-Dec-04	3.2	1.10E+01	3.40E-02	7.80E-13	4.56E-04
ER-12-2	---	1-Apr-03	4.3	1.50E+00	5.39E-03	6.90E-13	1.6E-04
ER-12-3	---	6-Jul-05	0.5	2.95E+00	4.43E-03	5.39E-13	1.0E-04
ER-12-4	---	25-Apr-06	< 1	N/A*	N/A*	5.70E-13	1.7E-04
ER-12-4	---	16-Aug-05	89.7	6.86E+00	6.93E-03	5.56E-13	1.7E-04
U12S	---	22-Aug-06	< 1	N/A*	N/A*	1.2E-12	3.7E-04
Springs - Rainier Mesa							
White Rock Springs	---	26-Sep-06	4.92	N/A*	N/A*	4.0E-11	2.0E-02
Captain Jack Springs	---	27-Sep-06	< 1	N/A*	N/A*	2.5E-11	3.54E-03
Springs							
Topopah Springs	---	28-Sep-06	12.48	N/A*	N/A*	5.1E-12	3.7E-04
Clean Wells - Pahute Mesa-Oasis Valley							
ER-EC-1	---	3-Jun-03	≤ 174	7.20E+00	1.28E-02	5.14E-13	1.64E-03
ER-EC-1	---	1-Feb-00	<1.5	5.90E+00	1.05E-02	5.46E-13	1.75E-03
ER-EC-2A	---	8-Jul-03	≤ 93	7.70E+00	1.52E-02	5.02E-13	9.15E-04
ER-EC-2A	---	27-Jul-00	<1.5	7.70E+00	1.58E-02	5.33E-13	1.11E-03
ER-EC-4	---	24-Jun-03	<1.5	5.90E+00	1.07E-02	4.80E-13	1.28E-03
ER-EC-4	---	17-Aug-00	<1.5	5.00E+00	9.54E-03	5.61E-13	1.77E-03
ER-EC-5	---	15-Jul-03	≤ 9.0	7.50E+00	1.62E-02	5.61E-13	2.95E-04
ER-EC-5	---	25-May-00	<1.5	6.30E+00	1.33E-02	6.53E-13	3.5E-04
ER-EC-6	---	10-Jun-03	≤ 64	6.60E+00	1.17E-02	5.07E-13	8.65E-04
ER-EC-6	---	10-Feb-00	<1.5	5.40E+00	9.86E-03	5.41E-13	7.9E-04
ER-EC-7	---	21-Jul-03	1.6	4.62E+01	4.80E-02	7.55E-13	9.47E-05
ER-EC-7	---	5-Jun-00	<1.5	3.65E+01	5.22E-02	1.18E-12	2.0E-04
ER-EC-8	---	1-Jul-03	5.4	8.00E+00	1.68E-02	4.90E-13	7.65E-04
ER-EC-8	---	12-Jul-00	<1.5	8.70E+00	1.80E-02	4.63E-13	8.8E-04
ER-18-2	---	17-Jun-03	<1.5	4.00E-01	4.13E-03	2.31E-13	9.38E-05
ER-18-2	---	21-Mar-00	<1.5	1.60E+00	1.70E-02	3.02E-13	1.3E-04

N/A* Data will be provided in the FY07 HRMP report when analyses are complete.

Table 2.7 Environmental well radiochemical data.

Well name	Test	Sample date	$^{234}U/^{238}U$	$^{234}U/^{238}U$ activity ratio	$^{234}U/^{235}U$	$^{235}U/^{238}U$	^{234}U	^{235}U	^{238}U
Unit *Half-life (a)* *Ref. date*		*date collected in field*	*ratio*	*ratio*	*ratio*	*ratio*	*(pCi/L)* *2.46E+05* *collect.*	*(pCi/L)* *7.04E+08* *collect.*	*(pCi/L)* *4.47E+09* *collect.*
Clean Wells - Frenchman Flat									
Water Well 5a	---	14-Aug-00	---	---	---	---	---	---	---
Water Well 5c	---	7-Aug-00	---	---	---	---	---	---	---
Water Well 5b	---	7-Aug-00	---	---	---	---	---	---	---
ER-5-4	---	5-Jul-01	7.46E-05	1.36	1.03E-02	7.25E-03	7.30E-01	2.50E-02	5.30E-01
ER-5-4 #2	---	21-Nov-02	7.19E-05	1.31	9.92E-03	7.25E-03	1.61E+01	5.70E-01	1.22E+01
UE-5c WW	---	8-Aug-00	---	---	---	---	---	---	---
UE-5 PW-3	---	9-Aug-00	---	---	---	---	---	---	---
ER-5-3	---	28-Mar-01	1.86E-04	3.40	2.57E-02	7.26E-03	1.12E+00	1.50E-02	3.30E-01
ER-5-3 #2	---	17-May-01	1.80E-04	3.29	2.48E-02	7.26E-03	5.60E-01	8.00E-03	1.70E-01
Water Well 4a	---	8-Aug-00	---	---	---	---	---	---	---
Clean Wells - Yucca Flat									
ER-2-1	---	3-Sep-03	1.48E-04	2.71	2.04E-02	7.25E-03	3.11E+00	5.30E-02	1.14E+00
ER-6-1 #2	---	16-Jan-03	2.30E-04	4.19	3.17E-02	7.25E-03	4.55E+00	5.00E-02	1.07E+00
ER-6-2	---	4-Aug-04	2.39E-04	4.35	3.30E-02	7.25E-03	3.20E+00	3.40E-02	7.24E-01
ER-7-1	---	17-Jul-03	1.88E-04	3.43	2.59E-02	7.25E-03	1.33E+00	1.80E-02	3.83E-01
WW2 (USGS HTH #2)	---	7-Sep-06	2.52E-04	4.59	3.48E-02	7.25E-03	1.61E+00	1.61E-02	3.45E-01
Clean Wells - Rainier Mesa									
ER-12-1	---	8-Dec-04	3.79E-04	1.62	5.22E-02	7.25E-03	1.43E+00	4.21E-02	8.68E-01
ER-12-2	---	1-Apr-03	1.79E-04	3.26	2.45E-02	7.30E-03	1.90E-02	2.70E-04	5.70E-03
ER-12-3	---	6-Jul-05	1.15E-04	2.09	1.58E-02	7.26E-03	1.30E+00	2.90E-02	6.12E-01
ER-12-4	---	25-Apr-06	1.14E-04	2.077	1.57E-02	7.26E-03	2.60E-01	5.76E-03	1.24E-01
ER-12-4	---	16-Aug-05	1.06E-04	1.93	1.46E-02	7.24E-03	1.92E-01	5.00E-03	9.90E-02
U12S	---	22-Aug-06	1.21E-04	2.21	1.67E-02	7.26E-03	6.89E-01	1.44E-02	3.08E-01
Springs - Rainier Mesa									
White Rock Springs	---	26-Sep-06	1.03E-04	1.88	1.42E-02	7.26E-03	9.97E-01	2.44E-02	5.23E-01
Captain Jack Springs	---	27-Sep-06	1.50E-04	2.73	2.06E-02	7.26E-03	6.21E-01	1.05E-02	2.24E-01
Springs									
Topopah Springs	---	28-Sep-06	1.06E-04	1.92	1.46E-02	7.25E-03	1.97E-01	4.70E-03	1.01E-01
Clean Wells - Pahute Mesa-Oasis Valley									
ER-EC-1	---	3-Jun-03	1.94E-04	3.54	2.66E-02	7.27E-03	1.13E+01	1.48E-01	3.17E+00
ER-EC-1	---	1-Feb-00	2.10E-04	3.82	2.89E-02	7.25E-03	1.05E+01	1.26E-01	2.71E+00
ER-EC-2A	---	8-Jul-03	2.74E-04	5.01	3.78E-02	7.25E-03	1.19E+01	1.10E-01	2.35E+00
ER-EC-2A	---	27-Jul-00	2.25E-04	4.11	3.09E-02	7.27E-03	1.28E+01	1.44E-01	3.08E+00
ER-EC-4	---	24-Jun-03	1.59E-04	2.90	2.19E-02	7.27E-03	3.99E+00	6.40E-02	1.36E+00
ER-EC-4	---	17-Aug-00	1.59E-04	2.90	2.18E-02	7.29E-03	3.97E+00	6.40E-02	1.39E+00
ER-EC-5	---	15-Jul-03	3.53E-04	6.45	4.85E-02	7.27E-03	7.27E+00	5.20E-02	1.12E+00
ER-EC-5	---	25-May-00	3.51E-04	6.41	4.82E-02	7.28E-03	7.20E+00	5.20E-02	1.11E+00
ER-EC-6	---	10-Jun-03	2.03E-04	3.71	2.80E-02	7.27E-03	6.79E+00	8.50E-02	1.81E+00
ER-EC-6	---	10-Feb-00	2.23E-04	4.07	3.07E-02	7.27E-03	6.52E+00	7.40E-02	1.58E+00
ER-EC-7	---	21-Jul-03	3.97E-04	7.26	5.48E-02	7.25E-03	4.57E+00	2.90E-02	6.22E-01
ER-EC-7	---	5-Jun-00	3.97E-04	7.26	5.46E-02	7.28E-03	5.19E+00	3.30E-02	7.10E-01
ER-EC-8	---	1-Jul-03	2.77E-04	5.06	3.82E-02	7.24E-03	8.22E+00	7.50E-02	1.61E+00
ER-EC-8	---	12-Jul-00	2.78E-04	5.08	3.82E-02	7.28E-03	8.18E+00	7.40E-02	1.59E+00
ER-18-2	---	17-Jun-03	6.98E-04	12.76	9.59E-02	7.29E-03	3.67E+01	1.33E-01	2.85E+00
ER-18-2	---	21-Mar-00	6.95E-04	12.70	9.56E-02	7.27E-03	3.54E+01	1.29E-01	2.76E+00

CHAPTER 3

Noble Gas Data

R. Lindvall, M. Zavarin

Chemical Sciences Division, Chemistry, Materials, Earth and Life Sciences
Lawrence Livermore National Laboratory

The following is a compilation of noble gas data collected by LLNL. **Table 1** is recently updated data from tables that appeared in the LLNL HRMP FY 2005 Progress Report. The noble gas data in the tables in the LLNL HRMP FY 2005 Progress Report contain errors and should not be used. Starting with this FY2006 HRMP Progress Report, noble gases will only be presented as the elemental totals, and not as single isotopes. Therefore **Table 3.1** and **Table 3.2** can serve as a reference link between the old and the new formats. **Table 3.3** contains historical data not presented in the HRMP reports. This is not a comprehensive list of all samples analyzed, but rather analyses that LLNL has been able to verify through archived data.

Table 3.1 Corrected Noble Gas Data for Hot Well Samples

Well name	Test	Sample date	^{20}Ne	Ne total	^{40}Ar	Ar total	Kr	^{130}Xe	Xe total
Unit			*atoms/g*	*atoms/g*	*atoms/g*	*atoms/g*	*atoms/g*	*atoms/g*	*atoms/g*
Hot Wells - Frenchman Flat									
UE5n	CAMBRIC	12-Feb-04	---	---	---	---	---	---	---
UE5n	CAMBRIC	19-Apr-01	4.66E+12	5.15E+12	8.30E+15	8.33E+15	---	1.14E+10	2.78E+11
UE5n	CAMBRIC	9-Sep-99	7.25E+12	8.01E+12	1.04E+16	1.04E+16	---	1.19E+10	2.90E+11
RNM-1	CAMBRIC	3-Jun-04	---	---	---	---	---	---	---
RNM-1	CAMBRIC	28-Jun-00	4.15E+12	4.58E+12	7.63E+15	7.66E+15	---	---	---
RNM-2S	CAMBRIC	10-Jul-03	6.49E+13	7.17E+13	---	---	---	3.63E+10	8.85E+11
RNM-2S	CAMBRIC	9-May-03	3.02E+12	3.34E+12	---	---	---	1.35E+10	3.29E+11
RNM-2S	CAMBRIC	14-Jun-00	5.50E+12	6.08E+12	9.11E+15	9.15E+15	---	---	---
RNM-2S	CAMBRIC	11-Oct-99	4.35E+12	4.81E+12	8.05E+15	8.08E+15	---	---	---
Hot Wells - Yucca Flat									
U4u PS2a	DALHART	9-Oct-03	1.20E+13	1.33E+13	---	---	---	1.08E+10	2.63E+11
U4u PS2a	DALHART	16-Aug-99	---	---	---	---	---	---	---
UE-7ns	BOURBON	13-Dec-05	---	---	---	---	---	---	---
UE-7ns	BOURBON	21-Aug-01	6.52E+12	7.21E+12	9.30E+15	9.34E+15	---	1.10E+10	2.68E+11
UE-2ce	NASH	12-Jul-05	---	---	---	---	---	---	---
UE-2ce	NASH	22-Aug-01	7.14E+12	7.89E+12	9.31E+15	9.35E+15	---	1.09E+10	2.66E+11
U-3cn PS#2	BILBY	28-Nov-03	---	---	---	---	---	---	---
U-3cn PS#2	BILBY	9-Dec-04	---	---	---	---	---	---	---
U-3cn PS#2	BILBY	18-Dec-01	7.41E+12	8.19E+12	9.30E+15	9.34E+15	---	1.00E+10	2.44E+11
Hot Wells - Pahute Mesa									
U20n PS1 DDh	CHESHIRE	15-Nov-05	---	---	---	---	---	---	---
U20n PS1 DDh	CHESHIRE	9-Jul-03	5.63E+12	6.22E+12	---	---	---	1.24E+10	3.02E+11
U20n PS1 DDh	CHESHIRE	12-Oct-99	5.70E+12	6.30E+12	6.45E+15	6.48E+15	---	---	---
U19ad PS1a	CHANCELLOR	27-Sep-04	---	---	---	---	---	---	---
U19q PS1d	CAMEMBERT	16-Jul-03	---	---	---	---	---	---	---
U19q PS1d	CAMEMBERT	21-Oct-98	7.73E+12	8.54E+12	---	---	---	---	---
U19v PS1ds	ALMENDRO	18-Apr-06	---	---	---	---	---	---	---
U19v PS1ds	ALMENDRO	23-Jul-03	5.19E+12	5.74E+12	---	---	---	1.69E+10	4.12E+11
U19v PS1ds	ALMENDRO	31-May-01	4.42E+12	4.89E+12	1.44E+16	1.45E+16	---	3.86E+10	9.41E+11
U19v PS1ds	ALMENDRO	26-Sep-00	---	---	---	---	---	---	---
U19v PS1ds	ALMENDRO	18-Aug-99	---	---	---	---	---	---	---
ER-20-5 #1	TYBO/BENHAM†	30-Nov-04	---	---	---	---	---	---	---
ER-20-5 #1	TYBO/BENHAM†	9-Jul-98	7.55E+12	8.34E+12	---	---	---	---	---
ER-20-5 #3	TYBO/BENHAM†	29-Nov-04	---	---	---	---	---	---	---
ER-20-5 #3	TYBO/BENHAM†	15-Nov-01	7.49E+12	8.28E+12	---	---	---	1.13E+10	2.76E+11
ER-20-5 #3	TYBO/BENHAM†	30-Apr-98	1.07E+13	1.18E+13	---	---	---	---	---
PM-2, 865	SCHOONER	26-Oct-05	---	---	---	---	---	---	---
PM-2, 985	SCHOONER	26-Oct-05	---	---	---	---	---	---	---
PM-2, 1970, main	SCHOONER	26-Oct-05	---	---	---	---	---	---	---
PM-2, 2625-1300	Schooner	26-Oct-05	---	---	---	---	---	---	---

† Both the TYBO and BENHAM tests are listed since the ER-20-5 well cluster was drilled in the near-field (~300 m from the surface ground zero) environment of the TYBO test.

Table 3.2 Corrected Noble Gas Data for Environmental Samples

Well name	Test	Sample date	^{20}Ne	Ne total	^{40}Ar	Ar total	Kr	^{130}Xe	Xe total
Unit			*atoms/g*	*atoms/g*	*atoms/g*	*atoms/g*	*atoms/g*	*atoms/g*	*atoms/g*
Clean Wells - Frenchman Flat									
Water Well 5a	---	14-Aug-00	9.43E+12	1.04E+13	1.58E+16	1.59E+16	---	---	---
Water Well 5c	---	7-Aug-00	5.64E+12	6.23E+12	9.86E+15	9.90E+15	---	---	---
Water Well 5b	---	7-Aug-00	5.52E+12	6.10E+12	9.00E+15	9.04E+15	---	---	---
ER-5-4	---	5-Jul-01	9.05E+12	1.00E+13	1.09E+16	1.09E+16	2.10E+12	1.19E+10	2.90E+11
ER-5-4 #2	---	21-Nov-02	4.50E+12	4.97E+12	8.22E+15	8.25E+15	1.81E+12	9.97E+09	2.43E+11
UE-5c WW	---	8-Aug-00	4.91E+12	5.42E+12	8.81E+15	8.85E+15	---	---	---
UE-5 PW-3	---	9-Aug-00	7.03E+12	7.77E+12	1.15E+16	1.15E+16	---	---	---
ER-5-3	---	28-Mar-01	8.44E+12	9.33E+12	9.83E+15	9.87E+15	---	---	---
ER-5-3 #2	---	17-May-01	4.52E+12	5.00E+12	4.73E+15	4.75E+15	1.02E+12	5.49E+09	1.34E+11
Water Well 4a	---	8-Aug-00	4.65E+12	5.14E+12	7.99E+15	8.02E+15	---	---	---
Clean Wells - Yucca Flat									
ER-2-1	---	3-Sep-03	6.92E+12	7.65E+12	9.62E+15	9.66E+15	2.02E+12	1.07E+10	2.62E+11
ER-6-1 #2	---	16-Jan-03	---	---	---	---	---	---	---
ER-6-2	---	4-Aug-04	3.68E+12	4.06E+12	5.13E+15	5.15E+15	1.19E+12	6.97E+09	1.70E+11
ER-7-1	---	17-Jul-03	4.33E+12	4.79E+12	7.40E+15	7.43E+15	1.81E+12	1.09E+10	2.66E+11
WW2 (USGS HTH #2)	---	7-Sep-06	4.12E+12	4.55E+12	6.82E+15	6.85E+15	1.53E+12	8.69E+09	2.12E+11
Clean Wells - Rainier Mesa									
ER-12-1	---	8-Dec-04	1.02E+13	1.12E+13	1.27E+16	1.28E+16	2.67E+12	1.50E+10	3.65E+11
ER-12-2	---	1-Apr-03	7.31E+12	8.08E+12	1.03E+16	1.03E+16	1.91E+12	4.77E+09	1.16E+11
ER-12-3	---	6-Jul-05	7.30E+12	8.07E+12	9.69E+15	9.73E+15	2.14E+12	1.16E+10	2.83E+11
ER-12-4	---	25-Apr-06	3.90E+12	4.31E+12	6.43E+15	6.46E+15	1.53E+12	9.78E+09	2.39E+11
ER-12-4	---	16-Aug-05	4.48E+12	4.95E+12	7.63E+15	7.66E+15	1.82E+12	1.19E+10	2.89E+11
U12S	---	22-Aug-06	2.01E+14	2.22E+14	3.72E+16	3.73E+16	1.29E+13	5.69E+10	1.39E+12
Springs - Rainier Mesa									
White Rock Springs	---	26-Sep-06	---	---	---	---	---	---	---
Captain Jack Springs	---	27-Sep-06	---	---	---	---	---	---	---
Springs									
Topopah Springs	---	28-Sep-06	---	---	---	---	---	---	---
Clean Wells - Pahute Mesa-Oasis Valley									
ER-EC-1	---	3-Jun-03	6.53E+12	7.21E+12	7.65E+15	7.68E+15	1.58E+12	9.38E+09	2.29E+11
ER-EC-1	---	1-Feb-00	7.29E+12	8.05E+12	9.11E+15	9.11E+15	---	9.59E+09	2.34E+11
ER-EC-2A	---	8-Jul-03	3.87E+12	4.28E+12	5.66E+15	5.68E+15	1.21E+12	7.91E+09	1.93E+11
ER-EC-2A	---	27-Jul-00	9.68E+12	1.07E+13	1.02E+16	1.02E+16	---	---	---
ER-EC-4	---	24-Jun-03	6.14E+12	6.78E+12	7.12E+15	7.15E+15	1.42E+12	8.07E+09	1.97E+11
ER-EC-4	---	17-Aug-00	6.93E+12	7.66E+12	8.52E+15	8.55E+15	---	---	---
ER-EC-5	---	15-Jul-03	4.73E+12	5.23E+12	6.50E+15	6.53E+15	1.34E+12	8.03E+09	1.96E+11
ER-EC-5	---	25-May-00	8.03E+12	8.88E+12	9.47E+15	9.51E+15	---	7.54E+09	1.84E+11
ER-EC-6	---	10-Jul-03	4.31E+12	4.76E+12	6.60E+15	6.63E+15	1.49E+12	9.26E+09	2.26E+11
ER-EC-6	---	10-Feb-00	6.24E+12	6.90E+12	8.74E+15	8.78E+15	---	9.39E+09	2.29E+11
ER-EC-7	---	21-Jul-03	4.87E+12	5.38E+12	7.38E+15	7.41E+15	1.59E+12	9.11E+09	2.22E+11
ER-EC-7	---	5-Jun-00	6.73E+12	7.44E+12	8.20E+15	8.23E+15	---	9.64E+09	2.35E+11
ER-EC-8	---	1-Jul-03	4.23E+12	4.68E+12	5.61E+15	5.63E+15	1.13E+12	6.73E+09	1.64E+11
ER-EC-8	---	12-Jul-00	4.67E+12	5.16E+12	6.43E+15	6.46E+15	---	---	---
ER-18-2	---	17-Jun-03	2.66E+12	2.94E+12	3.50E+15	3.51E+15	6.94E+11	4.43E+09	1.08E+11
ER-18-2	---	21-Mar-00	3.46E+12	3.83E+12	4.20E+15	4.22E+15	---	---	---

Table 3.3 Verified Noble Gas Data for Historical Samples

Sample	Date	latitude	Longitude	Ne total (atoms/ml)	Ar total (atoms/ml)	Kr total (atoms/ml)	Xe total (atoms/ml)
Big Spring, Ash Meadows	9/6/95	36°22'30"	116°16'25"	4.50E+12	6.53E+15	1.45E+12	1.92E+11
Crystal Pool Spring, Ash Meadows	9/6/95	36°25'13"	116°19'23"	4.51E+12	6.72E+15	1.42E+12	1.99E+11
Fairbanks Spring, Ash Meadows	9/6/95	36°29'26"	116°20'28"	4.72E+12	6.76E+15	1.43E+12	2.03E+11
Army Well #1, NTS, Area 22	5/12/93	36°35'30"	116°02'14"	4.75E+12	7.39E+15	7.99E+23	2.34E+11
J-12 Well, NTS, Area 25	5/13/93	36°45'54"	116°23'24"	4.49E+12	6.92E+15	7.48E+23	2.13E+11
Water Well 5c, NTS, Area 5	5/20/93	36°47'20"	115°57'49"	5.01E+12	8.45E+15	1.96E+12	2.72E+11
J-13 Well, NTS, Area 25	5/13/93	36°48'28"	116°23'40"	4.47E+12	6.70E+15	1.45E+12	2.08E+11
UE-5c Well, NTS, Area 5	5/13/93	36°50'11"	115°58'47"	4.71E+12	7.77E+15	1.75E+12	2.42E+11
Water Well 4, NTS, Area 6	5/20/93	36°54'18"	116°01'26"	4.54E+12	7.18E+15	1.65E+12	2.21E+11
Water Well C-1, NTS, Area 6	5/19/93	36°55'07"	116°00'34"	3.64E+12	4.91E+15	1.04E+12	1.53E+11
Water Well C, NTS, Area 6	5/19/93	36°55'08"	116°00'35"	3.68E+12	5.03E+15	1.04E+12	1.54E+11
Bailey Hot Spring, Oasis Valley	9/7/95	36°58'27"	116°43'18"	3.85E+12	6.04E+15	1.34E+12	1.90E+11
ER-6-1 Well, NTS, Area 6	11/23/92	36°59'04"	115°59'34"	7.98E+12	9.29E+15	1.96E+12	2.68E+11
Goss Spring, Oasis Valley	9/7/95	36°59'45"	116°42'51"	4.33E+12	7.03E+15	1.53E+12	2.12E+11
ER-3-1 Well, NTS, Area 3, (9/95)	9/11/95	37°01'33"	115°56'13"	3.30E+12	4.27E+15	8.93E+11	1.38E+11
U3-cn #5 Well, NTS, Area 3	1/29/97	37°03'34"	116°01'20"	5.65E+12	8.45E+15	1.93E+12	2.87E+11
UE-1q Well, NTS, Area 1	7/10/92	37°03'37"	116°03'30"	4.86E+12	8.01E+15	1.82E+12	2.64E+11
ER-12-1 Well, NTS, Area 12	1/6/93	37°11'06"	116°11'03"	2.82E+13	2.61E+16	4.49E+12	5.14E+11
UE-10j Well, Composite, NTS, Area 8	10/3/93	37°11'08"	116°04'53"	9.00E+12	1.23E+16	2.57E+12	3.41E+11
UE-10j Well, Zone 2, NTS, Area 8	3/20/97	37°11'08"	116°04'53"	8.83E+12	1.10E+16	2.26E+12	2.91E+11
UE-10j Well, Zone 3, NTS, Area 8	3/24/97	37°11'08"	116°04'53"	6.06E+12	8.61E+15	1.79E+12	2.51E+11
Watertown #1 Well, Emigrant Valley	8/16/95	37°14'40"	115°48'33"	4.47E+12	7.24E+15	1.59E+12	2.31E+11
ER-20-6 #3 Well, NTS, Area 20	12/16/96	37°15'33"	116°25'16"	1.40E+13	1.41E+16	2.51E+12	3.18E+11
ER-20-6 #2 Well, NTS, Area 20	11/27/96	37°15'35"	116°25'16"	1.22E+13	1.45E+16	2.44E+12	3.09E+11
ER-20-6 #1 Well, NTS, Area 20	12/17/96	37°15'36"	116°25'15"	5.39E+12	7.11E+15	1.53E+12	2.28E+11
Watertown #3 Well, Emigrant Valley	8/15/95	37°15'39"	115°50'03"	4.69E+12	7.10E+12	1.80E+12	2.56E+11
UE-19c Well, NTS, Area 19	8/13/92	37°16'08"	116°19'10"	3.79E+12	7.59E+15	2.02E+12	3.08E+11
Watertown #4 Well, Emigrant Valley	8/15/95	37°17'17"	115°56'12"	4.38E+12	7.99E+15	1.88E+12	2.57E+11
Alamo City Well #7, Pahranagat Valley	8/8/95	37°21'44"	115°10'06"	5.17E+12	8.63E+15	1.88E+12	2.67E+11
Spencer Well, Pahranagat Valley	8/6/95	37°23'42"	115°10'49"	6.03E+12	9.21E+15	2.07E+12	2.70E+11
Little Ash Spring, Pahranagat Valley	8/8/95	37°27'49"	115°11'30"	3.96E+12	6.45E+15	1.46E+12	2.21E+11
Crystal Springs, Pahranagat Valley	8/7/95	37°31'55"	115°13'59"	9.16E+12	9.75E+15	1.97E+12	2.83E+11
Hiko Spring, Pahranagat Valley	8/7/95	37°35'54"	115°12'52"	4.94E+12	7.50E+15	2.07E+12	2.60E+11

CHAPTER 4

Radionuclide Sorption to Tuff and Carbonate Rock

Pihong Zhao[1], Guillermo Atilio Blasiyh Nuño[2], Mavrik Zavarin[1], Qinhong (Max) Hu[1], and Rachel E. Lindvall[1]

[1]Chemical Sciences Division, CMELS
Lawrence Livermore National Laboratory

[2] VYP Consultores S.A.
San Martin 793, Piso 2 "B"
C1004AAO Buenos Aires, Argentina

Abstract

Batch sorption and desorption experiments were performed to determine the distribution coefficients (K_d) of Pu(IV), Np(V), U(VI), Cs and Sr to zeolitized tuff (tuff confining unit, TCU) and carbonate (lower carbonate aquifer, LCA) rocks in synthetic NTS groundwater. Alkaline and alkaline earth radionuclides (Cs and Sr) have very high and reversible K_ds on zeolitic tuff and very low K_ds on carbonate rock. Actinides have higher K_ds on carbonate rock than zeolitized tuff. The sorption mechanism on carbonate rock does not appear to be reversible and may involve actinide co-precipitation during dissolution and re-crystallization of carbonate minerals. The K_d for Pu(IV) as a function of rock particle size was also investigated in this study. Tuff particle size has little to no effect on Pu(IV) K_d due to the high matrix porosity of the rock. Particle size does affect Pu(IV) sorption to carbonate rock; a positive correlation between surface area and Pu sorption was observed. Due to the very low porosity of intact carbonate rock and the correlation of K_d with particle size, it is likely that the actinide K_ds in the field will be much lower (1-2 orders of magnitude or more) than those measured here for carbonate rock.

4.1 Introduction

To evaluate the effect of underground nuclear testing on groundwater beneath the Yucca Flat/Climax Mine corrective action unit (CAU), Nevada Test Site (NTS), the Underground Test Area (UGTA) Project is developing flow and transport models to predict the movement of contaminants and define a contaminant boundary. These models require specific hydrogeologic and transport parameter data. This includes K_d data that can be used to predict the radionuclide retardation in groundwater.

In the Yucca Flat basin of the NTS, 747 underground nuclear tests were conducted primarily within the tuff confining unit or the overlying alluvium (U.S. D.O.E., 1992). It is expected that the low permeability TCU will minimize radionuclide migration to the regional lower carbonate aquifer (LCA) that underlies the TCU. However, radionuclide migration may take place through fractures or by porous flow when radiologic source terms are located near the tuff-carbonate

interface. To understand and predict the migration behavior of radionuclides through the tuff and into the regional carbonate aquifer, radionuclide distribution coefficients (K_ds) in tuff and carbonate rock matrixes must be examined. Several studies investigating the sorption and retardation of radionuclides on Yucca Flat rocks have recently been completed (Zavarin et al., 2005a, 2005b, 2006; Ware et al., 2005). A report by Farnham et al. (2007) documents extensive transport data and data analyses for Yucca Flat / Climax Mine CAU and provides the primary reference to support parameterization of the Yucca Flat/Climax Mine CAU transport model. However, data regarding radionuclide sorption to LCA rock are still lacking, particularly with regards to the effect of surface area.

In the present work, we have studied the sorption of five selected radionuclides (Pu(IV), Np(V), U(VI), Cs and Sr) onto crushed TCU and LCA rock in synthetic NTS groundwater. Distribution coefficients (K_d) were measured in sorption and desorption batch experiments. The K_ds from this work are compared with values in the literature and sorption mechanisms are discussed.

4.2 Material and Method

4.2.1 Rock characteristics

Two rock samples, one from the Tuff Confining Unit (TCU) and one from the Lower Carbonate Aquifer (LCA) were obtained from the NTS core library and used in our study. The TCU rock sample was selected from core UE-7ba, and the LCA rock was selected from core ER-6-1. The cores were crushed to grain sizes of 2 mm or less. The dry sieving method was used to separate crushed rock into three size fractions: <75 μm, 75-500 μm and 500μm – 2mm. The mineral phases in the solids were analyzed using x-ray diffraction on a Scintag PAD-V diffractometer. Detailed analysis of the procedures was previously described by Zavarin et al. (2005a). **Table 4.1** lists the parameters and mineralogy of the two core samples. The surface area of the samples was measured using the BET method (**Table 4.2**).

Table 4.1 TCU and LCA core parameters and mineralogy

Tuff Confining Unit (TCU)

Depth (ft)	Bulk Density g/cm^3	Porosity %	Quartz %	Cristobalite %	Illite %	Na-Ca Feldspar %	K Feldspar %	Zeolite* %
1626.2-1627.0	1.64	30.9	11	3	1	31	37	17

Lower Carbonate Aquifer (LCA)

Depth (ft)	Bulk Density g/cm^3	Porosity %	Calcite %	Dolomite %
2732.2-2733.1	2.79	1.6	17	83

* Clinoptilotite / Heulandite

Table 4.2 BET measurements

Rock	Sieve size	S.A. m^2/g
TCU	75μm	17.7 ± 0.3
	75-500 μm	13.9 ± 0.01
	500μm -2mm	13.9 ± 0.04
LCA	75μm	0.70 ± 0.01
	75-500 μm	0.13 ± 0.01
	500μm -2mm	0.028 ± 0.006

4.2.2 Sorption solutions

Synthetic NTS groundwaters were used in our sorption/desorption experiments. The synthetic solution compositions were based on previous fracture flow-through experiments conducted at LLNL on the same tuff and carbonate rock (Zavarin et al., 2005a). The major ions were analyzed using ion chromatography. Solution pH values and IC analyses results are listed in **Table 4.3**.

Table 4.3 Major cation constituents in synthetic solution

	pH	Na	K	Mg	Ca	F	Cl	NO_2^-	NO_3^-	SO_4^{2-}	PO_4^{3-}
		mg/L									
TCU	8.6	94.6	7.1	0.49	3.1	0.05	17.2	<0.02	0.26	0.66	<0.04
LCA	8.4	59.6	12.2	17.8	23.8	0.01	140.7	0.235	15.0	0.62	0.045

4.2.3 Radionuclides

Radionuclides ^{237}Np, ^{238}U and ^{242}Pu and stable isotopes ^{88}Sr and ^{133}Cs were used in the experiment. The selected radionuclides represent a wide range of radionuclide sorption behavior. The stock solutions used as radionuclide spikes were analyzed using ICP-MS. The concentration of each radionuclide was chosen based on a combination of instrument detection limits, expected background levels (for Cs, Sr, and U), solubility limits and sorption linearity.

4.2.4 Batch sorption / desorption experiments

Batch sorption and desorption experiments were performed to determine the distribution coefficients (K_d) of Pu(IV), Np(V), U(VI), Cs and Sr on rocks from the TCU and LCA using synthetic NTS groundwater. Duplicate experiments were performed for each radionuclide/rock pair. Each solution/rock mixture was equilibrated for one day prior to spiking with an acidified radionuclide stock solution. In an effort to minimize a shift in pH, an equivalent amount of NaOH solution was added to each mixture during spiking. Different liquid to solid ratios were used in batch experiments based on the anticipated sorption affinities of the selected radionuclides to the rock samples. The sorption experiments were run for 12 days, and aliquots for analysis were taken at 1, 4, 6 and 12 days. For each analysis, the samples were centrifuged and an aliquot of supernatant was withdrawn from the top of the tube and measured by ICP-MS. At the termination of the sorption experiment, all the fluid was removed by centrifugation, a fresh

aliquot of the same volume of the initial sorption solution was introduced. The desorption experiments were run for 15 days. The initial desorption samples were taken within 2 hours, and additional samples were collected and analyzed at 8 and 15 days. **Table 4** summarizes the initial conditions used for each sorption experiment.

The K_d of a radionuclide is calculated using Equation 1:

$$K_d = \frac{C_0 - C_i}{C_i} \times \frac{V_s}{m_s} \qquad (1)$$

Where C_0 and C_i are the concentrations (or the activities) of a radionuclide in solution prior to and after sorption, respectively; V_s is the volume (in mL) of the sorption solution and m_s is the mass of the solid used in grams. In the sorption experiments where radionuclide sorption is very strong or very weak, large positive and negative errors in K_ds can be introduced, respectively, by the concentration ratio. In the desorption experiments, if sorption is weak and liquid to solid ratio is low, calculated K_ds are sensitive to the estimated volume of sorption solution remaining at the start of the desorption experiment. This affects both the concentration ratio and liquid to solid ratio in Equation 1. In our desorption experiments, the fluid remaining at the end of the sorption step was not measured. Instead, we estimated the volume of sorption solution to solid to be 1:1 (1mL of sorption solution remained for 1g of solid used) or 1:2 (0.5mL of sorption solution remained for 1g of solid used). Therefore, K_ds were calculated using two sorption fluid to solid ratios; we expect the actual desorption K_ds to be between these calculated values.

Table 4.4 Initial conditions used for each sorption experiments

Radionuclide	Rock sample	Sieve size, μm	Solution volume, mL	solid mass, g	Liquid:solid ratio	Radionuclide initial conc., M
Pu(IV)	TCU	<75	15.0	0.3	50:1	1.5E-8
Pu(IV)	TCU	75-500	15.0	0.3	50:1	1.5E-8
Pu(IV)	TCU	500μm-2mm	15.0	0.3	50:1	1.5E-8
Pu(IV)	LCA	<75	15.0	0.3	50:1	1.5E-8
Pu(IV)	LCA	75-500	15.0	0.3	50:1	1.5E-8
Pu(IV)	LCA	500μm-2mm	15.0	0.3	50:1	1.5E-8
Np(V)	TCU	75-500	10.0	2.0	5:1	8E-6
Np(V)	LCA	75-500	10.0	2.0	5:1	8E-6
U(VI)	TCU	75-500	10.0	2.0	5:1	5E-6
U(VI)	LCA	75-500	10.0	2.0	5:1	5E-6
Cs	TCU	75-500	15.0	0.3	50:1	1E-5
Cs	LCA	75-500	10.0	2.0	5:1	1E-5
Sr	TCU	75-500	15.0	0.3	50:1	1E-5
Sr	LCA	75-500	10.0	2.0	5:1	1E-5

4.3 Results and Discussion

4.3.1 Pu(IV) sorption and desorption

Pu(IV) sorption experiments were performed using TCU and LCA rocks with three different grain sizes. The initial ^{242}Pu concentration used was 1.5×10^{-8} M. At the termination of the sorption and desorption experiments, the solution pH ranged from pH 8.2-8.7 with averages of pH 8.4±0.1 and pH 8.5±0.1, respectively. In **Figure 4.1**, Pu K_ds obtained from both sorption and desorption experiment phases using three different particle sizes are plotted as a function of time. Samples were analyzed after 1, 4, 6 and 12 days. The first set of desorption samples were taken immediately after Pu-free solution was introduced to the sample. Samples were also collected and analyzed at 20 and 27 days from the start of sorption experiment (8 and 15 days after the start of the desorption phase). The vertical black line in **Figure 4.1** indicates the start of the desorption experiments.

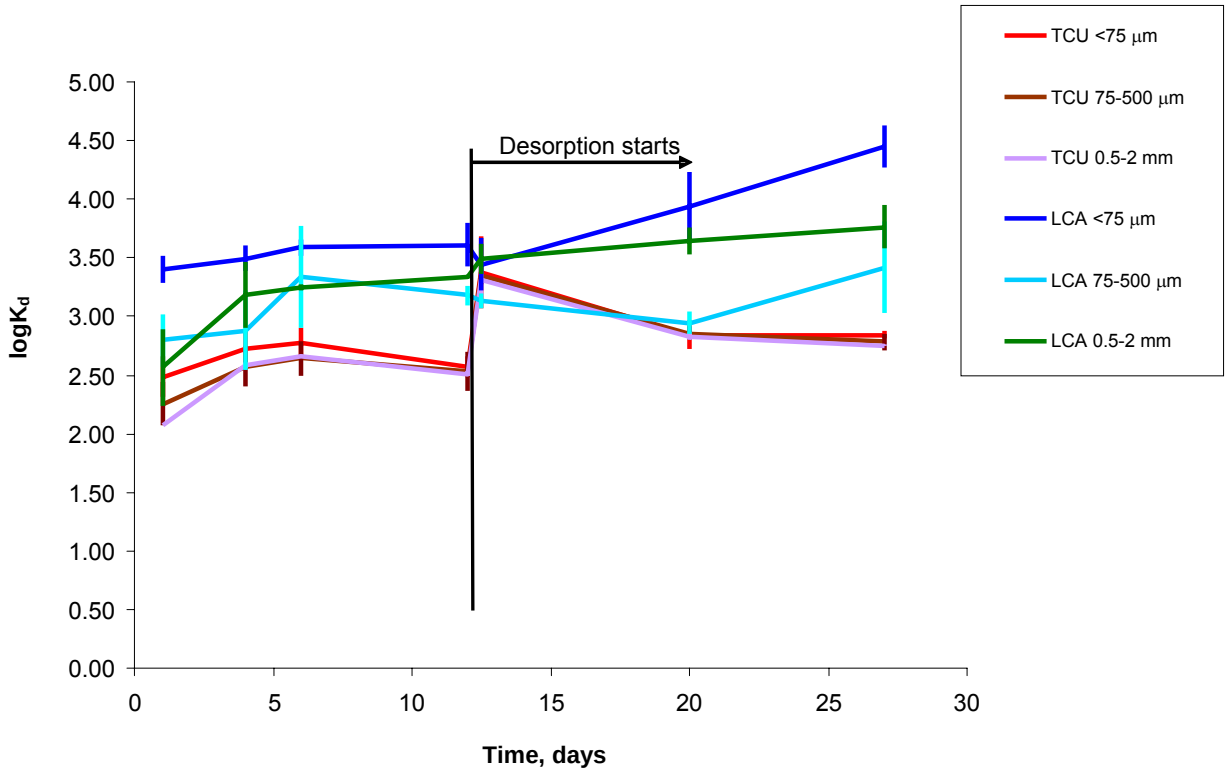

Figure 4.1 Pu(IV) K_d versus time. Error bars represent the measured range based on duplicate samples.

The sorption K_ds for both rock types reach a plateau by the 12th day. The Pu sorbs to both the LCA and the TCU rock samples, although the K_ds for the LCA are greater. The LCA consists primarily of calcite and dolomite minerals and the TCU is dominated by zeolite and feldspars.

In **Figure 4.1**, we would expect that a rate-limited sorption/desorption experiment should exhibit initially low K_ds that increase and finally plateau during the sorption phase followed by initially high K_ds that decrease and plateau during the desorption phase. For a reversible reaction, the sorption plateau and desorption plateau K_ds should be the same. At 12 days, the average K_d for Pu(IV) on TCU rock is $10^{2.5}$ mL/g. The initial desorption K_ds are about an order of magnitude higher but decrease to $10^{2.8}$ mL/g after 15 days of desorption. Although the sorption and desorption K_ds for Pu(IV) on TCU rock are not the same, the results suggest that Pu sorption to zeolitic rock is rate limited (on the scale of days) and essentially reversible.

Unlike the TCU data, Pu(IV) sorption to LCA rock does not appear to be reversible . Calcite is a slightly soluble mineral that has an inherently unstable surface (Stout and Carroll, 1992). Variability in K_d as a function of time in both sorption and desorption phases of the experiment are likely a result of this instability. Zachara et al. (1992) suggested that, for pure calcite minerals, 30 days of aging in a sodium bicarbonate solution may be sufficient to produce a more energetically stable calcite surface that is less prone to recrystallization. Only 1 day of aging was used in the experiments presented here. As a comparison, Zavarin et al. (2005b) reported a Pu(IV) K_d of $10^{3.0}$ mL/g on well aged calcite (BET of calcite 0.26 m^2/g) near pH 8. Assuming sorption is proportional to surface area, we would predict the Pu K_d on 75-500 mm LCA rock to be $10^{\sim 2.7}$ mL/g, about one order of magnitude lower than measured. The higher K_d in this study compared to Zavarin et al. (2005b) is likely due to re-crystallization of carbonate surfaces during the batch sorption/desorption experiments.

The sorption of Pu(IV) on both LCA and TCU rock was performed using three different particle size fractions (**Figure 2**). The measured surface area of the TCU rocks varied very little between the different particle size fractions (17.7m^2/g for <75 μm fraction and 13.9 m^2/g for the 75μm<x<500μm and 500μm<x<2000μm fractions). Clearly, the internal porosity of this rock contributes more to the surface area than particle size. Neither the BET surface area nor the measured Pu K_d varied substantially between the three TCU particle size fractions. For LCA rock, Pu K_ds at 1 day correlated much more strongly to surface area than at 12 days. This is consistent with the expectation that 1 day sorption data would be less affected by surface recrystallization effects. The large variation in BET surface area for the three LCA particle size fractions indicates that the surface area of the native LCA rock is very low indeed (<0.03 m^2/g).

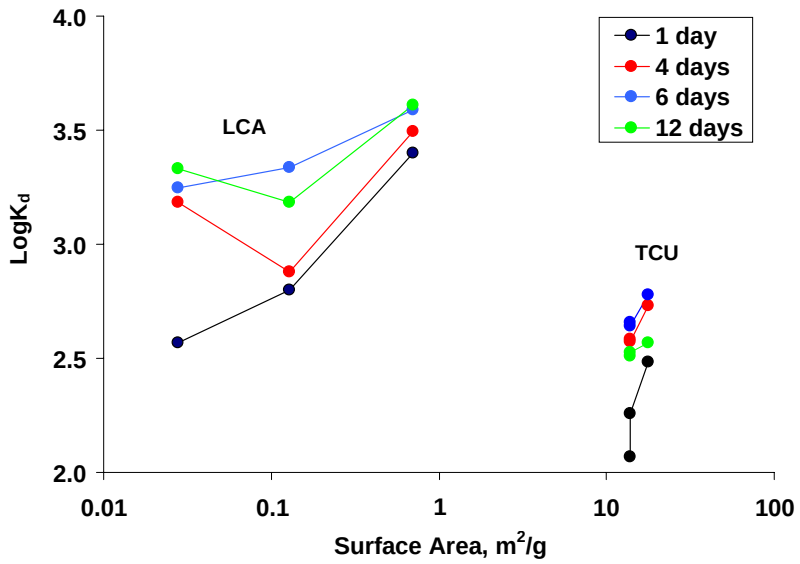

Figure 4.2 Pu(IV) K_d as a function of LCA and TCU rock surface area.

4.3.2 Np(V) sorption and desorption

Np(V) sorption experiments were performed using 75-500 μm particle size TCU and LCA rock. The initial ^{237}Np concentration used was 8×10^{-6} M; the liquid to solid ratio was 5:1. At the end of the sorption phase, the average solution pH for TCU and LCA samples was 8.2 and 9.5, respectively. The pH values increased 0.3 by the end of the desorption phase. The K_ds are plotted as a function of time in **Figure 3**.

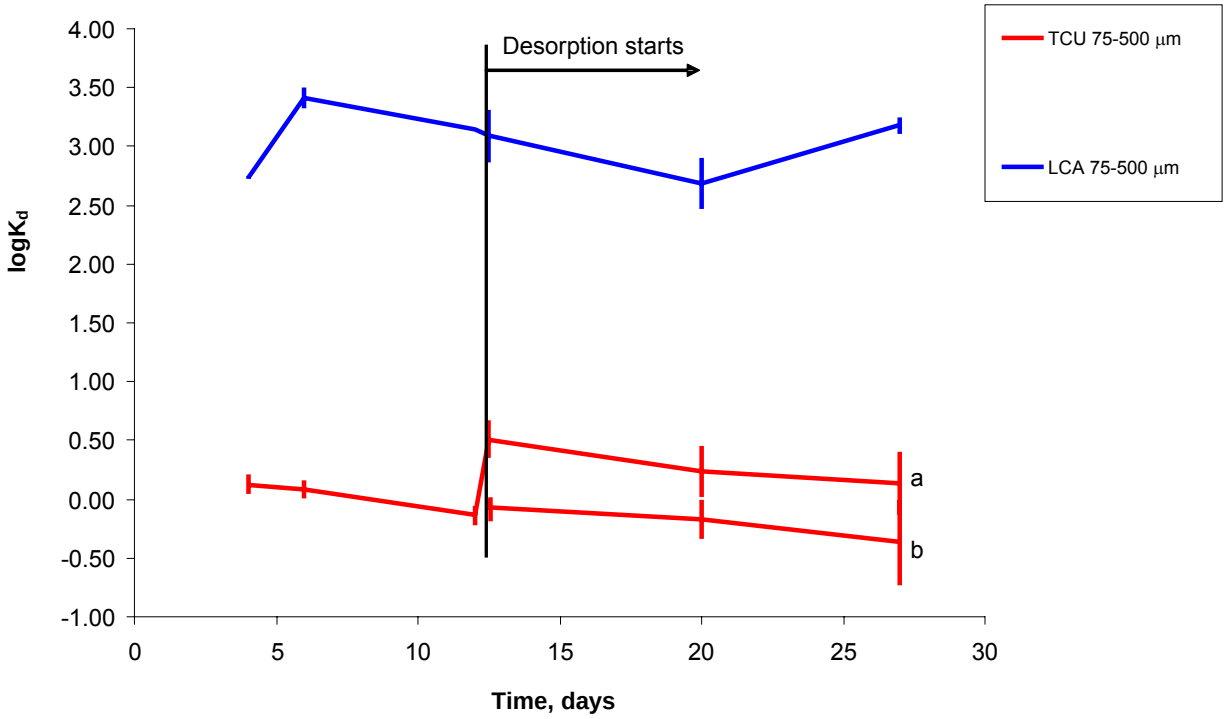

Figure 4.3 Np(V) K_d versus time. Error bars represent the measured range based on duplicate samples. Np(V) desorption K_d based on (a) 1:1 and (b) 1:2 solution to rock ratio at the end of sorption phase.

Np(V) has a high affinity for LCA rock with an average K_d of $10^{3.2}$ mL/g. Sorption and desorption trends are not consistent with rate-limited reversible sorption process; surface aging effects are likely. Nevertheless, the K_ds obtained from LCA sorption and desorption experiments are essentially the same within experimental uncertainty. In a previous study, Zavarin et al. (2005b) measured a K_d of $10^{1.6}$ mL/g for Np(V) sorption to aged calcite at pH 9.5 (BET surface area of 0.26 m^2/g). When corrected for surface area differences,the measured Np(V) K_d on aged calcite is more than an order of magnitude lower than measured here. As in the case of Pu, this suggests that re-crystallization of carbonate surfaces resulted in high apparent sorption K_ds.

In contrast to the LCA sample, weak Np(V) sorption was observed on TCU rock. The Np(V) K_d was $10^{-0.13}$ mL/g during the sorption phase. During desorption, the calculated K_ds are very uncertain and greatly affected by our estimate of solution remaining at the end of the sorption phase (**Figure 4.3**). Two estimates were used: 1:1 or 1:2 solution to rock ratio. The resulting desorption K_ds are plotted in **Figure 4.3**. The true desorption K_d is expected to fall within these two estimates. Given the high uncertainty in desorption K_d, we cannot determine whether sorption is rate limited or reversible. However, the affinity of Np(V) for the zeolitized tuff is clearly very low.

4.3.3 U(VI) sorption and desorption

U(VI) sorption experiments were performed using 75-500 μm particle size TCU and LCA rock. The initial uranium concentration used was 5×10^{-6} M; the liquid to solid ratio was 5:1. The pH values during sorption and desorption phases were constant with TCU and LCA average pHs of 8.6 and 9.8, respectively. The K_ds are plotted as a function of time in **Figure 4**.

U(VI) shows some measurable sorption on LCA rock with an average K_d of $10^{0.9}$ mL/g after 12 days. However, a plateau was never reached. The apparent K_d obtained from desorption experiments was initially 1 log unit higher than the sorption value and slowly decreased. However, the desoption K_d after 15 days ($10^{1.4}$ mL/g) was substantially higher that the sorption K_d. Kinetically-limited reversible sorption behavior is not observed. The U(VI) desorption K_d was estimated using a 1:1 or 1:2 solution to rock ratio at the end of the sorption phase. However, due to the relatively high sorption, the choice of ratio does not substantially affect the calculated desorption K_d (**Figure 4.4**).

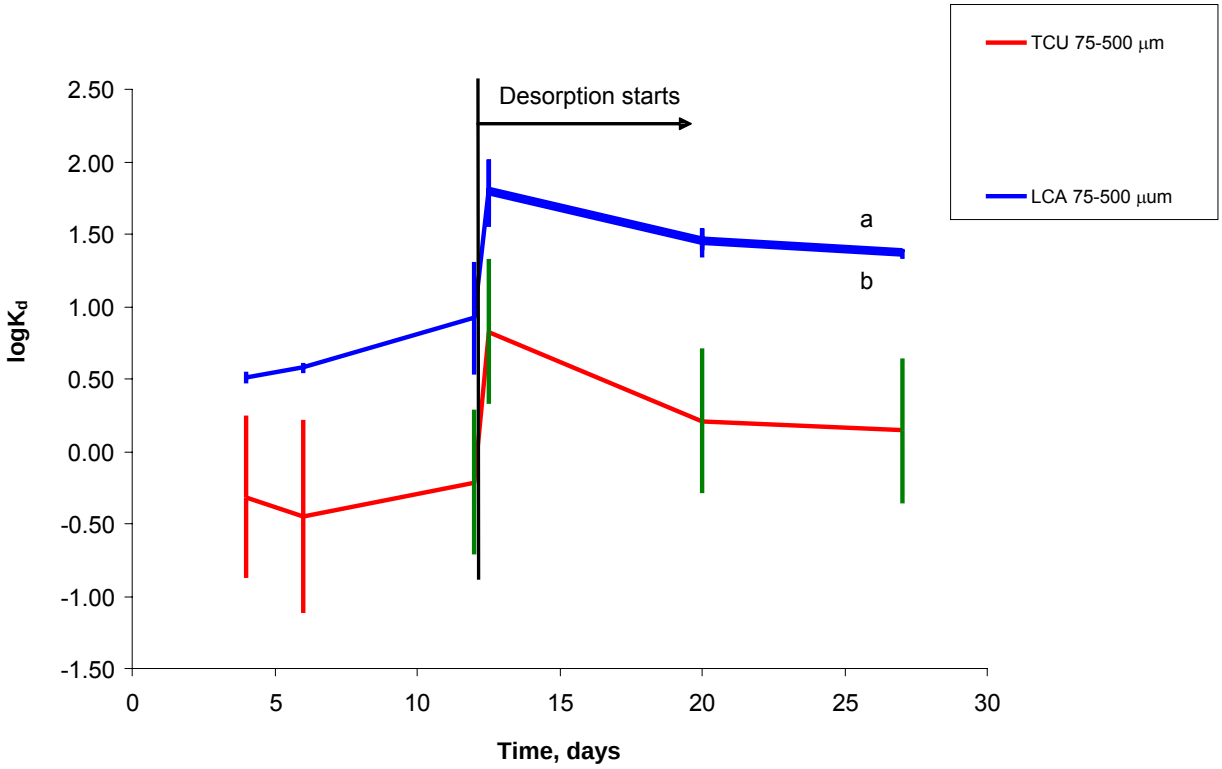

Figure 4.4 U(VI) K_d versus time. Error bars represent the measured range based on duplicate samples (green error bars were estimated due to apparent negative sorption in one sample). U(VI) desorption K_d based on (a) 1:1 and (b) 1:2 solution to rock ratio at the end of sorption phase.

For U(VI)-TCU system, very weak to no sorption was observed. One sample had very low but measureable U(VI) sorption while the other had no measurable sorption. The sorption K_d is less than 10^0 mL/g. The K_d during the desorption phase is not measurable with any level of certainty.

4.3.4 Cs sorption and desorption

Cs sorption experiments were performed using 75-500 μm particle size TCU and LCA rock. The initial Cs concentration was 1×10^{-5} M; the liquid to solid ratios were 50:1 and 5:1 for TCU and LCA rock, respectively. The pH values during sorption and desorption phases were constant with TCU and LCA average pHs of 8.7 and 9.7, respectively. The Cs K_ds are plotted as a function of time in **Figure 5**.

Cs has a very high affinity for TCU rock, as expected, with an average K_d of $10^{3.6}$ mL/g. The K_ds obtained from both sorption and desorption phases of the experiment are the same. The results indicate that sorption is reversible and that sorption/desorption rates are very fast (< 1 day). The choice of solution:rock ratio used in calculating the desorption phase K_d is not significant, as indicated in **Figure 4.5**.

Very weak Cs sorption to LCA rock was observed. The Cs sorption K_d was $10^{-0.6}$ mL/g. An apparently higher desorption phase K_d was calculated when either the 1:1 or 1:2 solution:rock ratio was used in calculating the desorption phase K_d. This would suggest that Cs sorption was not reversible. However, uncertainties in the desorption K_ds are too large to clain irreversible sorption with any certainty. Irregardless of the reversible or irreversible nature of Cs sorption, Cs retardation in carbonate rock is very low to negligible.

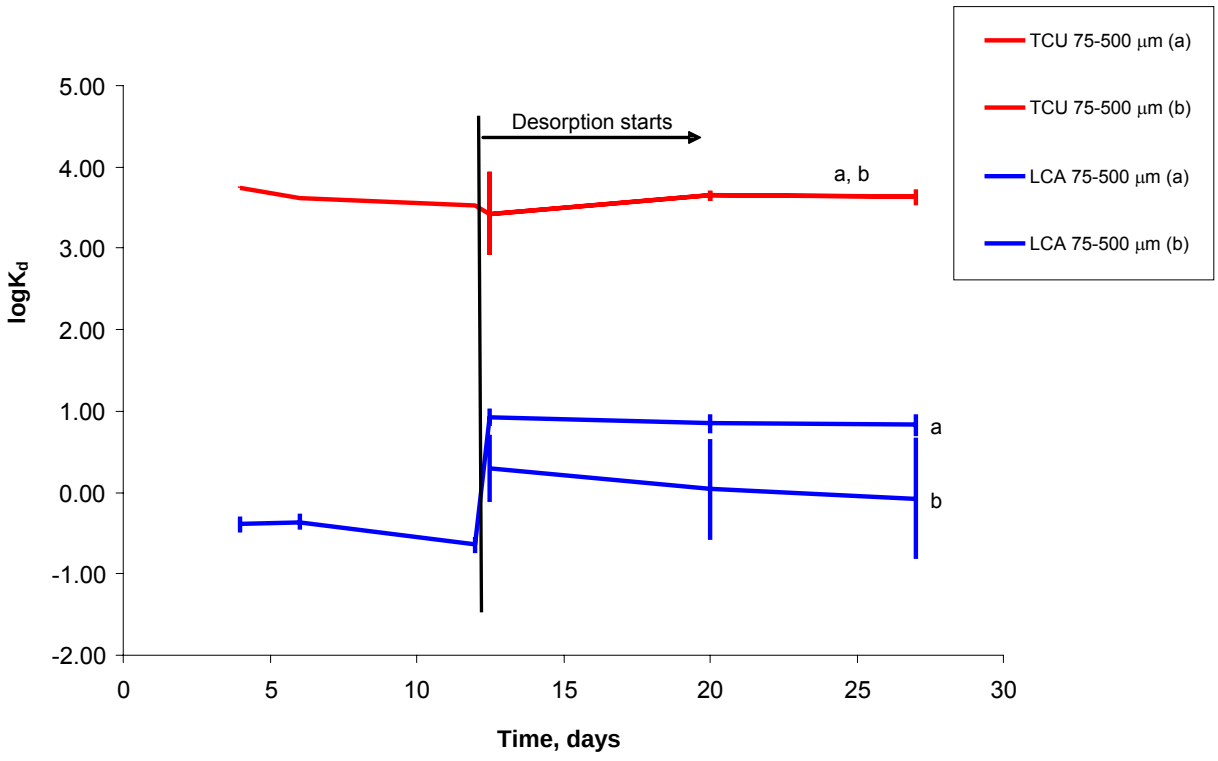

Figure 4.5 Cs K_d versus time. Error bars represent the measured range based on duplicate samples. Cs desorption K_d based on (a) 1:1 and (b) 1:2 solution:rock ratio at the end of sorption phase.

4.3.5 Sr sorption and desorption

The Sr sorption and desorption experiments were carried out using conditions similar to Cs experiments. The Sr sorption experiments were performed using 75-500 µm particle size TCU and LCA rock. The initial Sr concentration was $1x10^{-5}$ M; the liquid to solid ratios were 50:1 and 5:1 for TCU and LCA rock, respectively. The pH values during sorption and desorption phases were constant with TCU and LCA average pHs of 8.7 and pH 9.8, respectively. The Sr K_ds are plotted as a function of time in **Figure 4.6**.

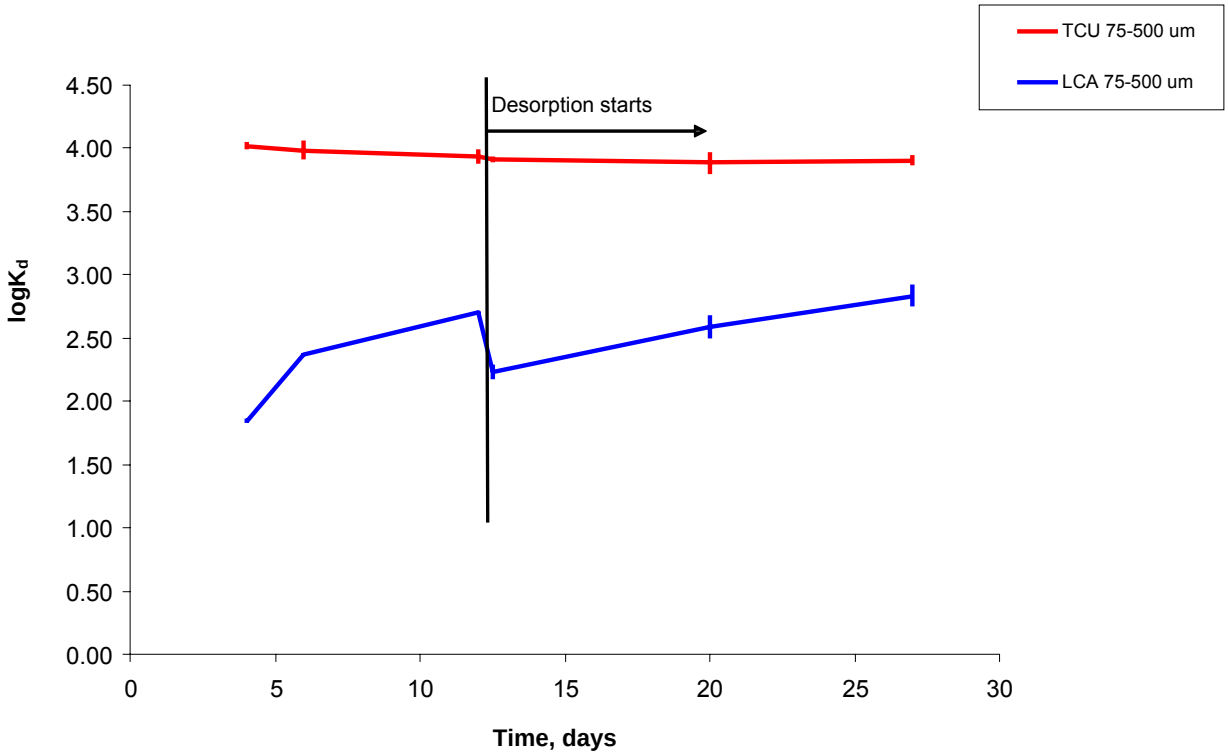

Figure 4.6 Sr K_d versus time. Error bars represent the measured range based on duplicate samples.

Sr sorption to TCU rock appears to be reversible and kinetically fast (< 1 day). Both sorption and desorption K_ds are $10^{3.9}$ mL/g. The Sr behavior is essentially identical to Cs with only a slightly higher K_d. Ion exchange of these ions with the dominant zeolite mineral in the TCU rock (clinoptilolite) is expected to be the primary sorption mechanism for both ions.

Moderate sorption of Sr to LCA rock was observed. However, a plateau was not reached during sorption or desorption . The apparent K_d obtained from desorption experiments was initially lower than the sorption value. The lower K_d may have resulted from dissolution of the carbonate mineral surface at the start of the desorption phase. Nevertheless, the K_d at the end of the desorption phase ($10^{2.8}$ mL/g) was slightly higher than at the end of the sorption phase ($10^{2.7}$ mL/g)K_d. The lack of sorption/desorption plateaus and reduced K_d at the start of the desorption phase suggest that Sr sorption is not controlled by kinetically-limited reversible sorption.

4.3.6 Comparison of radionuclide K_ds with literature values

Radionuclide K_ds for TCU and LCA rock at the end of the sorption and desorption experiment phases are listed in **Table 4.5**. For the actinides, sorption to LCA rock is always stronger than to TCU rock. The Pu(IV) and Np(V) affinity for LCA rock is very high. Based on comparisons with batch sorption experiments conducted on well-aged and pure calcite (Zavarin et al., 2005b), it is likely that the very high affinity is, in part, due to surface recrystallization effects. Much lower K_ds would be expected in the field. U(VI) sorption to LCA rock is very weak, consistent with pure calcite experiments conducted by Carroll and Bruno (1991). Moderate sorption of Pu(IV) but little to no sorption of Np(V) and U(VI) to TCU rock was observed. The obtained sorption and desorption curves as function of time suggest that the sorption is reversible, with sorption and desorption rates on the order of days. No indication of very slow desorption kinetics was observed in the TCU experiments.

For the alkaline and alkaline earth elements, sorption to LCA rock is much weaker than to TCU rock. Little to no sorption of Cs and moderately high sorption of Sr to LCA was observed. The relatively high Sr sorption is surprising and inconsistent with pure calcite sorption experiments conducted under similar conditions (Kd~$10^{0.5}$ mL/g in Parkman et al., 1998 and ~$10^{0.3}$ mL/g in Zachara et al., 1991). The sorption behavior observed here suggests Sr may have coprecipitated as a result of surface recrystallization. In the field, the sorption of both these elements is primarily controlled by ion-exchange reactions.

In support of UGTA project, Farnham et al., (2007) compiled literature data on distribution coefficients for Pu(IV), Np(V), U(VI), Cs and Sr sorption to various rocks and sediments. **Table 4.6** lists the range of K_ds for zeolitized tuff and carbonate rocks summarized by Farnham et al. (2007) and compares them to our experimental results. Most K_ds obtained in our study are within the reported range. However, it is important to note that recrystallization effects (Zavarin et al., 2005b) and estimates of native LCA rock surface areas (Zavarin et al., 2005a) would suggest that the measured K_ds are two or more orders of magnitude higher than what would be observed in the field. This correction to field conditions would dramatically reduce the predicted retardation of all radionuclides in the LCA. This is likely true for both our measurements and those reported in Farnham et al. (2007).

In the TCU sorption experiments, Np(V) and U(VI) K_ds are below the range reported in Farnham et al., (2007). It suggests that Np(V) and U(VI) transport rates in the the Yucca Flat TCU may be faster than previously estimated. Our measured Sr K_d is substantially higher than the range reported in Farnham et al., (2007) suggesting that Sr transport rates in the TCU may be substantially slower than previously estimated.

Table 4.5 Log(K_d) of radionuclide on TCU and LCA rock in Synthetic NTS groundwater.

		Sorption experiments		Desorption Experiments			
				1:1 remaining liquid:solid		1:2 remaining liquid:solid	
		log(K_d)	± error	**log(K_d)**	± error	**log(K_d)**	± error
Pu(IV)	TCU <75 µm	**2.57**	0.09	**2.84**	0.03	**2.84**	0.03
	TCU 75-500 µm	**2.53**	0.17	**2.79**	0.07	**2.79**	0.07
	TCU 0.5-2 mm	**2.51**	0.02	**2.76**	0.00	**2.75**	0.00
Pu(IV)	LCA <75 µm	**3.61**	0.19	**4.45**	0.17	**4.45**	0.17
	LCA 75-500 µm	**3.18**	0.08	**3.42**	0.39	**3.42**	0.39
	LCA 0.5-2 mm	**3.33**	0.00	**3.76**	0.19	**3.76**	0.19
Np(V)	TCU 75-500 µm	**-0.13**	0.08	**0.14**	0.26	**-0.36**	
	LCA 75-500 µm	**3.15**	0.01	**3.18**	0.07	**3.18**	0.07
U(VI)	TCU 75-500 µm	**-0.21**		**0.15**			
	LCA 75-500 µm	**0.92**	0.39	**1.39**	0.01	**1.36**	0.03
Cs	TCU 75-500 µm	**3.53**	0.01	**3.63**		**3.63**	
	LCA 75-500 µm	**-0.64**		**0.83**	0.13	**-0.07**	0.74
Sr	TCU 75-500 µm	**3.94**	0.06	**3.90**	0.04	**3.90**	0.04
	LCA 75-500 µm	**2.71**	0.01	**2.83**	0.09	**2.83**	0.09

Table 4.6. K_d values measured in this study and reported in Farnham et al. (2007).

		This study		
	Mineral	**log(K_d)**	± error	**Reported log(K_d) range**[a]
Pu(IV)	TCU	**2.51-2.57**[b]	0.17	**2-3.2**
	LCA	**3.18-3.61**[b]	0.21	**2-4**
Np(V)	TCU	**-0.13**	0.08	**0.08-1.05**
	LCA	**3.15**	0.01	**2-3.7**
U(VI)	TCU	**-0.21**		**0.2-1**
	LCA	**0.92**	0.39	**0-2.1**
Cs	TCU	**3.53**	0.01	**2.1-3.9**
	LCA	**-0.64**		**0.6-2**
Sr	TCU	**3.94**	0.06	**1.2-2.5**
	LCA	**2.71**	0.01	**0.7-1.2**

[a] Modified from Farnham et al. (2007)
[b] Log(K_d) were obtained from three different size fractions of the rock samples.

4.4 Conclusions

Batch sorption and desorption experiments were performed to determine the distribution coefficients (K_ds) of Pu(IV), Np(V), U(VI), Cs and Sr on tuff confining unit (TCU) and lower carbonate aquifer (LCA) rocks in synthetic NTS groundwater. In general, actinides have shown a greater affinity for LCA rock over TCU rock. However, the sorption mechanism observed in the lab may include actinide co-precipitation during dissolution and re-crystallization of carbonate minerals. Re-crystallization of calcite may have resulted in substantially higher Pu(IV) and Np(V) K_ds than would be observed in the field. This was also observed in the case of Sr sorption. Furthermore, the reactive surface area of LCA rock in the field will be much lower than the crushed material used here. The reduced surface area would further reduce the expected LCA radionuclide K_ds in the field. Thus LCA K_ds measured here and reported in Farnham et al. (2007) may be more than two orders of magnitude higher than would be expected in the field due to the changes in the surface area of the mineral due to recrystallization . This dramatically reduces the effectiveness of the LCA to retard these actinides.

The Pu(IV) K_d as functions of the particle size suggests that TCU rock particle size has little to no effect on measured K_d due to its high matrix porosity. The initial sorption of Pu(IV) on LCA was proportional to the surface area, but LCA dissolution and re-crystallization became an important factor impacting the sorption over time.

Cs and Sr sorption to TCU rock is very strong, reversible, and kinetically fast. The high sorption results from ion exchange on zeolite minerals (primarily clinoptilolite) in the zeolitized tuff. Sorption of these elements to LCA rock is rather weak, particularly when recrystallization and surface area effects are accounted for. We would expect their transport rates in LCA rock to be very high, and controlled primarily by the presence of absence of trace mineral phases that participate in ion exchange (e.g. fracture lining clay or zeolite minerals).

4.5 Acknowledgements

This work was funded by the Underground Test Area Project, National Nuclear Security Administration, Nevada Site Office. This work was performed under the auspices of the U.S. Department of Energy by Lawrence Livermore National Laboratory under Contract DE-AC52-07NA27344.

4.6 References

Carroll, S.A., and Bruno, J. (1991) Mineral-solution interaction in the U(VI)-CO2-H2O system, Radiochimica Acta, 52/53:187-193.

Department of Energy (2000) United States Nuclear Tests, July 1945-Sept. 1992. DOE NV-209 Rev. 15, Dec 2000).

Dosch, R.G., and A.W. Lynch. 1980. "Radionuclide Transport in a Dolomite Aquifer, Scientific Basis for Nuclear Waste Management." In Proceedings of the International Symposium, held in Boston, Massachusetts, on November 27-30, 1979. New York, NY: Plenum Press.

Farnham , I., Fryer, W., Pickens, J., Jones, T., Brown-King, C., Hand, J., Londergan, J., Bryant, N., Drellack, S.L., Zavarin, M. (2007) Phase I Contaminant Transport Parameters For The Groundwater Flow And Contaminant Transport Model Of Corrective Action Unit 97: Yucca Flat/Climax Mine, Nye County, Nevada. S-N/99205-096.

Parkman, R.H., J.M. Charnock, F.R. Livens, and D.J. Vaughan. (1998). A study of the interaction of strontium ions in aqueous solution with the surfaces of calcite and kaolinite, Geochimica et Cosmochimica Acta, 62:1481-1492.

Perkins, W.G., D.A. Lucero, and G.O. Brown. 1998. Column Experiments for Radionuclide Adsorption Studies of Culebra Dolomite: Retardation Parameter Estimation for Non-Eluted Actinide Species, SAND98-1005. Albuquerque, NM: Sandia National Laboratories.

Stout, D.L., and Carroll, S.A. (1992) A Literature Review of Actinide-Carbonate Mineral Interaction, SAND92-7328. Albuquerque, NM: Sandia National Laboratories.

Ware, S. D., A. Abdel-Fattah, M. Ding, P. W. Reimus, C. Sedlacek, M. Haga, E. Garcia and S. Chipera (2005) Radionuclide Sorption and Transport in the Lower Carbonate Aquifer and Tuff Confining Unit of Yucca Flat, Nevada Test Site, draft report, Los Alamos National Laboratory, Los Alamos, New Mexico.

Zachara, J.M., C.E. Cowan, and C.T. Resch. (1991). Sorption of divalent metals on calcite, Geochimica et Cosmochimica Acta, 55:1549-1562.

Zavarin, M., Johnson, M.P., Roberts, S.K., Pletcher, R., Rose, T. P., Kersting, A.B., Eaton, G., Hu, Q., Ramon, E., Walensky, J., and Zhao, P. (2005a) Radionuclide Transport in Tuff and Carbonate Fractures from Yucca Flat Nevada Test Site. UCLR-TR-219836, Lawrence Livermore National Laboratory, Livermore, California.

Zavarin, M., Roberts, S. K., Hakem, N., Sawvel, A.M., and Kersting, A.B. (2005b) Eu(III), Sm(III), Np(V), Pu(V), and Pu(IV) sorption to calcite. Radiochimica Acta **93**, 93–102.

Zavarin, M., Roberts, S.K., Reimus, P., Johnson, M.P. (2006) Summary of Radionuclide Reactive Transport Experiments in Fractured Tuff and Carbonate Rocks from Yucca Flat, Nevada Test Site. UCRL-TR-225271.

4.7 Appendix: Summary of K_d data.

Radionuclide	Rock mineral	Sieve size (μm)	Sorption log(K_d)					Desorption log(K_d)			
			1 day	4 days	6 days	12 days	pH @ 12days	12 days	20 days	27 days	pH @ 27days
Pu(IV)	TCU	<75	2.49	2.73	2.78	2.57	8.40	3.38	2.84	2.84	8.65
		75-500	2.26	2.58	2.64	2.53	8.45	3.35	2.85	2.79	8.60
		500-2mm	2.07	2.59	2.66	2.51	8.35	3.31	2.83	2.76	8.50
	LCA	<75	3.40	3.50	3.59	3.61	8.50	3.44	3.94	4.45	8.25
		75-500	2.80	2.88	3.34	3.18	8.40	3.13	2.94	3.42	8.45
		500-2mm	2.57	3.18	3.25	3.33	8.55	3.49	3.65	3.76	8.55
Np(V)	TCU	75-500		0.13	0.08	-0.13	8.15	0.51	0.23	0.14	8.45
	LCA	75-500		2.73	3.41	3.15	9.45	3.09	2.68	3.18	9.75
nat. U(VI)	TCU	75-500		-0.31	-0.45	-0.21	8.60	0.83	0.21	0.15	8.55
	LCA	75-500		0.51	0.58	0.92	9.70	1.81	1.46	1.39	9.80
Cs	TCU	75-500		3.74	3.62	3.53	8.70	3.43	3.65	3.63	8.70
	LCA	75-500		-0.39	-0.36	-0.64	9.70	0.92	0.85	0.83	9.70
Sr	TCU	75-500		4.02	3.98	3.94	8.70	3.92	3.89	3.90	8.60
	LCA	75-500		1.85	2.38	2.71	9.75	2.24	2.59	2.83	9.75

CHAPTER 5

Sorption and Desorption Rates of Neptunium and Plutonium on Goethite

By

Brian A. Powell, Annie B. Kersting, and Mavrik Zavarin

Glenn T Seaborg Institute, Chemistry, Materials, Earth and Life Sciences Directorate,
Lawrence Livermore National Laboratory

ABSTRACT

A series of flow-cell experiments were performed to examine Np(V) and Pu(V) sorption to and desorption from goethite. Np and Pu desorption occurred at a faster rate and to a greater extent than previously reported. However, the rate and extent of desorption decreased over time suggesting sample aging and/or hysteresis effects. The aging and/or hysteresis may result from redistribution of Np and Pu from weakly to more strongly sorbing sites. Differences between Np and Pu sorption were attributed to reduction of Pu(V) to Pu(IV) on the goethite surface. Reduction rates calculated from the current data compare favorably with previously measured Pu(V) reduction rates. However, Pu in the flow cell effluent (aqueous phase) was Pu(V), indicating that a significant fraction of sorbed Pu(IV) was reoxidized to aqueous Pu(V) during desorption. The presence of aqueous Pu(V) indicates that subsurface transport models must consider an equilibrium distribution of sorbed Pu(IV) and aqueous Pu(V). Based upon this work, it is recommended that Np and Pu subsurface transport models account for (1) differences in site affinities, (2) hysteretic and/or ageing effects, (3) differences in sorption affinities of Pu(IV) and Pu(V), and (4) redox transformation between the Pu species. Rates of sorption and desorption are relatively fast and are not likely to affect field-scale subsurface transport predictions.

5.1 Introduction

The presence of ^{237}Np and ^{239}Pu in the subsurface coupled with, 1) their long half-lives, 2) relative mobility of ^{237}Np in groundwater and, 3) the ability of Pu to be transported colloidally in groundwater make both actinides long-term risk drivers. Reactive transport models that accurately predict the mobility of actinides are needed to assess the risk of subsurface contamination resulting from nuclear weapons production and testing. Accurate predictive models are also required for risk assessment of any proposed subsurface nuclear waste repository. Incorporation of the coupled physical, chemical, and biological reactions controlling actinide subsurface transport into reactive transport models presents an enormous challenge. In some cases, simplified models that highlight the most important reactions may suffice. However, development of even a simplified subsurface transport model is complicated by the redox chemistry of actinides and the profoundly different geochemical behavior of their different

oxidation states. This is especially problematic for Pu as the similarity between reduction potentials of Pu(VI/V), Pu(V/VI), and Pu(VI/IV) in neutral solutions make Pu very sensitive to oxidation states changes (Allard et al., 1980). Under environmental conditions, plutonium may exist as Pu(III), Pu(IV), Pu(V), and Pu(VI) and Np is commonly found as Np(IV) or Np(V). Different oxidation states of Np and Pu give rise to different transport behavior. Neptunium tends to exist as Np(V) under oxidizing conditions and is relatively less sensitive to oxidation state changes, compared to Pu (Morse and Choppin, 1991).

In order to accurately predict Np and Pu subsurface mobility, a transport model must account for the fractional oxidation state distribution in a system as well as the sorption behavior of the oxidation state for each actinide. Traditionally, subsurface transport models employ bulk distribution coefficients that do not account for the differences in geochemical behavior between the various Pu oxidation states (CRWMS M&O, 2000). Reactive transport models incorporating only a linear distribution coefficient (K_d) can only be applied to systems whose parameters match those in which the K_d was determined. Therefore, a more holistic approach is desired that can account for system site heterogeneity as well as the effects of changes in system parameters such as pH and E_H on actinide speciation and sorption behavior. Critical data within such a model are the rates and reversibility of Np and Pu sorption/desorption reactions.

In this work, sorption and desorption rates of Np and Pu on synthetic goethite were measured. Goethite was chosen, as it is ubiquitous in the environment and is known to strongly interact with Np and Pu. Several researchers have examined the interaction of Np (Keeney-Kennicutt and Morse, 1984; Combes et al., 1992; Girvin et al., 1991; Nakayama and Sakamoto, 1991; Tockiyama, et al., 1995; Kohler et al., 1999; Nakata et al., 2000) and Pu (Keeney-Kennicutt and Morse, 1985; Sanchez, et al., 1985; Lu, et al., 1999; Powell et al., 2004; Powell et al., 2005; Lu et al., 2003; Khasanova et al., 2007) with iron (oxyhydr)oxides. Girvin et al., (1991) and Kohler et al. (1999) observed a strong interaction of Np(V) with amorphous iron oxydyroxide and hematite, respectively, and effectively modeled the data assuming a single Np(V) sorbing species. Tochiyama et al. (1995) observed greater sorption of Np(V) to goethite than to hematite and magnetite. Sorption of Pu to goethite is complicated by the surface mediated reduction of Pu(V) to Pu(IV) that has been observed by several researchers (Kenney-Kennicutt and Morse, 1985; Sanchez et al., 1985; Penrose et al., 1987; Powell et al., 2005; Khasanova et al., 2007). Sorption of Pu(V) was found to be similar to Np(V) initially. However, reduction of Pu(V) to Pu(IV) promotes further sorption due to the higher affinity of Pu(IV) for mineral surfaces, relative to Pu(V). Powell et al. (2004) determined an overall rate expression describing Pu(V) reduction by hematite and goethite as a function of solution pH. In continued studies, Powell et al., (2006) found that Pu(IV) was the dominant sorbed oxidation state for all synthetic minerals tested, even on oxidizing minerals such as pyrolysite (β-MnO_2).

In contrast to the numerous Np and Pu sorption studies on various minerals, Np and Pu desorption studies are limited. Time dependent data that can be used to calculate reliable desorption rates are essentially absent from the literature. Most Np desorption data has been obtained through batch methods and system perturbation (e.g. changes in pH or addition of a

complexant). Researchers frequently observed incomplete desorption of Np, suggesting that a fraction of Np is "irreversibly" sorbed. Kenney-Kennicutt and Morse (1984) observed sorption hysteresis in batch experiments with goethite in seawater and distilled water. Nakata et al., (2000) observed greater than 50% desorption of Np from hematite and magnetite into a 1M KCl solution. They also observed an increase in the fraction of unleachable Np over time, even after attempts to leach the Np from the surface with 0.1 M $K_2C_2O_4$. These observations indicate that a mechanism for strongly binding Np to iron oxide surfaces exists but needs further study.

The predominance of Pu(IV) on most mineral surfaces confounds attempts to directly examine the desorption behavior of each environmentally relevant Pu oxidation state individually. In batch experiments examining Pu desorption from hematite and goethite, less than 1% of the total sorbed Pu (added as either Pu(V) or Pu(IV)) was desorbed in J-13 well water and synthetic groundwater (Lu et al., 1999; Lu et al., 2003). In all cases, the oxidation state of the desorbed Pu was not determined. However, the similarity in the desorbed fraction of each system suggests that an equilibrium distribution was reached independent of the initial Pu oxidation state. Incomplete leaching of Pu was observed after re-suspending Pu equilibrated goethite in 0.6 M $HClO_4$ (Kenney-Kennicutt and Morse, 1985). Furthermore, the fraction of leachable Pu decreased with increasing equilibration time from 1 hour to 30 days (Kenney-Kennicutt and Morse, 1985). This suggests that Pu became more strongly associated with the solids phase over time. This "aging effect" was also observed by Powell et al (2004, 2005) in similar experiments with goethite, hematite, and magnetite.

Based upon the data discussed above, it appears that Np and Pu interaction with goethite is characterized by a combination of fast and slow, possibly hysteretic, sorption. In order to observe both fast and slow sorption/desorption reactions, a flow-through batch reactor can be employed. The experimental design used here is based upon the stirred flow technique developed by Carski and Sparks (1985). The reaction time between the influent solution and the solid phase can be varied by modifying the flow-rate. To determine if sorption/desorption is rate limited, the flow can be temporarily stopped. If a steady-state had not been reached, a change in the effluent concentration is observed when flow is resumed (Bar-Tal et al., 1990; Eick et al., 1990). *By utilizing a flow-through design in this work, we seek to determine the relative sorption and desorption rates of Np and Pu on goethite. An additional goal is to characterize the oxidation state of desorbed Pu.* The data are used to develop a conceptual model of Np and Pu sorption to goethite and gain insight into Np and Pu subsurface transport.

5.2 Materials and Methods

5.2.1 Synthetic Goethite Preparation and Characterization

Unless specified, all chemicals used in this work were ACS grade and used without further purification. Goethite was synthesized from $Fe(NO_3)_3{\cdot}9H_2O$ as described by Schwertmann and Cornell (1991). Briefly, 100mL of 1M $Fe(NO_3)_3{\cdot}9H_2O$ (Alfa Aesar) was mixed with 180 mL of 5M KOH (Alfa Aesar) in a 2L polypropylene bottle with a screw cap. A red precipitate immediately formed. The suspension was diluted to 2L using ultrapure H_2O (Milli-Q Gradient

System, >18 MΩ.cm resistivity) and immersed in a 70°C water bath for 3 days. The solids were dialyzed in ultrapure H_2O using 6-8k MWCO dialysis bags (Spectra/Por*). The dialysis water was changed periodically over a three day period until the conductivity of the dialysis water was the same as the ultrapure H_2O. The solids were isolated by filtration using 0.200 mm nylon filters and dried in an air oven at 40°C for five days.

A powder XRD pattern of the dried solids was obtained on a Scintag PAD-V diffractometer. Sharp, low intensity peaks confirmed goethite as the major phase using ICDD reference card 29-0713. Potentiometic titrations were performed using a Metrohm titrator at room temperature (20-22 °C) under a NaOH scrubbed Ar(g) purge of the reaction vessel headspace. A point of zero salt effect of 8.5 ± 0.1 was determined through potentiometric titrations of 10 g L^{-1} goethite suspensions in 0.001M, 0.01M, and 0.10M NaCl. Electron microscope images were obtained on a JEOL JSM-7401F scanning electron microscope (SEM) and a FEI Technai G2 20 X-Twin Scanning Transmission Microscope (STEM).

The synthesized material had a BET surface area of 15.8 m^2 g^{-1}, measured on a Micrometrics Gemini surface area analyzer. A goethite stock suspension was prepared; $NaHCO_3$ was added to the goethite suspension to speed equilibration with atmospheric $CO_2(g)$. Due to the long time frame (1-3 months) and constant stirring within the flow-cell, physical and chemical changes in the goethite may occur. Of concern is the change in particle size and reactive surface area due to mechanical breakdown of the particles in the stirred solution. To evaluate the potential breakdown of goethite particles, the stock suspension was continuously stirred for several months using a magnetic stir-bar. The surface area of the solids in the stock suspension after several months was 14 m^2 g^{-1}. The initial surface area of the material was similar, demonstrating that significant changes in goethite surface area during the flow-through tests was unlikely. However, SEM and TEM analysis of the goethite over the course of the Pu sorption/desorption experiment indicated some changes of goethite particle morphology. **Figure 5.1A** shows the initial synthetic goethite consisting of 1 to 3 μm long acicular crystals (needles), larger aggregates, and some 4-fold and 6-fold star shaped particles. At the end of the sorption step, both the needles and larger aggregates were observed along with a series of 100 to 1000 nm particles that were not readily seen in the initial goethite (**Figure 5.1B**). Presumably, the particles are pieces of goethite needles that were broken apart while stirring the suspension. At the end of the experiment, there were very few fine needles observed in SEM and TEM images (**Figure 5.1C** and **5.1D**, respectively). However, there was a marked increase in the number of small particle fragments. The destruction of the goethite needles would not be expected to cause a marked increase in the bulk surface area. However, such a change may affect Np/Pu sorption behavior by generating more reactive surface sites. It is possible that the <100 nm particles generated could pass through the flow-cell filter. Filtration tests on the effluent were conducted to check for the influence of colloids. However, no attempt was made to determine the possibility of a change in the reactive surface area. Therefore, effects (if any) of such a phenomena must be considered.

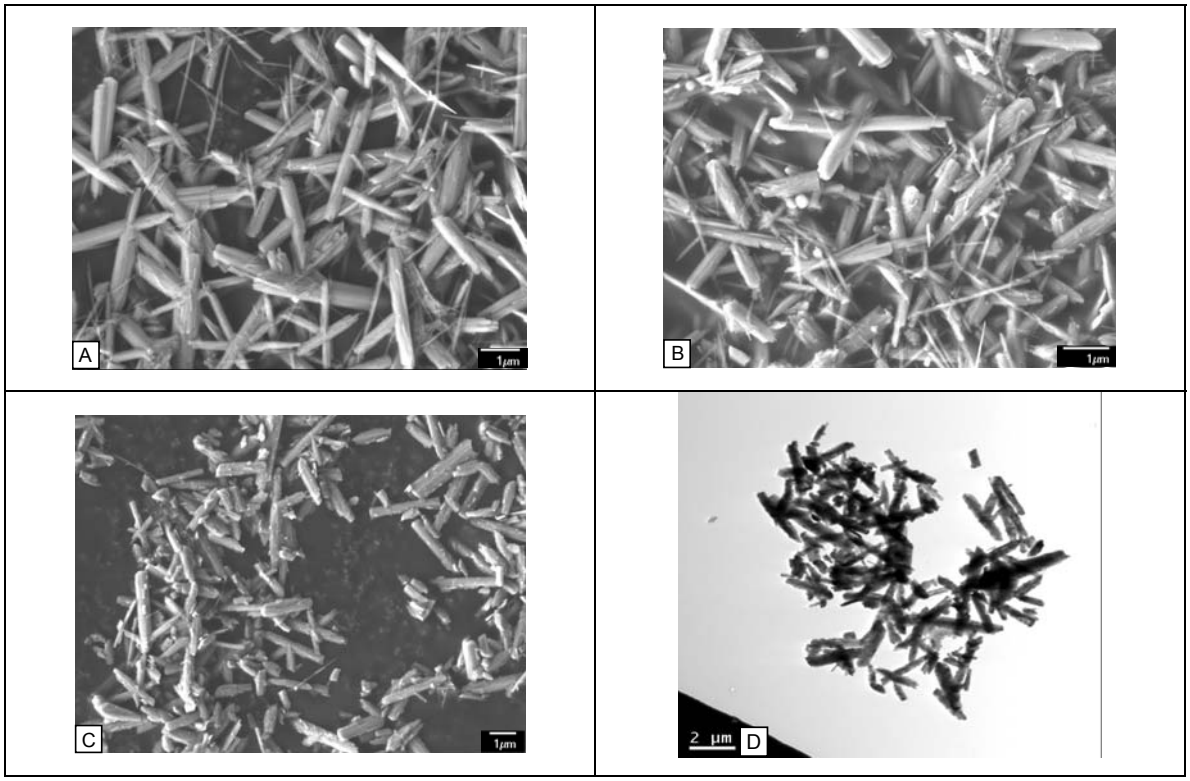

Figure 5.1 SEM and TEM images of synthetic goethite at various stages of the Pu sorption and desorption flow-through experiments. (A) SEM image of initial synthetic goethite; (B) SEM image of goethite at end of sorption step; (C) SEM and (D) TEM image of goethite at end of experiment.

5.2.2 ^{237}Np, $^{238/242}$Pu, and ^{3}H Analysis

Concentrations of ^{237}Np, $^{238/242}$Pu, and ^{3}H were determined on a Packard Tricarb 2550TR/XL Liquid Scintillation Analyzer in Ecolume (MP Biomedicals) cocktail. Alpha/Beta discrimination was used to accurately separate ^{237}Np from the ^{233}Pa daughter during liquid scintillation counting (LSC). The discriminator setting was determined by generating an alpha/beta spillover curve using separated ^{237}Np and ^{233}Pa. Separated ^{237}Np and ^{233}Pa were obtained using Biorad AG 1x8 anion exchange resin and silica gel as described elsewhere (Pickett, et al., 1994; and Hardy et al., 1958). The LSC peaks generated by ^{238}Pu and ^{242}Pu are coincident and have no other interference. Therefore, the total alpha peaks were summed to determine the Pu concentration.

In some cases the concentration of Pu in the effluent was too low to be determined by direct LSC analysis of the effluent. In these cases, the effluent from between 2 to 5 chamber volumes was combined and the Pu was coprecipitated with manganese oxide as follows. The combined solution was acidified to pH ~2 with 1M HCl then $KMnO_4$ was added to generate a 0.5 mM $KMnO_4$ solution. The solution was mixed on an orbital shaker for one hour then adjusted to pH 9

with 1M NaOH. Then 0.1 M $MnCl_2$ was added in 50 mL increments until the observed precipitate aggregated and no further precipitate was formed. Typically a 5x to 10x excess of Mn(II) over Mn(VII) was used. The suspension was centrifuged 10 minutes at 4500 rpm and the supernatant was discarded. The dark precipitate was dissolved with 1mL 1.0 M $NH_2OH{\cdot}HCl$ then 2 mL 1 M HNO_3. The entire solution was transferred to a liquid scintillation vial for Pu analysis. This method was found to provide quantitative recovery of Pu through analysis of replicate aliquots of the Pu working solution diluted 600x. Therefore, no recovery tracer was used when analyzing effluent samples.

Oxidation state analysis of the Pu working solution and effluent samples was performed using lanthanum fluoride coprecipitation and solvent extraction. The use of two techniques to allow comparison is desirable since techniques for the determination of Pu oxidation state distribution in less than 10^{-8} M Pu solutions are inherently indirect. The concentration of Pu used in this work was too low to employ more traditional spectroscopic techniques to characterize Pu oxidation state distribution (Cleveland, 1979, Conradson et al., 1998, Wilson et al., 2005). The techniques reported here consider Pu(IV), Pu(V), and Pu(VI). Pu(III) is not quantified in the separation scheme as under our experimental conditions it will be unstable (Cleveland, 1979). Separation of Pu oxidation state by lanthanum fluoride was based on the method described by Kobashi et al. (1998). Briefly, an aliquot of a Pu containing solution was diluted by at least 2x in a solution containing 0.8 M HNO_3, 0.25 M H_2SO_4, 0.01 M $La(NO_3)_3$, and 0.005 M $KMnO_4$. The permanganate was substituted for dichromate used by Kobashi et al. (1998) as a holding oxidant to prevent reduction of Pu(V) to Pu(IV) by the high HF concentration during analysis. Then a small aliquot of concentrated HF was added to make a 0.2 M HF solution. The Pu(III) and Pu(IV) coprecipitate, leaving Pu(V) and Pu(VI) in the aqueous phase. The solution was mixed for 10 minutes then centrifuged 3 minutes at 8000 rpm. The Pu concentration in the supernatant was determined by LSC and represents the Pu(V/VI) fraction. The Pu(IV) fraction is calculated by difference.

Separation of Pu oxidation states by solvent extraction was accomplished using 0.5 M bis-(ethylhexyl)-phosphoric acid (HDEHP) in xylene and 0.025 M 4-benzyol-3-methyl-1-phenyl-2-pyrazolin-5-one (PMBP) in xylene as the extractants (Foti and Freiling, 1964; Bertrand et al., 1983; Nitsche et al., 1988; Neu et al., 1994). An aliquot of Pu containing solution was acidified to pH ~0 using HCl then contacted with either the HDEHP or PMBP organic phase for 5 minutes in a 2 mL centrifuge vial. The vial was centrifuged 1 minute to aid phase separation then aliquots from both the aqueous and organic phases were removed for Pu analysis via LSC. A 0.025 M PMBP solution selectively extracts Pu(IV) from a pH 0 aqueous phase, leaving Pu(V) and Pu(VI) behind. A 0.5 M HDEHP solution selectively extracts Pu(IV) and Pu(VI) into the organic phase, leaving Pu(V) in the aqueous phase. The Pu oxidation state distribution in the working solution was determined using both HDEHP and PMBP as extractants. Measurements of the Pu oxidation states in the effluent from flow-through experiments was only determined using PMBP. Therefore the results are reported as either Pu(IV) or Pu(V/VI), allowing direct comparison with the lanthanum fluoride coprecipitation results.

5.2.3 ^{237}Np and $^{238/242}$Pu Working Solution Preparation

A 1.5 mM ^{237}Np(V) stock solution was purified by anion exchange then used to prepare a 3.2 μM ^{237}Np working solution in 5mM NaCl/0.7 mM $NaHCO_3$ at pH 8. An aliquot of a ^{3}H stock solution in H_2O was added to achieve a ^{3}H tracer concentration of 1000 cpm mL^{-1}. The ^{3}H was used as a non-reactive tracer. To ensure equilibration with atmospheric CO_2(g), the solution was stirred uncapped for >3 days prior to use. A filter was placed over the bottle to prevent dust infiltration. The pH of the stock solution was 8.03 and the final ^{237}Np concentration was 3.2 μM.

A 1.2 μM Pu stock solution in 1M HNO_3 containing 8% ^{238}Pu and 92% $^{239/240}$Pu by mass was used to prepare the Pu working solutions used in this work. The exact isotopic distribution was measured by ICP-MS and HPGe spectroscopy. A small aliquot of the stock solution was evaporated to dryness then dissolved in 0.5 mL 1.0 M HCl/0.2 mM $KMnO_4$. The solution was wrapped in Al foil and left for 8 hours to oxidize all Pu to Pu(VI). The solution was diluted approximately 200x with 5 mM NaCl to the pH range 2-3. A 10 μL aliquot of 0.01 M $MnCl_2$ was added to precipitate any remaining permanganate. The solution was then passed through a 100 nm nylon syringe filter into a Teflon bottle, adjusted to pH 3 using NaOH and left for 5 days to allow autoreduction of Pu(VI) to Pu(V). An aliquot of a ^{3}H stock solution was added to yield a final ^{3}H concentration of 1000 cpm mL^{-1}. Also, 0.1 M $NaHCO_3$ was added to buffer the pH to 8 and speed equilibration with atmospheric CO_2(g). Similar to the Np working solution, the Pu working solution was stirred uncapped for 3 days to ensure equilibration with atmospheric CO_2(g). The final pH of the solution was 8.05 and the final Pu concentration was 2.6 nM. Oxidation state analysis of the working solution indicated the solution was <1% ± 1% Pu(IV), 97% ± 4% Pu(V), and 3% ± 4% Pu(VI) by solvent extraction and 6% ± 3% Pu(IV) and 94% ± 3% Pu(V/VI) by lanthanum fluoride coprecipitation. The error is propagated from LSC data. However, an estimate of at least 5% error for these indirect oxidation state measurements is suggested.

5.2.4 Flow-through stirred cell experiments

Flow-through experiments were performed using a Millipore 10mL ultrafiltration stirred cell fitted with a 100 nm pore size Millipore polycarbonate filter. Sorption and desorption steps were employed similar to those described by Eick et al. (1985) and Strawn and Sparks (2000). The background solution used in flow-cell experiments was 5 mM NaCl/0.7 mM $NaHCO_3$ adjusted to pH 8 and stirred for 2 weeks prior to use to ensure equilibration with atmospheric CO_2(g). The pH of the background solution was 8.05 at the start of both the Np and Pu flow-through experiments. In one step of the Pu flow-through experiment, a 5 mM NaCl solution adjusted to pH 5 with HCl was used as the background solution.

The goethite and background solution were added to the cell to generate a 2 g L^{-1} suspension. All masses and volumes were determined gravimetrically by weighing the cell before and after each addition. A Minipuls 2 peristaltic pump was used to maintain the flow rate of 12 mL hr^{-1}. A magnetic stirplate was used to ensure adequate mixing. The goethite was equilibrated with the

background solution with at least 50 pore volumes of the background solution. An Eldex fraction collector was used to collect fractions of the effluent at specified intervals. The exact volume of each fraction was determined gravimetrically and the pH was measured.

The "sorption step" of each experiment was started by draining the background solution from the influent and effluent lines. Then either the Np or Pu working solution was pumped through the influent tubes then connected to the flow-cell. Time zero was defined as the time at which the first drop of effluent was collected. At a flow rate of 12 mL hr^{-1}, the residence time within the 10 mL cell was 50 minutes. To determine if sorption was rate limited, the flow was stopped for various intervals ranging from 30 minutes to 17 days; effectively changing the residence time to the time of the stopped-flow period. If the concentration of Np or Pu in the effluent decreased after flow was resumed, the sorption reaction was rate-limited within the 50 minute residence time during normal flow. The flow-cell was weighed during each stopped-flow period to gravimetrically determine the exact solution volume. The standard deviation of suspension volume within the flow-cell was 0.1 mL throughout the experiments.

After the sorption step where Np or Pu had been loaded onto the goethite, a desorption step was initiated where the Np-free or Pu-free background solution was pumped through the system. The influent and effluent lines were drained and thoroughly rinsed with the background solution and drained again. The influent line was re-attached to the flow-cell. For Np experiment, the desorption step was started immediately after the sorption step was finished. For the Pu experiment, flow was stopped and the system was stirred for 2.5 days before beginning the desorption step. The difference in the two systems is due to the differing sorption rates of Np and Pu as will be discussed below. The desorption step was run exactly as described for the sorption step except for the influent solution did not contain Np, Pu, or tritium. Similar to the sorption step, the flow was periodically stopped to determine if desorption was rate-limited.

The total volume of each effluent fraction was determined gravimetrically. The pH was measured with an Orion ROSS semi-micro glass electrode and a Orion 5-star multimeter. Samples were prepared to determine the Np, Pu, and tritium concentrations using LSC as described above. The oxidation state of Pu in selected fraction was also measured as described above. Although the effluent passed through a 0.100 μm filter upon exiting the flow cell, additional filtration tests were run on selected fractions to determine if any colloidal species were present. This was especially relevant in Pu systems where Pu colloids may form from precipitation of Pu(IV) hydrolysis products (Neck and Kim, 2001). Effluent fractions were passed through 3k MWCO Microsep centrifugal filters then aliquots of the filtrate were analyzed via LSC. The first 0.5 mL of the filtrate was discarded to allow equilibration of the filter with the effluent which was found to minimize sorption of the actinides to the filtration membrane.

At specified stopped-flow periods, 10 μL aliquots of the suspension were removed for further SEM and TEM analysis. The subsamples were immediately dried at 40°C to minimize further reaction.

5.2.5 Data Analysis

5.2.5.1 Approximation of Effluent ^3H and Np Concentration

The fraction of Np or Pu sorbed at any point can be calculated by difference as

$$C_{solid} = \frac{V\ (C_{influent} - C_{effluent})}{m} \quad (1)$$

Where C_{solid} is the solid phase concentration of Np or Pu, $C_{influent}$ is the influent concentration, $C_{effluent}$ is the effluent concentration, V is the volume of the fluid and m is the mass of the solids. Therefore, the total activity of Np or Pu remaining in the cell could also be calculated by summing the solid phase concentration over the desired flow range. The total solid phase concentration and the measured effluent concentration were used to calculate an apparent K_d as:

$$K_d = \frac{C_{solid}}{C_{aqueous}} \quad (2)$$

A general mass balance equation for describing flow of a non-reactive solute was shown by Bar-Tal (1990, and references therein).

$$\frac{dC_{cell}}{dt}V_{cell} = (C_{influent} - C_{effluent})Q + m\frac{dS}{dt} \quad (3)$$

Where C_{cell} is the concentration in the cell, V_{cell} is the volume of the cell, Q is the flow rate, S is the sorbed concentration, and t is time. For a non-sorbing tracer, such as ^3H used in this work, equation 2 is simplified to:

$$\frac{dC_{cell}}{dt}V_{cell} = (C_{influent} - C_{effluent})Q. \quad (4)$$

The solution to equation 3 as reported by Bar-Tal et al. (1990 and references therein) is:

$$C_{effluent} = C_{influent}[1 - e^{-\frac{Q}{V_{cell}}t}] \quad (5)$$

For the desorption step where $C_{influent} = 0$ and $C_{effluent}=C_{cell}$ at the start of the desorption step (t_d), equation 3 can be simplified to:

$$C_{effluent} = C_{cell,t_d}e^{-\frac{Q}{V_{cell}}t} \quad (6)$$

Although examination of the non-equilibrium processes are one of the main objectives of this work, results from a simple model assuming equilibrium distribution of Np are discussed below to aid in a qualitative discussion of the data. Using the apparent K_d values calculated from stopped flow periods, retardation factors (R) were calculated using the equation:

$$R = 1 + \frac{\rho_b K_d}{\eta_e} \quad (7)$$

Where ρ_b is the bulk density and η_e is the effective porosity. The effective porosity was assumed to be one and the bulk density was set equal to the goethite concentration. The retardation factor can be employed in Equation 3 to account for sorption/desorption processes of Np. Making the assumption of steady state allows the far-right term of Equation 3 to be set to zero such that the effluent concentration during the sorption step can be written as:

$$C_{effluent} = C_{influent}[1 - \exp(-\frac{(Q/V_{cell})}{R}t] \quad (8)$$

Applying the same initial conditions and assumptions as equation 5. Likewise assuming the same initial conditions and assumptions as equation 6, the Np effluent profile during the desorption step can be written as:

$$C_{effluent} = C_{cell,t_d} \exp(-\frac{Q/V_{cell}}{R}t) \quad (9)$$

Again, this simple model is not meant to provide a rigorous description of the sorption behavior in these systems. As will be discussed below, the assumption of steady-state conditions is technically invalid. The model is only meant to aid in a qualitative discussion of the data.

5.2.5.2 Calculation of Pu sorption rate constants

Psuedo-first order sorption rate constants were calculated from the stopped flow data during the sorption step using Equiation 10 below

$$[Pu]_t = [Pu]_o e^{-k_{sorp}t} \quad (10)$$

Where, $[Pu]_t$ is the effluent Pu concentration after the stopped flow period, $[Pu]_o$ is the effluent Pu concentration at the start of the stopped flow period, t is the duration of stopped flow, and k_{sorp} is the pseudo-first order sorption rate constant.

5.3 Results and Discussion

5.3.1 Np Interactions with Goethite in Flow Cell

5.3.1.1 Np Sorption Step

The Np and ^{3}H flow cell data are presented in **Figure 5.2**. The figure shows the relative breakthough of Np and ^{3}H. As expected, 99.9% of the tritium was recovered in the effluent. The solid line represents a theoretical non-reactive tracer modeled with equations 4 and 5. Overall, there is a good fit to the ^{3}H effluent curve data for the sorption step. The fraction of Np in the effluent during the sorption step is lower than the ^{3}H effluent demonstrating loss of Np from the

aqueous phase due to sorption to goethite. There was a slight change in the aqueous Np concentration during the 2 hour and 21 hour stopped flow (noted as points A and B, respectively, in **Figure 5.2**). Under these solution conditions, Np sorption had almost reached a steady state within the 50 minute solution residence time.

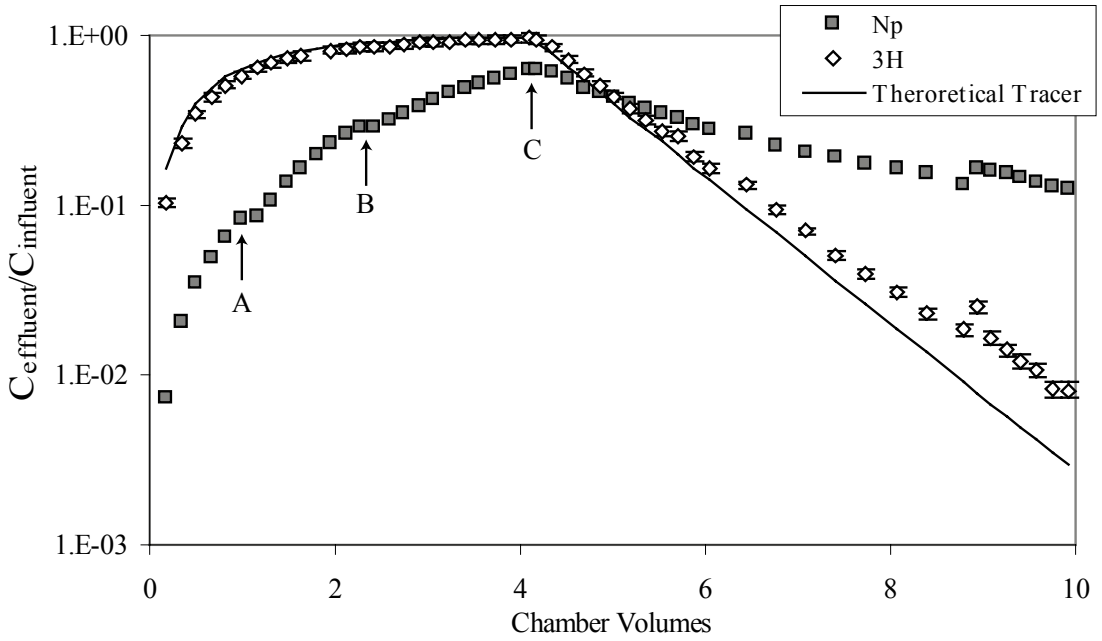

Figure 5.2 Np and ^{3}H effluent profile from stirred flow-cell. During the sorption step (0 to 4 chamber volumes) the background solution amended with 3.2 μM Np and 1000 cpm mL^{-1} ^{3}H was pumped through the flow-cell. During the sorption step (>4 chamber volume) only the background solution was pumped through the flow-cell. Arrows indicate periods of stopped flow for A) 2 hours, B) 21 hours, C) 0.5 hours, also start of the desorption step. Solid line represents theoretical non-reactive tracer calculated using Equations 5 and 6 for the sorption and desorption steps, respectively. System parameters: flow-rate = 12 mL hr^{-1}; Cell volume = 10 mL.

A Np-geothite sorption/desorption isotherm is plotted in **Figure 5.3**. The aqueous Np concentration tended to decrease slightly between 1 hour and 1 day. However, the change was relatively small, indicating that steady state had nearly been achieved after 1 hour. The measured effluent Np concentrations and the calculated Np solid phase concentrations from the flow-cell experiment can be directly compared to these batch isortherm data (**Figure 5.3**). The flow-cell data during the sorption phase match the 1 hour batch isotherm data quite well, consistent with the 50 minute residence time allowed in the flow-cell experiments. At the highest Np concentration, the 1 hour and 1 day batch isotherm data as well as the flow-cell data deviate significantly, suggesting that steady-state is not reached after one hour under high surface loading conditions.

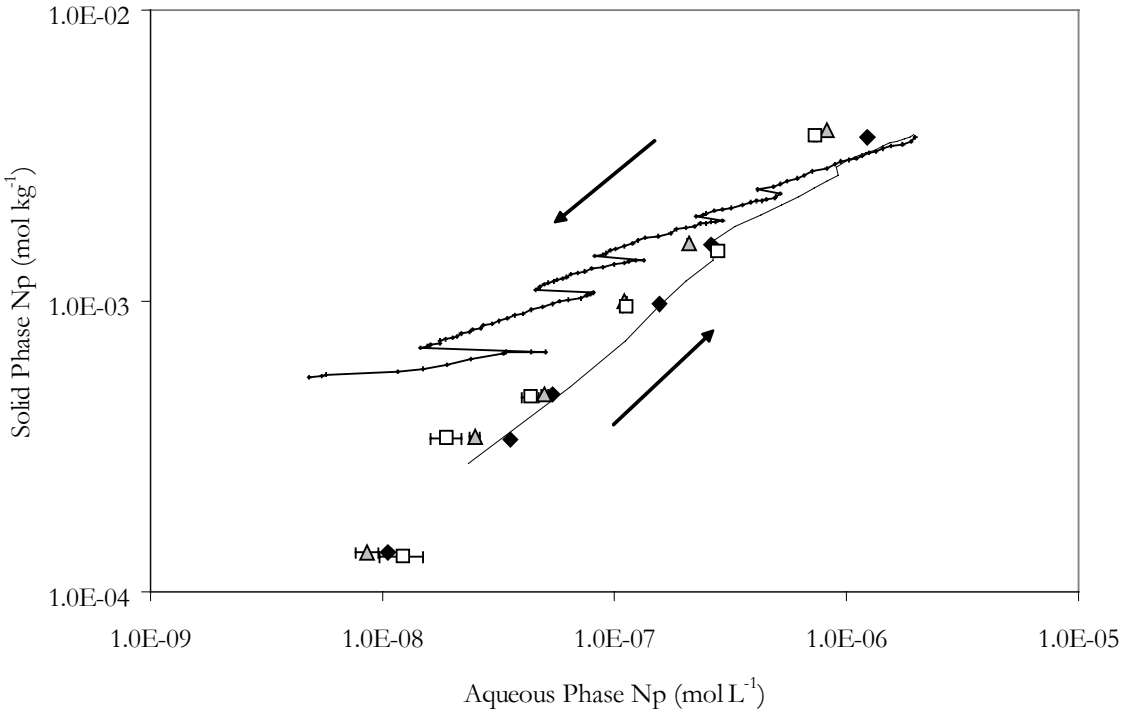

Figure 5.3 Np-goethite sorption/desorption isotherm. Sorption data collected after 1 hour (◆) and 1 day (△). Desorption data collected after 30 days (□).Isotherm solution conditions match those from flow-through experiment. Data from flow-through cell experiment collected during sorption step (thin, dotted line) and the desorption step (solid line) plotted. Arrows indicate forward direction of time during experiment. During periods of active flow, the aqueous Np concentration decreased since the desorption was rate-limited and the system moved further from equilibrium (away from the isotherm line). During periods of stopped flow, the aqueous Np concentration would increase as the system approached equilibrium as indicated by the approach to the isotherm line.

5.3.1.2 Np Desorption Step

After the Np working solution had been pumped through the flow-cell for four chamber volumes, the desorption step was started (**Figure 5.2**). It took approximately 30 minutes to drain and clean the influent and effluent lines and resume flow with the Np-free background solution. Note that the influent concentration of ^{3}H and ^{237}Np are technically zero during the desorption step but the initial data points of the desorption step are plotted in **Figure 5.2** so that the data can be compared with the sorption data. The fraction of ^{3}H in the effluent relative to the influent decreases to less than 1% within a few chamber volumes, consistent with the expected behavior of a non-reactive tracer. The solid line again represents a theoretical non-reactive tracer modeled with equations 4 and 5. The tritium values measured during the experiment after 6 chamber volumes are elevated compared to the modeled data. This represents an artifact of incomplete separation between the ^{3}H and ^{233}Pa LSC signals.

While the overall concentration of Np decreases over time, the Np concentration relative to the tracer increases. The concentration of Np in the effluent relative to the tracer represents Np that has desorbed from the goethite. It is more convenient to discuss the Np desorption data in terms of the absolute effluent Np concentration as shown in **Figures 5.3** and **5.4**. **Figure 5.4** shows the Np aqueous concentration in the flow cell for both the sorption and desorption steps. During the desorption process, the flow-cell was stopped six times (A-F on Fig. 5.4). The increase in Np effluent concentration following each of the stopped-flow periods indicates that the system did not achieve steady state and that Np desorption was rate limited within the 50 minute solution residence time allowed during active flow.

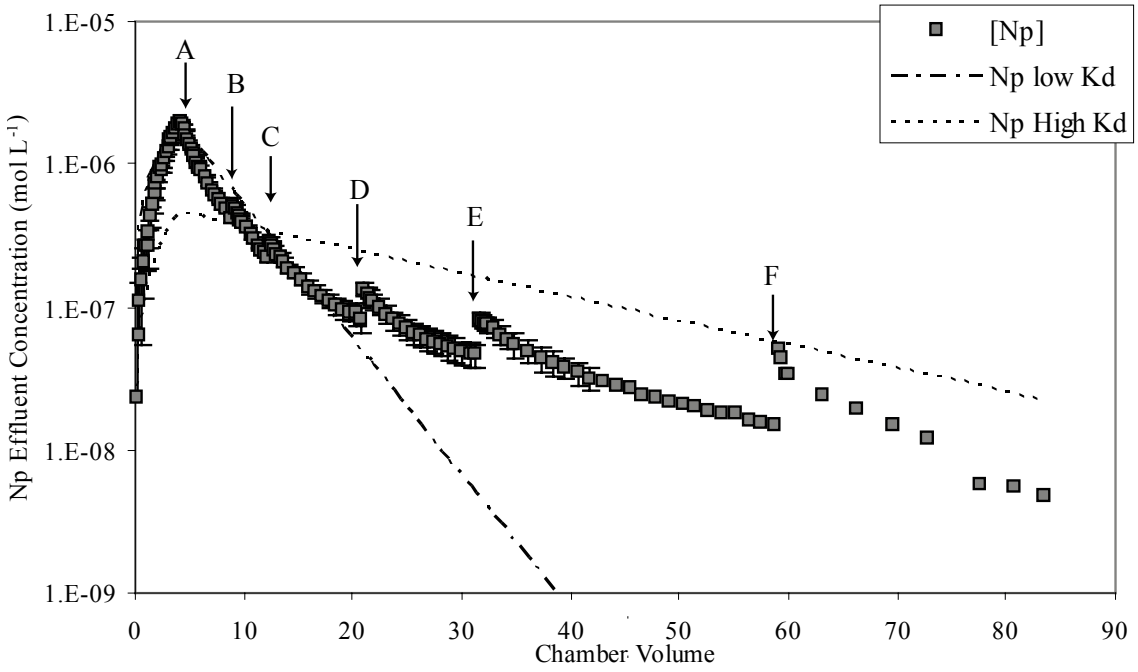

Figure 5.4 Np aqueous concentration in the flow-cell effluent representing both sorption and desorption steps. During the sorption step (0 to 4 chamber volumes) the background solution amended with 3.2 μM Np was pumped through the flow-cell. During the sorption step (4 to 83 chamber volumes) only the background solution was pumped through the flow-cell. Arrows indicate periods of stopped flow for A) start of desorption step, flow stopped 30 minutes, B) 0.9 days, C) 2.8 days, D) 3.7 days, E) 5.8 days, and F) 17.2 days. Dashed lines represent theoretical effluent profile calculated using Equations 8 and 9 for the sorption and desorption steps, respectively. The maximum (13000 L kg-1) and minimum (1860 L kg-1) Kd values from the stopped flow periods were used to calculate the retardation factors (R) using equation 2. System parameters: Flow-rate = 12 mL hr-1; Cell volume = 10 mL; Background solution: 5 mM NaCl, 0.7 mM NaHCO3, pH 8.

The flow-cell data from the desorption step are compared to the batch sorption isotherm data in **Figure 5.3**. Clearly, the partitioning of Np in the flow-cell deviates significantly from the batch

sorption isotherm data during both flow and stop-flow periods. During flow, the desorption rate of Np was not rapid enough to sustain the aqueous Np concentration within the cell and the system moved away from steady state (i.e. the data from the desorption step move away from the batch sorption isotherm data. During the stop-flow periods, as more time was allowed for Np to desorb, the aqueous Np concentration increased and the data approach the batch isotherm data.

The batch desorption isotherm data in **Figure 5.3** was generated by replacing the solution in the samples used to generate the sorption isotherm and allowing the modified samples to equilibrate for 30 days. The data agreement between the 1 day sorption isotherm and the 30 day desorption isotherm indicate that 1 day and 30 days are upper limits required to reach steady state for the sorption and desorption reactions, respectively. These boundaries agree with the data from the flow-cell experiment. Sorption was found to reach steady state within 1 day during from the flow-through data. For the desorption rate, the Np partitioning during the desorption step came closest to reaching the batch isotherm data after a stopped flow period of 17.2 days.

The duration of the desorption stop-flow periods ranged from 0.9 to 17.2 days and a constant Np aqueous concentration was never reached. Throughout the same period, the solid phase Np concentration decreased by approximately one order of magnitude. Attempts to model the Np breakthrough in **Figure 5.4** using either the minimum (1860 L kg^{-1}) or maximum (13000 L kg^{-1}) K_d values calculated from the stopped flow periods were unable to match the data. As noted above, this is an oversimplified model only intended to demonstrate the changing K_d value with surface load. At high Np solid phase concentrations, the low K_d value more closely approximates the data. Conversely, the high K_d value provides a better fit when the Np solid phase concentration was relatively lower. This changing behavior is proposed to be due to the effects of both strongly and weakly sorbing sites.

Dzombak and Morel (1990) proposed that two types of sorption sites influence cation sorption behavior on iron oxides; low affinity sites that control the bulk of observed sorption of cations, anions, and protons as well as a smaller set of high-affinity cation bonding sites. The curvature of the sorption isotherm shown in **Figure 5.3** indicates the influence of multiple sorption sites. At high Np solid phase concentrations, the strong sorption sites are full and Np desorption will primarily be controlled by weakly sorbing sites. As Np desorbs from the weakly sorbing sites and the overall Np solid phase concentration decreases, the Np partitioning will be primarily controlled by the strongly sorbing sites. In this model, only a small fraction of the total sorption sites are proposed to be "strongly" sorbing sites.

In our experiments, the Np solid phase concentrations at the beginning and end of the desorption steps were 3.7 μM $g^{-1}_{goethite}$ and 0.5 μM $g^{-1}_{goethite}$, respectively. If we assuming an average site density of 2.3 sites nm^{-2} for iron oxides (Dzombak and Morell, 1990), the Np surface load decreases from 7% to 1% from the beginning to the end of the desorption step, respectively (see **Figure 5.5**). When examining Np(V) sorption to hematite, Kohler et al., (1999) noted that for adsorption densities above 5% of the total hematite site concentration, the slope of sorption isotherms decreased below one, indicating that Np(V) was interacting with weaker sorption sites.

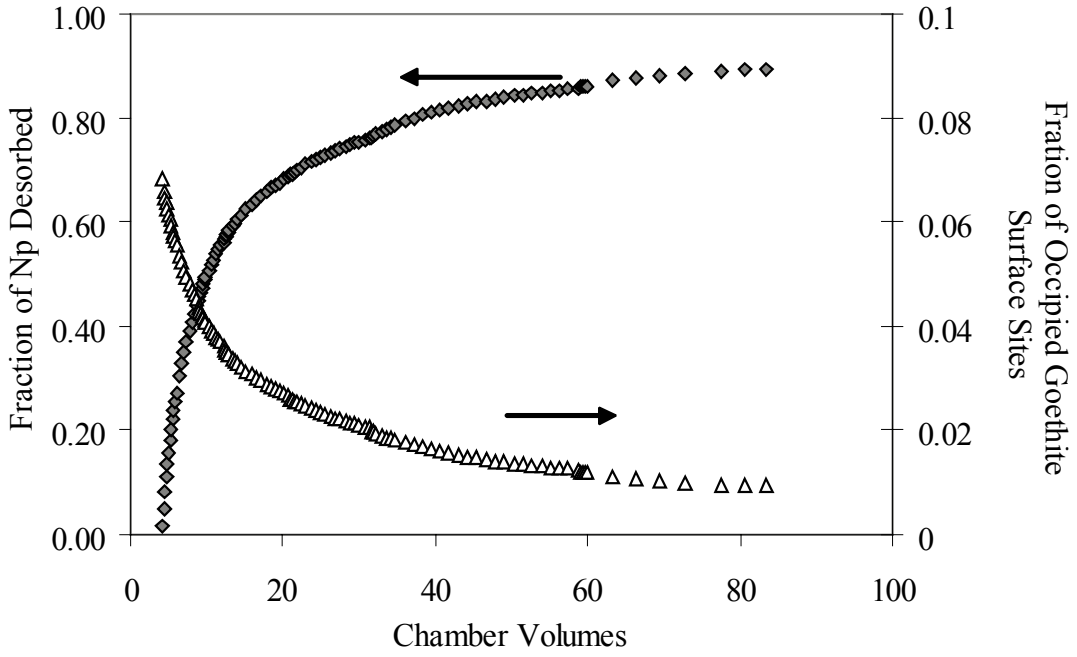

Figure 5.5 Fraction of Np desorbed during flow-through desorption step at pH 8 (◆) and fraction of goethite sites occupied by Np(V) assuming 2.3 sites nm^{-2} (Δ, plotted on secondary y-axis).

After passing 83 chamber volumes through the flow-cell 12% ± 3.7% of the Np remained sorbed. This apparent irreversible sorption has been previously observed in Np sorption studies. Nakata et al., (2000) found that after Np was sorbed to hematite for 1 week, 24% remained sorbed after attempts to desorb the Np with 1 M KCl and 0.1 $K_2C_2O_4$ in sequential steps. In column experiments utilizing untreated loess and loess treated to remove $CaCO_3$ and organic matter, 23% and 45%, respectively, of the sorbed Np was recovered in the effluent (Weijuan et al., 2003). Kenney-Kennicutt and Morse (1984) observed approximated 66% desorption of Np from goethite in deionized water and seawater, indicating the sorption reaction was not completely reversible. As shown in **Figure 5**, the total amount of Np desorbed was still increasing at the end of the experiment. It is uncertain whether or not complete recovery of the sorbed Np would have been achieved. This is presumed to be the result of Np partitioning to strongly sorbing sites which likely have considerably slower desorption kinetics and higher sorption affinities. However, this does not necessarily imply that the reaction is irreversible.

5.3.2 Pu Interactions with Goethite in Flow-through Cell

5.3.2.1 Pu Sorption Step

Sorption and desorption behavior of Pu to goethite was markedly different than Np. The relative effluent profile during the sorption step and the initial phase of the desorption step are shown in **Figure 5.6**. As seen in the Np experiment, the ^3H tracer effluent concentration becomes equal to

the influent concentration after a few column volumes. This is consistent with the profile of a non-reactive tracer as calculated by equation 4. The concentration of Pu in the effluent during the sorption step remained below 1% of the influent concentration as the first few chamber volumes were passed through the flow-cell indicating that the majority of Pu was sorbed. The concentration of Pu in the effluent continued increased throughout the sorption step. The maximum observed effluent Pu concentration of 10% was reached after approximately 8 chamber volumes. Presumably this maximum effluent concentration would be higher if flow was not periodically interrupted during the sorption step (**Figure 5.6**).

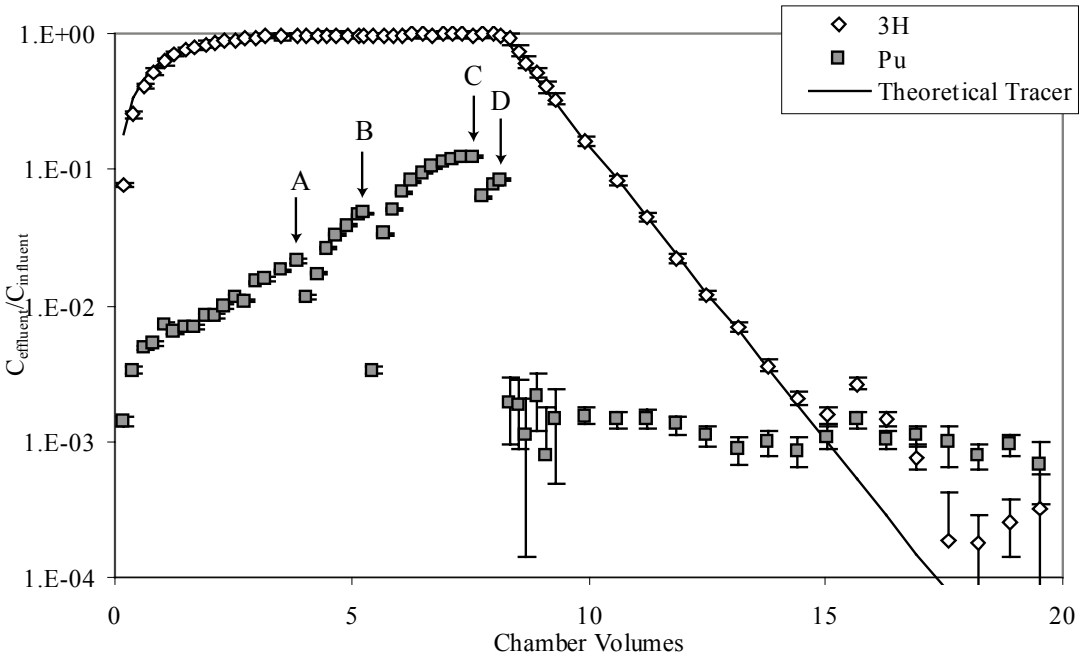

Figure 5.6 Pu and ^{3}H effluent profile from stirred flow-cell at pH 8. During the sorption step (0 to 8.3 chamber volumes) the background solution amended with 2.6 nM Pu(V) and 1000 cpm mL^{-1} ^{3}H was pumped through the flow-cell. During the desorption step (started at point D above) only the background solution was pumped through the flow-cell. Arrows indicate periods of stopped flow for A) 1 hours, B) 18.5 hours, C) 1 hour, and D) 66 hours (also start of the desorption step). Solid line represents theoretical non-reactive tracer calculated using Equations 5 and 6 for the sorption and desorption steps, respectively. System parameters: Flow-rate = 12 mL hr^{-1}; Cell volume = 10 mL; Background solution: 5 mM NaCl, 0.7 mM $NaHCO_3$, pH 8.

To test for the presence of real or pseudo colloids, selected effluent fractions were passed through 3k MWCO filters and the Pu concentration in filtrate was measured. In effluent fractions from 5.8 and 6.8 chamber volumes, 102 ± 4% and 96 ± 2%, respectively, of the effluent Pu passed through the filter, indicating that the Pu was soluble or present at a particle size less than the 3k MWCO filter pore size (estimated on the order of 1 to 4 nm). Results from oxidation state measurements of the effluent Pu from chamber volumes 6.3 and 7.6 showed that Pu was 95 ± 5% and 97 ± 4% Pu(V/VI), respectively. Therefore, Pu was mostly likely soluble as the initial Pu(V) species.

Flow was stopped for either 1 hour or 18 hours during the sorption step (noted as points A, B, and C in **Figure 5.6**). Upon resuming flow, a drop in the aqueous Pu concentration was observed indicating that additional Pu sorption occurred during the stop-flow period. Thus, sorption of Pu to goethite appears to be significantly rate-limited within the 50-minute solution residence time in the flow-cell.

Relative to the Np system, the rate-limited sorption was far more pronounced. Owing to the absence of a known reducing agent and the observed stability of Np(V) in circum-neutral solutions, reduction of Np(V) to Np(IV) was not expected in these systems. Additionally, reduction of Np(V) on ferric iron oxides has not been previously observed (Combes et al., 1992; Nakata et al., 2000). Conversely, reduction of Pu(V) to Pu(IV) by iron oxides and other minerals surfaces has been observed (Kenney-Kennicutt and Morse, 1985; Sanchez et al., 1985; Penrose et al., 1987; Kersting et al, 2005; Powell et al., 2005, Powell et al., 2006; Khassanova 2007). Furthermore Pu(IV) was observed as the stable solid phase oxidation state even on oxidizing manganese minerals (Powell et al., 2006). Powell et al., (2005) found that Pu(V) was temporarily stable on goethite surfaces before reducing to Pu(IV), indicating reduction was the rate limiting step rather than sorption. Based upon these observations, the rate limitation observed in the current work was presumed to be due to surface mediated reduction of Pu(V) to Pu(IV). Conceptually, as Pu(V) reduces to Pu(IV) on the goethite surface, more Pu(V) is sorbed to approach a steady state partitioning of Pu between the solid and the aqueous phase.

Table 5.1 lists psuedo first-order sorption rate constants that were calculated from the stopped flow data using Equation 10. The constants calculated from the 2 hour stopped flow periods compare favorably the value of 0.47 hr^{-1} calculated from the overall rate expression reported by Powell et al., (2005). Powell et al. (2005) reported that at pH 8 greater than 90% of the Pu(V) was sorbed and reduced to Pu(IV) in goethite suspensions within 24 hours. Therefore, the sorption rate constant of 0.14 ± 0.02 hr^{-1} calculated from the 18.5 hour stopped flow period was likely artificially low as the measurement was made when the system was close to reaching a steady-state. Similar to the rate constants reported by Powell et al. (2005), these rate constants are assumed to represent the overall reaction describing both sorption and reduction of Pu(V). However, based on Np(V) sorption data, Pu(V) reduction is the rate-limiting step.

Table 5.1 Apparent pseudo first-order Pu-goethite sorption rate constants

Time of Stopped Flow (hours)	sorption rate (hr^{-1})
1.0	0.62 ± 0.05
18.5	0.14 ± 0.02
1.0	0.69 ± 0.04

5.3.2.2 Pu Desorption Step at pH 8

The data collected during the sorption step indicate that sorption of Pu(V) was rate limited. Flow was stopped for 66 hours (2.5 days, noted as event D in **Figure 5.6**) prior to beginning the desorption step to allow the system to approach steady state. As shown in **Figure 5.6**, the ^{3}H effluent concentration drops to less than 1% of the initial influent concentration within approximately 5 chamber volumes, as expected. After 15 chamber volumes, the ^{3}H was almost completely evacuated and fell below the relative Pu concentration line in **Figure 5.6**, indicating that Pu was also desorbing from goethite (**Figure 5.6**). It is interesting to compare the fraction of Pu desorbed within the first chamber volume with batch Pu sorption experiments in goethite suspensions reported by Lu et al., (1999). Upon replacing the Pu-amended solution used in a batch sorption step with a Pu-free solution, Lu et al., (1999) reached 0.3% to 0.9% of the initial Pu concentration in goethite suspensions with natural and synthetic groundwaters. In this work, 0.2% of the initial Pu influent concentration was reached within the first chamber volume of Pu-free background solution, consistent with the results of Lu et al. (1999). However, Pu continued to desorb as the background solution was passed through the flow-cell.

The sorption and desorption steps are replotted in **Figure 5.7** in terms of the absolute effluent Pu concentration. At the end of the sorption step (noted as event "A" in **Figure 5.7**) the effluent Pu concentration was $2.16 \pm 0.05 \times 10^{-10}$ M. After the flow was stopped for 66 hours and the desorption step was started, the effluent Pu concentration had dropped two orders of magnitude to $4.9 \pm 2.5 \times 10^{-12}$ M. As Pu-free background solution was passed through the flow-cell, the effluent Pu concentration steadily decreased during active flow. An increase in the effluent Pu concentration was observed following stop-flow periods ranging in duration from 16 to 161 hours, indicating that Pu desorption was rate-limited within the 50 minute flow-cell residence time. To test the effect of the solution residence time, the flow rate was reduced to 3 mL hr^{-1} for a short period between chamber volumes 84.3 and 94.4 (noted as event "E" in **Figure 5.7**). The reduced flow-rate increased the solution residence time to 3.3 hours and a slight increase in the effluent Pu concentration was observed, again demonstrating that desorption of Pu was rate-limited. **Table 5.2** lists the Pu effluent concentration at the beginning of the stopped flow periods and the effluent concentration after restarting flow. Similar aqueous Pu concentrations are reached following the stopped flow periods, with an average value of 3.60×10^{-12} M and a standard deviation of 6.4×10^{-13} M. Based upon this observation, it may be assumed that the system had reached or was close to reaching steady state during the stopped flow periods. The similar K_d values listed in **Table 5.4** for stopped flow periods of 96 and 162 hours also indicate the system was close to steady state. Measurements of the effluent Pu oxidation state indicated primarily Pu(V/VI) as shown in **Table 5.3**. Due to the low Pu concentrations, the measurements have extremely high error, making a rigorous assessment difficult. However, it can be qualitatively stated that Pu was predominantly in an oxidized (Pu(V/VI) state.

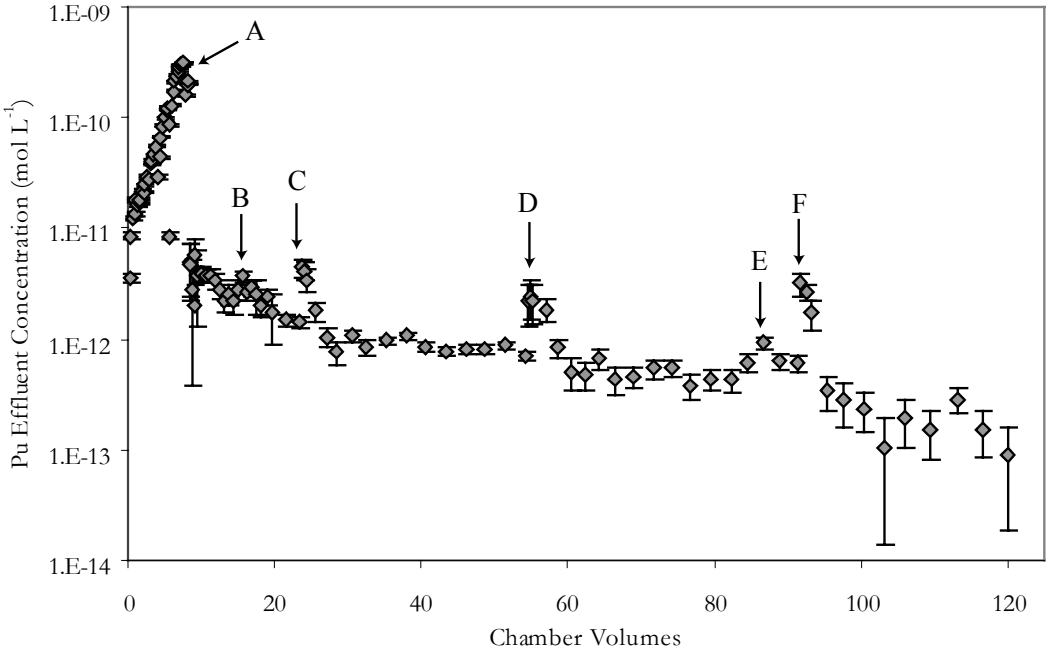

Figure 5.7 Pu aqueous concentration in the flow-cell effluent representing both sorption and desorption steps at pH 8. During the sorption step (0 to 8.3 chamber volumes) the background solution amended with 2.6 nM Pu(V) and 1000 cpm mL^{-1} ^3H was pumped through the flow-cell. During the desorption step (started at point D above) only the background solution was pumped through the flow-cell. Arrows indicate periods of stopped flow for A) start of desorption step, 66.0 hours, B) 16.3 hours, C) 42.0 hours, D) 96.0 hours, E) flow-rate decreased to 3 mL hr^{-1}, and F) 161.2 hours. System parameters: Flow-rate = 12 mL hr^{-1}; Cell volume = 10 mL; Background solution: 5 mM NaCl, 0.7 mM $NaHCO_3$, pH 8.

Table 5.2 Effluent Plutonium Concentrations at the Start and End of Stopped-flow Periods

Duration of stopped flow (h)	Pu effluent concentration at start of stopped flow period (mol L^{-1})	Pu effluent concentration after resuming flow (mol L^{-1})	K_d after resuming flow (L g^{-1})
System pH 8			
16.3	$2.79 \pm 0.53 \times 10^{-12}$	$3.70 \pm 0.47 \times 10^{-12}$	$2.82 \pm 0.18 \times 10^{6}$
42.0	$1.43 \pm 0.16 \times 10^{-12}$	$4.47 \pm 0.87 \times 10^{-12}$	$2.33 \pm 0.23 \times 10^{6}$
96.0	$7.00 \pm 0.74 \times 10^{-13}$	$3.04 \pm 0.94 \times 10^{-12}$	$3.42 \pm 0.53 \times 10^{6}$
161.2	$6.13 \pm 1.06 \times 10^{-13}$	$3.18 \pm 0.78 \times 10^{-12}$	$3.26 \pm 0.40 \times 10^{6}$
System pH 5			
22.0	$1.10 \pm 0.09 \times 10^{-11}$	$9.13 \pm 0.72 \times 10^{-11}$	$1.13 \pm 0.89 \times 10^{5}$
63.3	$1.36 \pm 0.11 \times 10^{-11}$	$2.84 \pm 0.23 \times 10^{-10}$	$3.61 \pm 0.29 \times 10^{4}$
64.5	$9.07 \pm 0.88 \times 10^{-12}$	$2.87 \pm 0.23 \times 10^{-10}$	$3.51 \pm 0.28 \times 10^{4}$
141.8	$6.87 \pm 0.65 \times 10^{-12}$	$1.95 \pm 0.16 \times 10^{-10}$	$5.07 \pm 0.41 \times 10^{4}$
289.5	$5.50 \pm 0.53 \times 10^{-12}$	$1.88 \pm 0.14 \times 10^{-10}$	$5.16 \pm 0.40 \times 10^{4}$

Table 5.3 Oxidation State Analysis of Pu in Effluent During Flow-through Experiment.

Chamber Volume	Fraction Pu(V/VI)	Fraction Pu(IV)	Analysis Technique
Sorption Step at pH 8			
6.3	95% ± 5%	5% ± 7%	CP
7.6	97% ± 4%	3% ± 7%	CP
Desorption Step at pH 8			
17.6	68% ± 24%	32% ± 25%	CP
19.5	83% ± 41%	17% ± 42%	CP
25.6	91% ± 27%	9% ± 28%	CP
25.6	97% ± 29%	3% ± 29%	SX
57.1	81% ± 28%	19% ± 28%	CP
57.1	73% ± 25%	27% ± 25%	SX
Desorption Step at pH 5			
130.4	98% ± 5%	2% ± 7%	CP
130.9	91% ± 6%	9% ± 8%	CP
132.7	96% ± 4%	4% ± 7%	CP
133.0	96% ± 5%	4% ± 7%	CP
133.3	100% ± 5%	0% ± 7%	CP
141.7	99% ± 4%	1% ± 6%	CP
142.0	94% ± 4%	6% ± 6%	SX
143.6	94% ± 4%	6% ± 7%	SX
154.4	90% ± 4%	10% ± 6%	CP
155.8	82% ± 4%	18% ± 6%	CP
154.7	84% ± 4%	16% ± 6%	SX
156.5	92% ± 5%	8% ± 7%	SX

SX = Solvent Extraction Oxidation State Analysis
CP = LaF_3 Coprecipitation Oxidation State Analysis

Table 5.4 Filtration Analysis of Pu in Effluent During Flow-through Experiment.

Cumulative Chamber Volume	Soluble Fraction[a]
5.8[b]	102% ± 4%
6.8[b]	96% ± 2%
133.9[c]	96% ± 5%
134.5[c]	98% ± 6%
135.1[c]	106% ± 7%
155.1[c]	91% ± 5%
157.2[c]	102% ± 10%
158.7[c]	94% ± 30%

[a]Fraction passing through 3K MWCO filter
[b]Measurement during sorption step
[c]Measurement during desorption step at pH 5

Despite reaching similar effluent Pu concentrations following periods of stop-flow, a steady decrease in the effluent Pu concentration during active flow was observed throughout the pH 8 desorption step. This observation suggests there is a type of "aging" effect that caused desorption of Pu to become more unfavorable over the course of the experiment. Unlike experiments with Np where the solid phase Np concentration was significantly changing during the desorption step, the sorbed Pu concentration only changed slightly over the course of the pH 8 desorption step. **Figure 5.8** shows that only 0.5% of the sorbed Pu was desorbed after passing 122 chamber volumes of Pu free solution through the flow cell. This corresponds to a minimal change in the Pu density on the goethite surface. At the end of the sorption step, the solid phase Pu concentration was $1.04 \pm 0.02 \times 10^{-8}$ mol_{Pu} $g^{-1}_{goethite}$ (2.5 ppm). Again assuming a site density of 2.3 sites nm^{-2}, the Pu occupied only 0.02% of the available surface sites. After desorbing 0.5% of the sorbed Pu during the pH 8 desorption step, the change in the solid phase Pu concentration was within the experimental error reported above. Therefore, the decrease in the effluent Pu concentration cannot be attributed to a changing solid phase Pu concentration as hypothesized for the Np systems examined above.

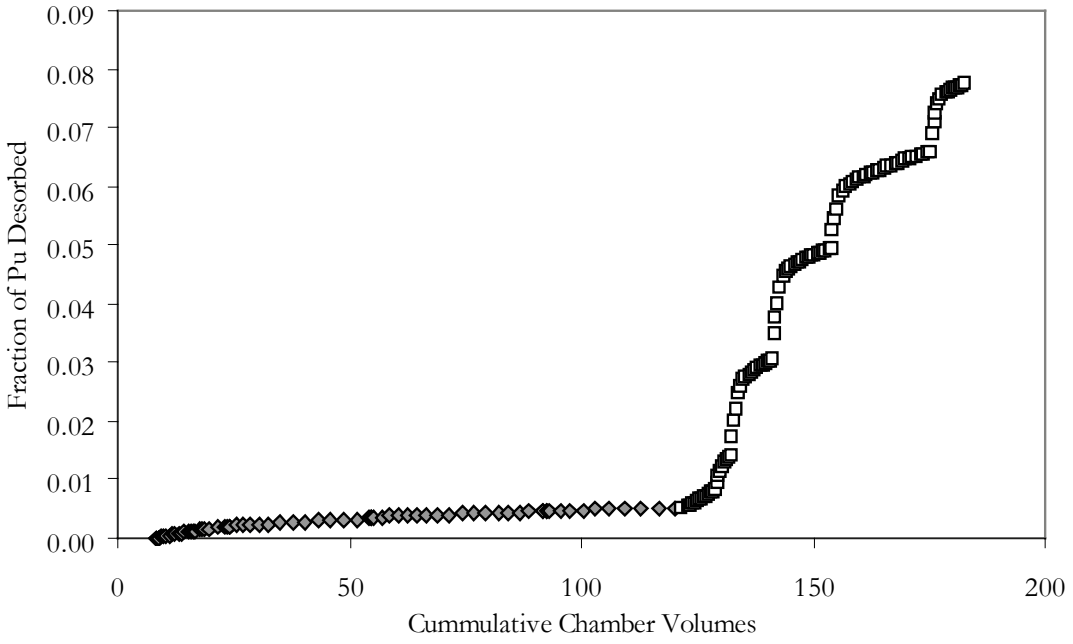

Figure 5.8 Fraction of Pu desorbed during flow-through desorption step at pH 5 (□) and pH 8 (◆). The fraction of occupied goethite sites changed from 1.95×10^{-4} to 1.80×10^{-4} throughout the course of the experiment, assuming 2.3 sites nm^{-2}.

Two possible mechanisms that can account for the observed decrease in Pu effluent concentration are 1) surface mediated precipitation of $Pu(OH)_4(s)$ and 2) re-partitioning of plutonium to more energetically favorable, strongly sorbing sites as proposed for the Np systems above. Both of these possible mechanisms assume that Pu is capable of desorbing and partitioning to different sites on the mineral surface. In the precipitation scenario, the concentration of desorbed Pu near the mineral surface could increase to a saturation level where plutonium hydrous oxides

precipitate. Efforts to observe discrete Pu precipitates on the mineral surface using transmission electron microscopy (TEM) and energy dispersive X-ray spectroscopy (EDS) were unsuccessful, indicating that Pu was widely distributed across the mineral surface. Furthermore, oxidation state analysis indicated that desorbed, aqueous Pu was in the soluble pentavalent state (**Table 5.3**). While disproportionation of Pu(V) could possibly generate insoluble Pu(IV), that mechanism is unlikely as the neutral pH and the relatively low total Pu concentration in the system make Pu(V) disproportionation unfavorable. Based upon this logic, it does not appear that Pu precipitation is responsible for the observed "aging" effect of the system.

Similar to the proposed involvement of strong and weak sorption sites in the Np systems discussed above, the "aging" effect may be the result of Pu repartitioning to more energetically favorable, strongly sorbing sites. It can be assumed that trace metals will initially partition to weak sorption sites due to their relatively high concentration compared with strong sorption sites. Desorption and readsorption of Pu over time will increase the probability that Pu will partition to a strongly sorbing site. Inherent in this mechanism is the assumption that the Pu desorption rate from strongly sorbing sites is slower than the desorption rate from weakly sorbing sites. This phenomenon will be discussed in more detail in the following sections describing a conceptual model of Np and Pu subsurface transport.

5.3.2.3 Pu Desorption Step at pH 5

After passing 120 chamber volumes of pH 8 background solution through the flow-cell, the influent solution was replaced with a pH 5, 5 mM NaCl solution. There was a marked increase in the aqueous Pu concentration as the effluent pH increased (**Figure 5.9**). After ~5 chamber volumes (cumulative chamber volumes 125-130), the effluent Pu concentration remained steady with an average concentration of 1.07×10^{-11}M and standard deviation of 3.2×10^{-13}M. Following the stopped flow periods, the effluent Pu concentration were observed increase further, indicating that desorption of Pu was rate limited at pH 5 as well as pH 8. **Table 5.2** lists the maximum observed effluent Pu concentration following the stopped flow periods. The maximum effluent Pu concentrations were approximately 2 orders of magnitude greater than the concentrations reached during the pH 8 stop-flow periods. The highest concentrations were reached following the 63.3 and 64.5 hours stop-flow periods. A slight decrease in the effluent Pu concentration was observed for the 141.8 and 289.5 hour stop-flow periods. There was also a corresponding increase in the K_d when increasing the duration of the stopped flow from ~64 hours to 141.8 and 289.5 hours. The effluent Pu concentration measured following 141.8 hour and 289.5 hour stop-flow periods are within the measured error. However, they are both outside the measured error for the 63.3 and 64.5 hour stop-flow periods. Therefore, it appears that at least 142 hours were required for the system to reach steady state.

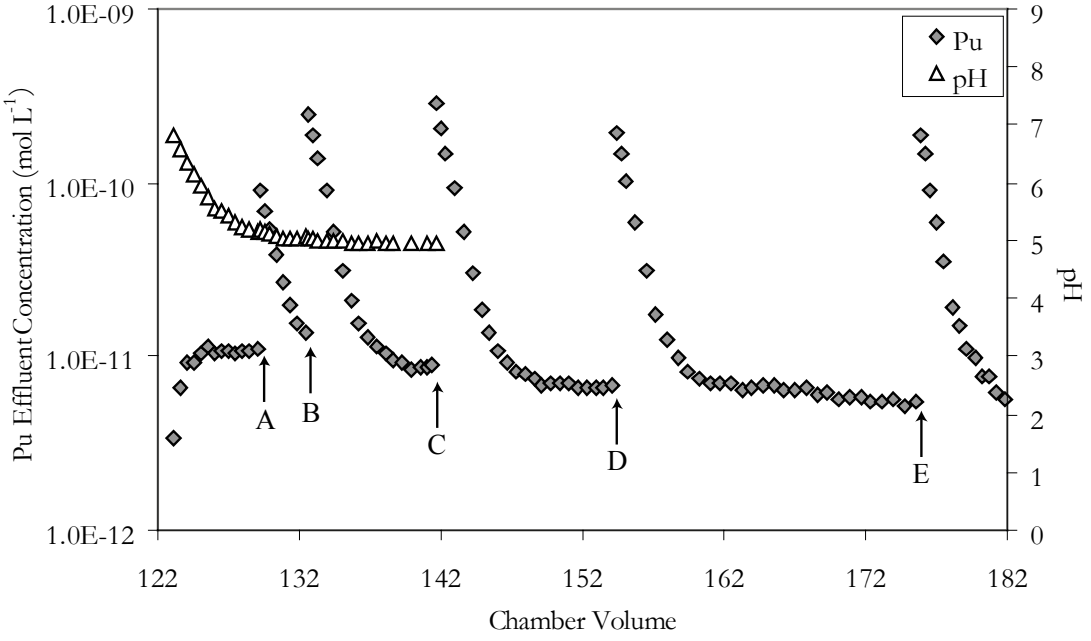

Figure 5.9 Pu aqueous concentration in the flow-cell effluent during desorption step at pH 5. After 120 chamber volumes, the background solution was replaced with a pH 5, 5mM NaCl solution. The changing effluent pH values are plotted on the y-axis up to 140 chamber volumes, after which the pH remained 5.0 ± 0.05. Arrows indicate periods of stopped flow for A) 0.5 hours, B) 22.0 hours, C) 63.3 hours, D) 64.5 hours, E) 141.8 hours, and F) 289.5 hours. System parameters: Flow-rate = 12 mL hr^{-1}; Cell volume = 10 mL Background solution: 5 mM NaCl, pH 5.

Over the course of the pH 5 desorption step, an additional 7.2% of the sorbed Pu was desorbed after passing 60 chamber volumes through the flow-cell (**Figure 5.8**). This resulted in the solid phase Pu concentration decreasing from $1.04 \pm .01 \times 10^{-8}$ mol_{Pu} $g_{goethite}^{-1}$ to $9.63 \pm .01 \times 10^{-9}$ mol_{Pu} $g_{goethite}^{-1}$ and a statistically insignificant change in the fraction of goethite sites occupied. Aliquots of the effluent were passed through 3k MWCO filters to determine if adjustment of the pH resulted in the release of any colloidal particles. The six measurements listed in **Table 5.4** verify that all effluent Pu was soluble and not associated with a colloidal phase. Furthermore, due to the higher effluent Pu concentrations, more precise measurements of the Pu oxidation state were possible. Results using both solvent extraction and lanthanum fluoride coprecipitation shown in **Table 5.3** indicate that Pu was primarily present in an oxidized (V/VI) state. Therefore, it appears that all the desorbed Pu measured throughout the experiment was present in the aqueous phase as soluble Pu(V). It is a reasonable assumption that the solid phase Pu was predominantly Pu(IV) based upon the discussion of the sorption behavior above and the numerous observations of goethite mediated reduction of trace Pu(V) to Pu(IV) (Kenney-Kennicutt and Morse, 1985, Sanchez et al., 1985, Penrose et al., 1987, Kersting et al., 2005). Therefore the significant fraction of desorbed Pu (7.7% total) appears to be re-oxidizing, although an exact mechanism cannot be drawn from these data.

At pH 5, the effluent Pu concentration reached during active flow appeared to steadily decease over time, similar to the system at pH 8. Again it appears an "aging" effect was observed where Pu was becoming more strongly associated with the solid phase over time. This effect may also be responsible for the slight decrease in the effluent Pu concentrations following the stopped flow periods as discussed above.

5.3.2.4 Pu Desorption Step- return system to pH 8

To further examine the effects of pH on Pu desorption, the influent solution was returned to the pH 8, 5mM NaCl/0.7 mM $NaHCO_3$ solution initially used in these experiments. Data discussed below are not shown. After the pH increased to 8.0, the effluent Pu concentration decreased. After the pH became stable at 8.0, a steady effluent Pu concentration was observed for 25 chamber volumes with an average value of 3.1×10^{-13} M (SD = 7.0×10^{-14} M, n=6). This Pu concentration is close to the value of 1.9×10^{-13} (SD 7.6×10^{-14} M, n=8) for the last 10 chamber volumes of the initial pH 8 desorption step. Therefore, the system is behaving exactly as expected if the pH had remained at pH 8 rather than being lowered to pH 5. In other words, lowering the system to pH 5 did not "reset" the sorption sites and allow Pu desorption to progress as it did at the beginning of the experiment. This observation indicates that the "aging" effect observed in these experiments is not easily perturbed.

This behavior supports that hypothesis that both Np and Pu become associated with more energetically favorable, strong sorption sites over time. Desorption from strongly sorbing sites will be less favorable and likely proceed slower and to a lesser extent. Therefore, as more Pu associated with strongly sorbing sites, less aqueous Pu would be expected. Since similar Pu concentrations were observed at the end of the first pH 8 desorption step and upon returning the system to pH 8, it appears that the Pu associated with strong sorption sites at pH 8 were undisturbed by the pH adjustment.

5.4 Summary and Conclusions

By utilizing a flow-cell experimental design, the rate and extent of Np and Pu interactions with goethite were investigated. Np and Pu were loaded onto goethite slowly without ever exceeding solubility. The rate-limitation of Np(V) sorption to goethite was relatively small compared with Pu(V). The difference between the sorption behavior was attributed to surface mediated reduction of Pu(V) to Pu(IV), while no redox changes of Np(V) were observed or expected. Reaction rates describing loss of aqueous Pu(V) compared favorably to reported rates Pu(V) reduction to Pu(IV) on goethite (Powell et al., 2005).

Sorption of both Np and Pu was reversible although hysteretic. During the sorption step, Np was loaded on the goethite solids to a solid phase concentration of 3.7 μM $g^{-1}_{goethite}$ which corresponded to occupation of approximately 7% of the surface sites. Desorption of Np appeared to require between 6 and 17 days to reach a steady state. After passing 83 chamber volumes of Np-free background solution through the flow-cell, 12% ± 3.7% of the Np remained sorbed to goethite. The Np remaining on the goethite is most likely associated with a small fraction of strongly sorbing sites, exhibiting considerably slower desorption kinetics.

Pu was loaded to a solid phase concentration of $1.04 \pm 0.02 \times 10^{-8}$ mol_{Pu} $g^{-1}_{goethite}$ (2.5 ppm), corresponding to occupation of 0.02% of the surface sites. Only 0.5% of the sorbed Pu was desorbed after passing 122 chamber volumes of pH 8, Pu-free solution through the flow-cell. An additional 7.2% was desorbed by passing 83 chamber volumes of pH 5, Pu-free solution through the cell. In both pH 5 and pH 8 systems, effluent Pu was found to be predominantly soluble and in an oxidized state (Pu(V/VI)). Lowering the influent pH to 5 resulted in an increase in the aqueous Pu concentration between 2 and 3 orders of magnitude, relative to pH 8. The increased Pu concentration is the result of a decreased affinity of Pu for solid phases and increased Pu solubility with decreasing pH.

Desorption of Pu was found to be rate-limited in both pH 8 and pH 5 systems. Based upon the duration of stopped flow events, it appears that Pu desorption took between 4 and 6 days to reach a steady state. The effluent Pu concentration observed during active flow decreased over the course of the experiment, indicating an "aging" effect whereby it was more difficult to desorb Pu. However, similar aqueous Pu concentrations and K_d values were observed in pH 8 systems following stopped flow periods indicating that the observed "aging" has a minimal effect on the steady state distribution of Pu in the systems. However, the "aging" effect may have influenced the pH 5 system as there was a slight increase in the K_d values reached following stopped flow periods. It was hypothesized that the "aging" effect was due to either aggregation of discrete Pu hydroxide precipitates at the mineral surface or by redistribution of solid phase Pu to more strongly sorbing sites. Attempts to observed discrete Pu solids via TEM/EDX were unsuccessful. Therefore, it is proposed that over time Pu redistributed to more strongly sorbing sites. The influence of both strong and weak sorption sites was also proposed to explain the behavior of Np in the same systems.

These data have shown that Np and Pu partitioning cannot be described using only a single, linear distribution coefficient. This is especially true for Pu systems where surface-mediated reduction of Pu(V) to Pu(IV) allows for the simultaneous presence of at least two oxidation states with drastically different sorption behavior. Sorption of Np and Pu appears to be influenced by interaction with sorption sites that have varying affinities for Np and Pu. The redistribution of Np and Pu from weakly sorbing sites to more strongly sorbing sites was proposed to explain the observed hysteresis. Presumably desorption from strongly sorbing sites will be slower than from weakly sorbing site. Therefore, experiments run for much longer durations are required to determine desorption rates from strongly sorbing sites, if the reaction is indeed reversible.

Another confounding factor is the influence of pH on the sorption of Pu and the relative distribution of Pu(V) and Pu(IV). The pH of the bulk phase will influence the sorption affinity of both Pu(IV) and Pu(V) as well as the overall solubility of Pu. In the absence of additional complexing agents, as the pH of a suspension decreases there is a corresponding increase in the aqueous Pu concentration as the predominantly cationic Pu species are repelled from the mineral surface. Additionally the solubility and oxidation state distribution is drastically effected by pH (Neck et al., 2007). Measurements of the oxidation state distribution of aqueous Pu within a saturated Pu hydrous oxide suspension indicate Pu(V/VI) as the dominant aqueous oxidation

state(s). Recently, Neck et al. (2007) modeled Pu solubility in the presence of oxygen where PuO_2(s,hyd) is partially oxidized to a mixed oxide product PuO_{2+x}(s,hyd). A solubility product for Pu(V) solids coassociated within PuO_{2+x}(s, hyd) was incorporated to control the Pu(V) aqueous concentration (Neck et al., 2007). In the current work and previous work, aqueous Pu(V) was observed in equilibrium with Pu sorbed to a mineral surface as Pu(IV) (Powell et al., 2004, 2005). This observation is somewhat analogous to Pu solubility studies discussed above. A small fraction of solid phase Pu(IV) may be oxidized by dissolved oxygen and partition to the aqueous phase as Pu(V). Then the aqueous phase Pu(V) concentration would be limited by sorption of Pu(V) and surface-mediated reduction to Pu(IV). Based on the predominance of solid phase Pu(IV), the reduction rate would be considerably faster than the oxidation rate. This is analogous to the relatively fast sorption rate observed in this work, relative to the desorption rate. A similar observation was made by Kaplan et al., (2004) where incorporation of an oxidation rate 5 orders of magnitude slower than the reduction rate was necessary to accurately fit Pu transport in 12 year field lysimeter studies.

Based upon this work, it is recommended that efforts to model Np and Pu subsurface transport use a conceptual model assuming reversible sorption to sites with varying affinities for Np and Pu. Furthermore, it is imperative that differences between the sorption behavior of Pu(IV) and Pu(V) be considered and accounted for. The general behavior of Pu in these systems appears to be analogous to solubility studies. Therefore, Pu sorption could be conceptualized assuming both Pu(IV) and Pu(V) partition to the solid phase based upon their relative sorption affinities and that the maximum possible aqueous Pu(V) concentration is determined by the presence of dissolved oxygen and the solubility of PuO_{2+x}(s,hyd).

Acknowledgements: Portions of this work were performed under the auspices of the U.S. Department of Energy by the University of California, Lawrence Livermore National Laboratory under Contract W-7405-Eng-48, during fiscal year 2006.

5.5 References

Allard, B., Kipatsi, H., Liljenzin, J. O. (1980) Expected Species of Uranium, Neptunium, and Plutonium in Neutral Aqueous Solutions *J. Inorg. Nucl. Chem.* 42, 1015-1027.

Bar-Tal, A., Sparks, D. L., Pesek, J. D., Feigenbaum, S. (1990) Analyses of adsorption kinetics using a stirred-flow chamber: I. Theory and critical tests. *Soil. Sci. Soc. Am. J.* 54, 1273-1278.

Bertrand, P. A., and Choppin, G. R. (1982) Separation of Actinides in Different Oxidation States by Solvent Extraction *Radiochim. Acta* 31, 135-137.

Carski, T. H. and Sparks, D. L. (1985) A Modified Miscible Displacement Technique for Investigating Adsorption-Desorption Kinetics in Soils *Soil Sci. Soc. Am. J.* 49, 1114-1116.

Cleveland, J. M. (1979) *The Chemistry of Plutonium.* American Nuclear Society. La Grange Park, IL.

Combes, J. M., Chisholm-Brause, J., Brown, G. E. Jr., Parks, G. A., Conradson, S. D., Eller, P. G., Triay, I. R., Hobart, D. E., Meijer, A. (1992) EXAFS Spectroscopic Study of Neptunium(V) Sorption at the a-FeOOH/Water Interface *Environ. Sci. Tech.* 26, 376-382.

Conradson, S. D., Mahamid, I. A., Clark, D. L., Hess, N. J., Hudson, E. A., Neu, M. P., Palmer, P. D., Runde, W. H., Tait, C. D. (1998) Oxidation State Determination of Plutonium Aquo Ions Using X-Ray Absorption Spectroscopy *Polyhedron* 17(4) 599-602.

CRWMS M& O (Civilian Radioactive Waste Management System Management and Operating Contractor). 2000. *Unsaturated Zone and Saturated Zone Transport Properties*. Civilian Radioactive Waste Management System Management and Operating Contractor, Las Vegas, Nevada, ANL-NBS-HS-000019.

Dzombak, D. A. and Morel, F. M. M. (1990) Surface Complexation Modeling: Hydrous Ferric Oxide. John Wiley and Sons, Inc., New York.

Eick, M. J., Bar-Tal, A., Sparks, D. L., Feigenbaum, S. (1990) Analyses of Adsorption Kinetics Using a Stirred-Flow Chamber: II. Potassium-Calcium Exchange on Clay Minerals *Soil Sci. Soc. Am. J.* 54, 1278-1282.

Foti, S. C., and Freiling, E. C. (1964) the Determination of the Oxidation States of Tracer Uranium, Neptunium, and Plutonium in Aqueous Media *Talanta* 11, 385-392.

Girvin, D. C., Ames, L.L., Schwab, A. P., McGarrah, J. E. (1991) Neptunium Adsorption on Synthetic Amorphous Iron Oxyhydroxide *J. Coll. Inter. Sci.* 141(1), 67-78.

Hardy, C. J., Scargill, D., Fletcher, J. M. (1958) Studies on Protactinium(V) in Nitric Acid Solutions *J. Inorg. Nucl. Chem.* 7, 257-275.

Keeney-Kennicutt, W. L. and J. W. Morse (1984). "The interaction of Np(V)O2+ with common mineral surfaces in dilute aqueous solutions and seawater." Marine Chemistry **15**: 133-150.

Keeney-Kennicutt, W. L. and J. W. Morse (1985). "The redox chemistry of Pu(V)O2+ interaction with common mineral surfaces in dilute solutions and seawater." Geochimica et Cosmochimica Acta **49**(12): 2577-2588

Kersting A. B.; Zhao P.; Zavarin M.; Sylwester E. R.; Allen P. G.; Williams R. W. (2005) Sorption of Pu(V) on Mineral Colloids. In *Colloidal-Facilitate Transport of Low-Solubility Radionuclides: A Field, Experimental, and Modeling Investigation*; (eds. A. B. Kersting and P. W. Remus). Report UCRL-ID-149688. Lawrence Livermore National Laboratory, Livermore, CA. pp. 67-87.

Khasanova, A. B., Shcherhina, N.S., Kalmykov, S. N., Teterin, Yu A., Novikov, A. P. (2007) Sorption of Np(V), Pu(V) and Pu(IV) on Colloids of Fe(III) Oxides and Hydrous Oxides and MnO_2 *Radiochemistry* 49(4), 419-425 (Originally published in Radiokhimiya, 2007, 49(4), 367-372.

Kobashi, A., Choppin, G. R., Morse, J. W. (1998) A study of the techniques for separating plutonium in different oxidation states. *Radiochim. Acta* **43**, 211-215.

Kohler, M., Honeymann, B. D., Leckie, J. O. (1999) Neptunium(V) sorption to hematite (α-Fe_2O_3) in aqueous solutions: The effect of CO_2. *Radiochim. Acta* 85, 33-48.

Kobashi, A., and Choppin, G. R. (1988) A study of Techniquioes for Separating Plutonium in Different Oxidation States *Radiochim. Acta* 43, 211-215.

Lu, N., Cotter, C. R., Kitten, H. D., Bentley, J., Triay, I. R., (1999) Reversibility of sorption of plutonium-239 onto hematite and goethite colloids. *Radiochim. Acta* 83, 167-173.

Lu, N., Reimus, P. W., Parker, G. R., Conca, J. L., Triay, I. R. (2003) Sorption Kinetics and Impact of Temperature, Ionic Strength, and Colloid Concentration on the Adsorption of Plutonium-239 by Inorganic Colloids *Radiochim. Acta* 91, 713-720.

Morse, J. W. and G. R. Choppin (1991). "The Chemistry of Transuranic Elements in Natural-Waters." Reviews in Aquatic Sciences **4**(1): 1-22.

Nakata, K., Nagasaki, S., Tanaka, S., Sakamoto, Y., Tanaka, T., Ogawa, H. (2000) Sorption and Desorption Kinetics of Np(V) on Magnetite and Hematite *Radiochim. Acta* 88, 453-457.

Nakayama, S. and Y. Sakamoto (1991). "Sorption of neptunium on naturally-occurring iron-containing minerals." Radiochimica Acta **52-3**(P1): 153-157

Neu, M., Hoffman, D. C., Roberts, K. E., Nitsche, H., Silva, R. J. (1994) Comparison of Chemical Extractions and Laser Photoacoustic Spectroscopy for the Determination on Plutonium Species in Near-Neutral Carbonate Solutions *Radiochim. Acta* 66/67, 251-258.

Neck, V. and Kim, J. I. (2001) Solubility and Hydrolysis of Tetravalent Actinides *Radiochim. Acta* 89, 1-16.

Nitsche, H., Lee, S. C., Gatti, R. C. (1988) Determination of Plutonium Oxidation States at race Levels Pertinent to Nuclear Waste Disposal *J. Nucl. Radioanal. Chem.* 124(1), 171-185.

Powell, B. A., R. A. Fjeld, D. I. Kaplan, J. T. Coates and S. M. Serkiz (2004). Pu(V)O-2(+) adsorption and reduction by synthetic magnetite (Fe3O4). *Environmental Science & Technology* **38**(22): 6016-6024

Powell, B. A., Duff, M. C., Kaplan, D. I., Bertsch, P. M., Coates, J. T., Eng, P., Fjeld, R. A., Hunter, D. B., Newville, M., Rivers, M. L., Serkiz, S. M., Sutton, S. R., Triay, I. R., Vaniman, D. T. (2006) Plutonium Oxidation and Subsequent Reduction by Mn(IV) Minerals in Yucca Mt. Tuff *Environ. Sci. Tech.* 40(11), 3508-3514.

Pickett, D. A., Murrell, M. T., Williams, R. W. (1994) Determination of Femtogram Quantities of Protactinium in Geologic Samples by Thermal Ionization Mass Spectrometry *Anal. Chem.* 66, 1044-1049.

Powell, B. A., Fjeld, R. A., Kaplan, D. I., Coates, J. T., Serkiz, S. M. (2005) $Pu(V)O_2^+$ Adsorption and Reduction on Synthetic Goethite (α-FeOOH) and Hematite (α-Fe_2O_3) *Environ. Sci. Tech.* 39(7), 2107-2114.

Sanchez, A. L., Murray, J. W., Sibley, T. H. (1985) The Adsorption of Plutonium IV and V on Goethite *Geochim. Cosmo. Acta* 49, 2297-2307.

Penrose, W. R., Metta, D. N., Hylko, J. M., Rinckel, L. A. (1987) Chemical Speciation of Plutonium in Natural Waters *J. Environ. Radioactivity* 5, 169-184.

Schwertmann, U. and Taylor, R. M. (1989) Iron Oxides. In *Minerals in Soil Environments*. (eds. J. B. Dixon and S. B. Weed). Soil Science Society of America, Madison, Wisconsin. pp. 379-438.

Schwertmann, U. and Cornell, R. M. (1991) *Iron Oxidies in the Laboratory: Preparation and Characterization.* VCH Publishers Inc., New York, NY.

Strawn, D. G. and Sparks, D. L. (2000) Effects of soil organic matter on the kinetics and mechanisms of Pb(II) sorption and desorption in soil. *Soil Sci. Soc. Am. J.* 64, 144-156.

Tochiyama, O., S. Endo and Y. Inoue (1995). "Sorption of Neptunium(V) on Various Iron-Oxides and Hydrous Iron-Oxides." *Radiochimica Acta* **68**(2): 105-111.

Thompson, R. C. (1982) Neptunium – The Neglected Actinide: A Review of the Biological and Environmental Literature *Radia. Res.* 90, 1-32.

Weijuan, L., Zuyi, T., Liangtian, G., Shushen, L. (2003) Sorption and desorption of neptunium(V) on loess: batch and column experiments. *Radiochim. Acta* 91, 575-582.

Wilson, R. E., Hu, Y., Nitsche, H. (2005) Detection and quantification of Pu(III, IV, V, and VI) using a 1.0 meter liquid core waveguide. *Radiochim. Acta* 93, 203-206.

DISTRIBUTION

Organizations:

U.S. Department of Energy
National Nuclear Security Administration
Nevada Site Office
Technical Library
P.O. Box 98518
Las Vegas, NV 89193-8518

U.S. Department of Energy
National Nuclear Security Administration
Nevada Site Office
Public Reading Facility
P.O. Box 98521
Las Vegas, NV 89193-8521

U.S. Department of Energy
Office of Scientific and Technical Information
P.O. Box 62
Oak Ridge, TN 37831-0062

Individuals:

Stacey Alderson
MS 439
7710 W. Cheyenne Ave.
Las Vegas, NV 89129

Chris Andres
Nevada Department of Conservation
& Natural Resources
Division of Environmental Protection
2030 E. Flamingo Rd, Suite 230
Las Vegas, NV 89119-0818

Naomi Becker
P.O. Box 1663, MS T003
Los Alamos NM 87545

Pat Bodin
NNSA/NSO
P.O. Box 98518
Las Vegas, Nevada 89193-8518

Steven F. Carle
Lawrence Livermore National Lab
P.O. Box 808, L-231
Livermore, California 94551-9900

Bruce Crowe
NNSA/NSO
MS 505
P.O. Box 98518
Las Vegas, Nevada 89193-8518

Jeff Daniels
Lawrence Livermore National Lab
P.O. Box 808, L-072
Livermore, California 94551-9900

Barb Deshler
Stoller-Navarro Joint Venture
7710 W. Cheyenne Ave.
Las Vegas, Nevada 89129

Dee Donithan
Desert Research Institute
755 E. Flamingo
Las Vegas, Nevada 89119

Dave Donovan
SNWA Resources
1900 E. Flamingo
Suite 253
Las Vegas, NV 89119

Sig Drellack
NSTec
P.O. Box 98521 MS/NLV 082
Las Vegas, Nevada 89193-8521

Doug Duncan
U.S. Geological Survey
411 National Center
Reston, VA 20192

Brad Esser
Lawrence Livermore National Laboratory
P.O. Box 808, L-231
Livermore, California 94551-9900

Dave Finnegan
Los Alamos National Laboratory
P.O. Box 1663, MS-J514 C-NR
Los Alamos, New Mexico 87545

Robert Graves
U.S. Geological Survey
160 N. Stephanie Street
Henderson, NV 89074-8829

Ward Hawkins
Los Alamos National Laboratory
P.O. Box 1663, MS-F665 / EES-11
Los Alamos, New Mexico 87545

Ron Hershey
Desert Research Institute
2215 Raggio Parkway
Reno, Nevada 89512

Bruce Hurley
NNSA/NSO
P.O. Box 98518
Las Vegas, Nevada 89193

Britt Jacobson
Nevada Department of Conservation
& Natural Resources
Division of Environmental Protection
2030 E. Flamingo Rd, Suite 230
Las Vegas, NV 89119-0818

Roger Jacobson
Desert Research Institute
2215 Raggio Parkway
Reno, Nevada 89512

Jackie Kenneally
Lawrence Livermore National Laboratory
P.O. Box 808, L-236
Livermore, California 94551-9900

Annie Kersting
Lawrence Livermore National Laboratory
P.O. Box 808, L-231
Livermore, California 94551-9900

Ed Kwicklis
Los Alamos National Laboratory
Box 1663, T003
Los Alamos, New Mexico 87545

Randy Laczniak
U.S. Geological Survey
160 N. Stephanie Street
Henderson, NV 89074-8829

Stephen Leedom
NNSA/NSO
P.O. Box 98518
Las Vegas, Nevada 89193

Joseph Leising
SNWA Resources
1900 E. Flamingo
Suite 253
Las Vegas, NV 89119

Rachel Lindvall
Lawrence Livermore National Laboratory
P.O. Box 808, L-231
Livermore, California 94551-9900

Reed Maxwell
Lawrence Livermore National Laboratory
P.O. Box 808, L-208
Livermore, California 94551-9900

John McCord
Stoller-Navarro Joint Venture
7710 W. Cheyenne Ave.
Las Vegas, NV 89129

Mark McLane
Nevada Department of Conservation &
Natural Resources
Division of Environmental Protection
2030 E. Flamingo Rd, Suite 230
Las Vegas, NV 89119-0818

Christine Miller
Stoller-Navarro Joint Venture
7710 W. Cheyenne Ave.
Las Vegas, NV 89129

Ken Ortego
NSTec
P.O. Box 98521 M/S NSF 082
Las Vegas, Nevada 89193-8521

Jim Paces
U.S. Geological Survey
P.O. Box 25046, MS 963
Denver Federal Center
Denver, CO 80225

Gayle Pawloski
Lawrence Livermore National Laboratory
P.O. Box 808, L-221
Livermore, California 94551-9900

Zell Peterman
U.S. Geological Survey
P.O. Box 25046 M/S 963
Denver Federal Center
Denver, Colorado 80225

Greg Pohll
Desert Research Institute
2215 Raggio Parkway
Reno, Nevada 89512

David Prudic
US Geological Survey
333 West Nye Lane Rm 203
Carson City, Nevada 89706

Paul Reimus
Los Alamos National Laboratory
P.O. Box 1663, MS-J534 CST-7
Los Alamos, New Mexico 87545

Timothy Rose
Lawrence Livermore National Laboratory
P.O. Box 808, L-236
Livermore, California 94551-9900

Greg Ruskauff
Stoller-Navarro Joint Venture
7710 W. Cheyenne Ave.
Las Vegas, Nevada 89129

Chuck Russell
Desert Research Institute
755 E. Flamingo
Las Vegas, Nevada 89119

Michael Singleton
Lawrence Livermore National Laboratory
P.O. Box 808, L-231
Livermore, California 94551-9900

David K. Smith
Lawrence Livermore National Laboratory
P.O. Box 808, L-171
Livermore, California 94551-9900

Jim Thomas
Desert Research Institute
2215 Raggio Parkway
Reno, Nevada 89512

Bonnie Thompson
U.S. Geological Survey
160 N. Stephanie Street
Henderson, NV 89074-8829

K.C. Thompson
Environmental Restoration Division
NNSA/NSO
P.O. Box 98521 MS 505
Las Vegas, Nevada 89193-8521

Andy Tompson
Lawrence Livermore National Laboratory
P.O. Box 808, L-208
Livermore, California 94551-9900

Rick Waddell
GeoTrans Inc.
363 Centennial Parkway
Suite 210
Louisville, CO 80027

Bill Wilborn
Environmental Restoration Division
NNSA/NSO
P.O. Box 98515 MS 505
Las Vegas, Nevada 89193-8521

Ross Williams
Lawrence Livermore National Laboratory
P.O. Box 808, L-231
Livermore, California 94551-9900

Jon Wilson
U.S. Geological Survey
160 N. Stephanie Street
Henderson, NV 89074

Andy Wolfsberg
Los Alamos National Laboratory
Box 1663, MS T003
Los Alamos, New Mexico 87545

Jeff Wurtz
Stoller-Navarro Joint Venture
MS 439
7710 W. Cheyenne Ave.
Las Vegas, Nevada 89129

Vefa Yucel
NSTec
P.O. Box 98521 MS/NLV 81
Las Vegas, Nevada 89193-8521

Mavrik Zavarin
Lawrence Livermore National Laboratory
P.O. Box 808, L-231
Livermore, California 94551-9900

Pihong Zhao
Lawrence Livermore National Laboratory
P.O. Box 808, L-231
Livermore, California 94551-9900

Technical Information Department • Lawrence Livermore National Laboratory
Lawrence Livermore National Security, LLC • Livermore California 94550